DEPARTMENT OF ENGINEERING
UNIVERSITY OF MESSINA

Assessment of zerovalent iron/lapillus granular mixtures for the remediation of heavy metal-contaminated groundwater

Silvia Simonetti

This dissertation is submitted for the degree of Doctor of Philosophy in Civil, Environmental and Safety Engineering (XXXV Cycle)

Curriculum: Geotechnical Engineering (ICAR/07)

Head of doctoral school: Prof. Gaetano Bosurgi

Tutor: Prof. Nicola Moraci

Co-tutor: Ing. Stefania Bilardi

Academic year 2021/2022

Index

List of figures

List of tables

INTRODUCTION

Objectives and Methodological Framework of the PhD Thesis

Groundwater contamination by heavy metals has a significant impact on the ecosystem and human health due to the high level of toxicity of metals mainly released into the environment by industrial activities or uncontrolled waste disposals (Rajendran et al., 2022). Nowadays groundwater remediation requires the use of sustainable technologies able to reduce greenhouse gas emissions during their implementation and operation and capable of guaranteeing the drinking or agricultural uses of the water resource. A permeable reactive barrier (PRB) can represent a solution to this issue.

A PRB consists of a reactive and permeable diaphragm placed into the aquifer to intercept the contaminated plume, without energy input but using the natural hydraulic gradient, and to stop the contaminant propagation.

In Italy, the remediation of contaminated sites is regulated by Part IV - Title V of Legislative Decree 152 of 2006. According to Annex 3 of the V Title of the L.D. 152/2006 a PRB is classified among the containment measures of a contaminated site. These interventions have the aim to avoid contaminant propagation. Given the growing importance of the sustainability concept, in 2012 the SuRF Italy (Sustainable Remediation Forum) is born with the aim of drafting a document, the so-called White Book published in 2014, which declines the concept of sustainability to remediation technologies. This document defines sustainable remediation *"The management and remediation process of a contaminated site, aimed at identifying the best solution, which maximizes the benefits of its execution from an environmental, economic and social point of view through a decision-making process shared with the stakeholders "*.

With reference to the PRB, the same White Book places this remediation technology among the sustainable technologies to be applied in the future. This technology, which does not involve energy consumption for its operation, and which does not produce visible impacts on the surface (being the intervention underground), is characterized by a low environmental impact. In addition, it is possible to use the site during the aquifer remediation and this aspect generates a low social impact. Finally, the economic impact is also low as the technique does not have high construction costs compared to other possible technologies.

Zero valent iron is the most used reactive material for the construction of chemical-physical PRBs, as it is able to treat water contaminated by chlorinated organic solvents, heavy metals, radionuclides or mixed contaminations (for example heavy

metals and chlorinated solvents) (ITRC, 2005; Faisal et al., 2018). Although there are examples of a good longevity of this reactive medium in full scale (Wilkin et al., 2014), there are numerous cases where a significant reduction of the barrier permeability occurred (Henderson and Demond, 2007). This phenomenon is due to the formation of iron oxides and hydroxides that due to their expansive nature reduce the porosity and permeability of the barrier (Cao et al., 2021; Hu et al., 2018). Mixing ZVI with another granular medium is a well-established strategy able to prevent the corrosion process of iron by water and its constituents from causing a change in permeability (Bilardi et al., 2020; Hu et al., 2020; Moraci et al., 2017; Ruhl et al., 2014). The role of the admixing agent, like sand or volcanic materials (e.g., pumice, lapillus, zeolites), is to separate iron particles and avoid that the aggregation of ZVI particles can cause clogging phenomena (Hu and Noubactep, 2019; Hu et al., 2020; Limper et al., 2018; Ullah et al., 2020b; Yang et al., 2022).

The dispersion rate of ZVI cannot be establish a priori since the iron corrosion process, and the resulting formation of its corrosion products, depends on groundwater chemical composition and its flow velocity (Madaffari et al., 2017).

This thesis has the aim to deepen the long-term hydraulic behaviour of PRB composed of ZVI and lapillus and find a strategy able to improve its longevity. For this purpose, initially the efficacy of a multilayer configuration was evaluated towards the removal of heavy metals as copper (Cu), nickel (Ni) and zinc (Zn). This configuration consists of two sequential layers having different volumetric ratios (v.r.) between ZVI and lapillus (i.e., 5:95-20:80, 10:90-20:80).

Further objectives of the thesis were the study of i) the influence of geochemical parameters on the long-term behaviour of the ZVI/lapillus granular mixture; i) the effectiveness of lapillus in the removal of heavy metals and iii) the effectiveness of a ZVI/lapillus granular mixture aged with water.

Thesis organization

The first chapter of this thesis focuses on the theme of contamination of soil and water in Europe, with a look at the geographical distribution of contaminated sites with particular reference to heavy metals. The main remediation technologies currently used for the remediation of groundwater are discussed. In particular, the theme of PRB is deepened with the description of the main existing configurations, the main construction techniques and the design phases. The state of the art relating

to the application of ZVI is summarized with particular reference to aspects inherent the long-term behaviour of ZVI.

The second chapter describes the characteristics of the materials and of the contaminated solutions used in the experimentation, the apparatus used to test the granular mixtures and the instruments necessary to evaluate the hydraulic and reactive performance.

The third chapter deals with the comparison between two multilayer configuration of a Fe^0/lapillus granular mixture for PRB and a single-layer configuration with reference to the hydraulic conductivity and the long-term effectiveness towards Cu, Ni, and Zn removal. Specifically, three column tests called A, B and C were conducted. Column A identifies a monolayer configuration with Fe^0/lapillus v.r. 20:80; Column B identifies a column filled with a double layer of the ZVI/lapillus granular mixture. In the first layer, the two materials are mixed with a v.r. equal to 10:90 and in the second layer with a v.r. equal to 20:80. In column C, ZVI and lapillus are mixed with a v.r. equal to 05:95 in the first layer and with a v.r. equal to 20:80 in the second layer. The three columns are compared in terms of hydraulic and reactive behaviour over time and along the reactive medium thickness. Furthermore, the exhaust material taken from the three columns was subjected to SEM-EDX analysis.

The column tests described in the fourth chapter were conducted with the purpose of analysing the hydraulic and reactive behaviour of a Fe^0/lapillus mixture (v.r. equal to 10:90) as the geochemical parameters of the contaminated solution vary. Five columns (named E, F, G, M) were conducted. In Column M the reactive medium is permeated with Cu, Ni and Zn. The solution that feeds Column E contains Cu, Ni, Zn with $CaCO_3$. The solutions that feed Columns F and G contain Ni and Zn dissolved in distilled water with $NaHCO_3$ or with $CaCO_3$ and $NaHCO_3$ respectively. The four columns are compared in terms of hydraulic and reactive behaviour over time and along the reactive medium thickness.

The fifth chapter investigates the ability of lapillus to remove Cu, Ni and Zn (column D). The trends in the concentration of contaminants and pH over time and along the thickness of the medium are compared with data relating to Fe0/lapillus mixture (Column M).

The column tests described in the sixth chapter were carried out with the aim of simulating the behaviour of the reactive medium placed upstream of the inlet section of the PRB which has not yet come into contact with the contamination flow. A ZVI/lapillus granular mixture was permeated with distilled water (Column H_0) and subsequently with a contaminated solution of Cu, Ni and Zn (Column H_1). Both solutions were prepared with distilled water containing $CaCO_3$ diluted in it.

The conclusions chapter summarizes the main results achieved by the research conducted, providing useful suggestions in the design of ZVI-PRB.

1 GROUNDWATER REMEDIATION THROUGH REACTIVE PERMEABLE BARRIERS

1.1 Introduction

The remediation of contaminated sites is currently a challenge on a global scale. Research in these fields aims both at perfecting existing technological solutions and at devising new ones. This chapter aims to frame the topic of the research activity, presenting the European data concerning soil pollution by heavy metals and the state of the art of reactive permeable barriers for groundwater remediation, with relative advantages and problems concerning long-term performance.
The working principle of the PRB technology is described, along with the main configurations, dimensions and construction techniques. Subsequently, the main design phases of a PRB are summarized with particular reference to the characterization of the site, selection of the reactive medium, laboratory tests for the design of the barrier and selection of the most suitable construction method. The state of the art relating to the application of zero valent iron is summarized, the main removal mechanisms against heavy metals and the aspects inherent in the long-term behaviour of zero valent iron.

1.2 Contaminated sites

Since 2000, the European Environment Agency (EEA) has produced six reports on the state of the art of contaminated sites in Europe. The Joint Research Centre of the European Commission published in 2018 (Pérez and Eugenio, 2018) an update to the data collection of May 2014 regarding the CSI 015 indicator "Progress in the management of Contaminated Sites in Europe" (Van Liedekerke et al., 2014). The European Soil Data Centre (ESDAC) of the European Commission conducted a project to collect and manage contaminated site data collected through the European Environment Information and Observation Network (EIONET). Specifically, EIONET includes 28 member states of the European Union (EU-28) together with Iceland, Liechtenstein, Norway, Switzerland, Turkey and countries that have collaborated in the Western Balkans: Albania, Bosnia, Herzegovina, the former Yugoslav Republic of Macedonia, Montenegro and Serbia as well as Kosovo (Figure 1.1). Data collection concerned the management of contaminated sites, the remediation objectives and technologies, the contribution

of polluting activities to local soil contamination, environmental impacts and expenditure.

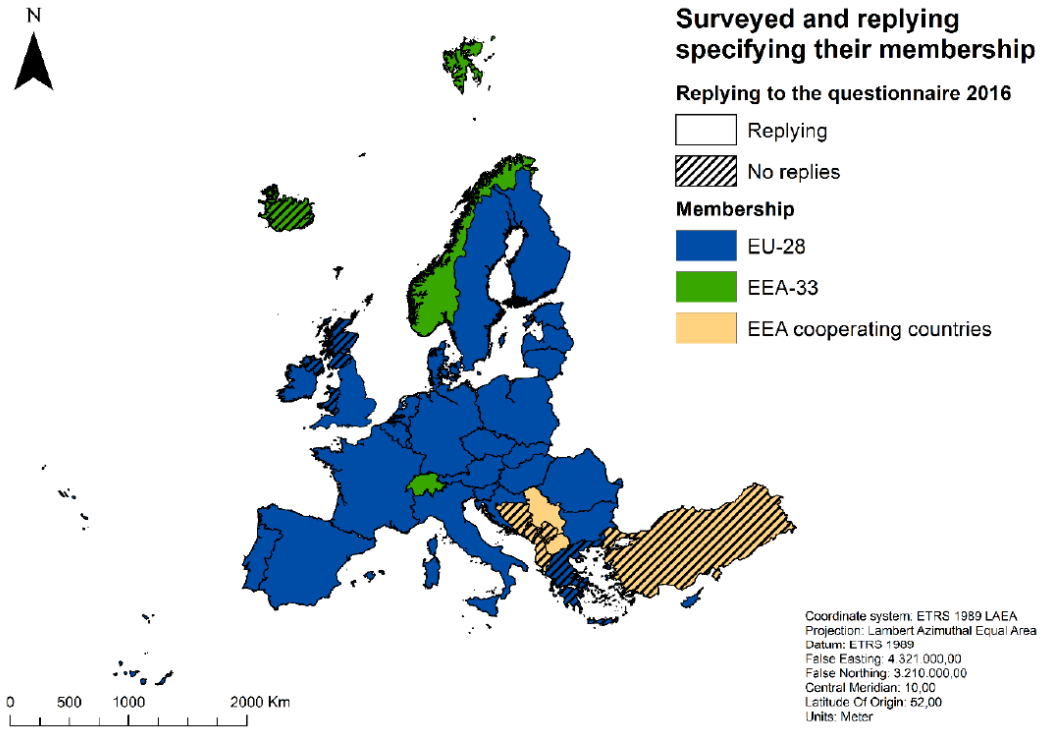

Figure 1.1 31 replying out of 39 surveyed, with their membership (EU, EEA, EEA cooperating countries in the western Balkans) (JRC Technical Reports, 2018).

In the 2011 data collection period, the ESDAC introduced the following parameters: "Potentially Contaminated Site" (PCS), "Contaminated Site" (CS) and "Site under remediation."

A contaminated site (CS) is a well-defined area in which the presence of soil contamination has been confirmed; such contamination represents a potential risk to humans, water, ecosystems or other receptors. Risk management measures (e.g., remediation) may be required depending on the severity of the risk of adverse impact on receptors within the current or planned use of the site.

A "potentially contaminated site" (PCS) is a site where unacceptable, but unverified soil contamination is suspected, and detailed investigations are needed to ascertain whether there is an unacceptable risk of adverse receptor impacts.

A distinction is also made between "estimated" and "identified" sites.

Data on the extent of local soil contamination in Europe in 2016 are available for 29 countries, including 25 member states of the European Union. In the EU-28, estimates reveal the possible existence of around 2.8 million sites where polluting activities have occurred/conducted.
In 2016, more than 650,000 sites where polluting activities occurred/conducted were registered in the national and regional inventories of the interviewed countries; more than 76,000 new sites have been registered since the last financial year. From the 2011 estimates, a significant effort has been made to remediate these contaminated sites with over 5,000 new sites undergoing remediation or RRM among the countries surveyed. Also, since 2011, a reduction in the number of sites undergoing remediation has been reported by Belgium (Flanders), Estonia, Italy, Latvia, Norway and Slovakia.

A key aspect for remediation research and development, analysed by Van Liedekerke et al. (2014) consists of the percentage of contaminants affecting the soil and fluid matrices. A similar distribution of contaminants affecting soil and groundwater can be inferred from the analysis results shown in Figure 1.2. Heavy metals represent the dominant category of contaminants. Mineral oils are the second most encountered category.

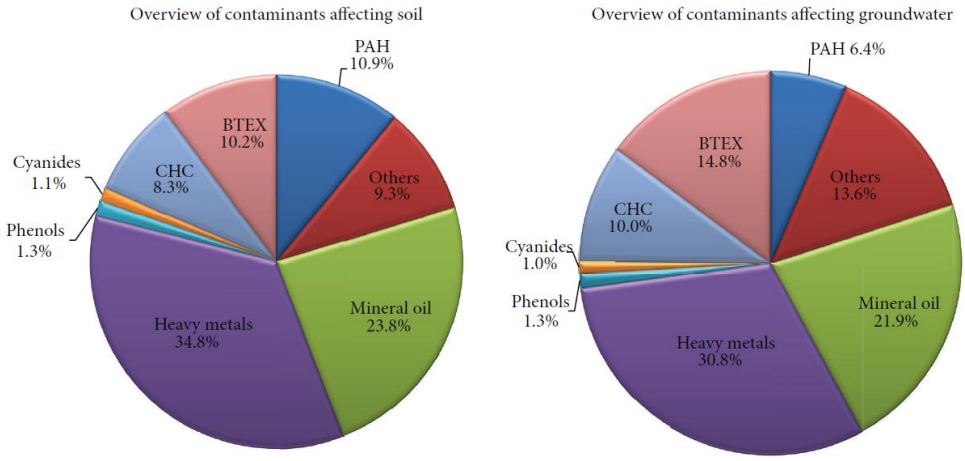

FIGURE 4: Distribution of contaminants affecting soil and groundwater in Europe.

Figure 1.2 Distribution of contaminants affecting soil and groundwater in Europe (Panagos et al., 2013).

The collection of EIONET-CSI data can be supplemented with data on heavy metals provided by other projects such as the European Pollutant Emissions and Transfer

Registry (E-PRTR) and data on the chemical characteristics of water and soil available after the statistical framework survey on land use/coverage area (LUCAS) soil survey, aimed at digital mapping of the soil to overcome the disadvantages due to the problem of privacy in identifying contaminated soil.
As regards the activities that most contribute to soil contamination, waste disposal and treatment represent 38% of the sources of local soil contamination out of the total of sources identified, industrial and commercial activities represent 34%, while sites agricultural and wastewater treatment plants account for 8%. For industrial and commercial activities, on the other hand, the production sector, including the metallurgical, chemical, oil and energy production industry, represents 60% of the contamination, while the service sector, mainly petrol stations, represents 33% (Panagos et al., 2013).

Lado et al. (2008) modelled the spatial distribution of eight heavy metals, analysing soil data from 28 European countries. Image 1.3 focuses attention on the quantities of copper, nickel and zinc. According to the results of this study, a higher concentration of Cu was found mainly in the countries of southern Europe (e.g., Greece, Italy and Andalusia) and in some areas of the United Kingdom. Ballabio et al. (2018) continue this study to obtain an updated map of the distribution of copper in the soils of 25 member states of the European Union (Fig. 1.4). The concentration of copper in the soil is higher in agricultural land; the combined effect of a high pH and the presence of organic carbon and clay promotes the accumulation of copper in soils with vineyards and fruit trees.
Looking at the distribution of Nickel, the LUCAS 2009-2012 sampling campaign reveals an average concentration in Europe of 18 mg/kg. High values of Ni are found mainly in central Greece, northern Italy, central Pyrenees, northern Scandinavia, Slovakia and Croatia and show a strong correlation between the Ni content and the magnitude of earthquakes, as seismic activity it is indirectly related to the concentrations of some heavy metals.
Zinc has a high concentration in Central Europe and Great Britain, with values mainly related to agriculture. They are also inversely correlated with distance from roads (Lado et al., 2008).

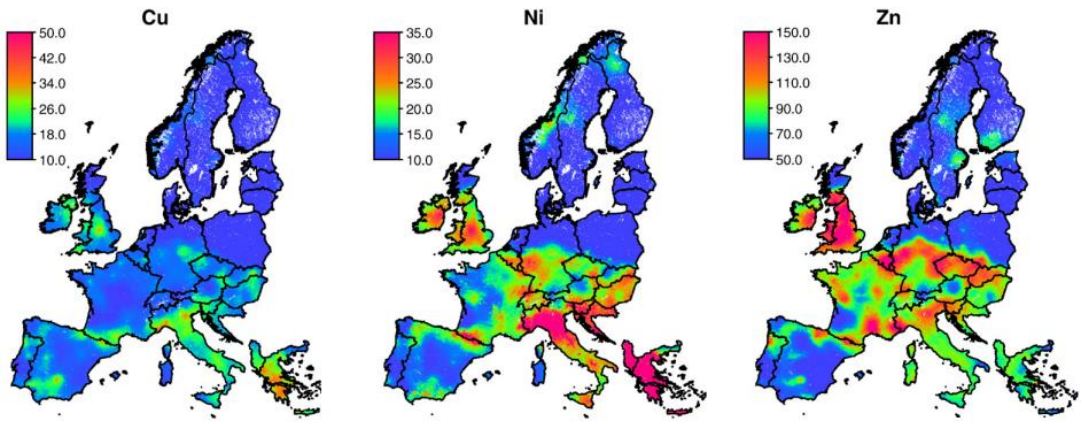

Figure 1.3 Maps of heavy metal concentration in topsoils [mg kg^{-1}] (Lado et al., 2008). All maps are available on-line via the http://eusoils.jrc.it website

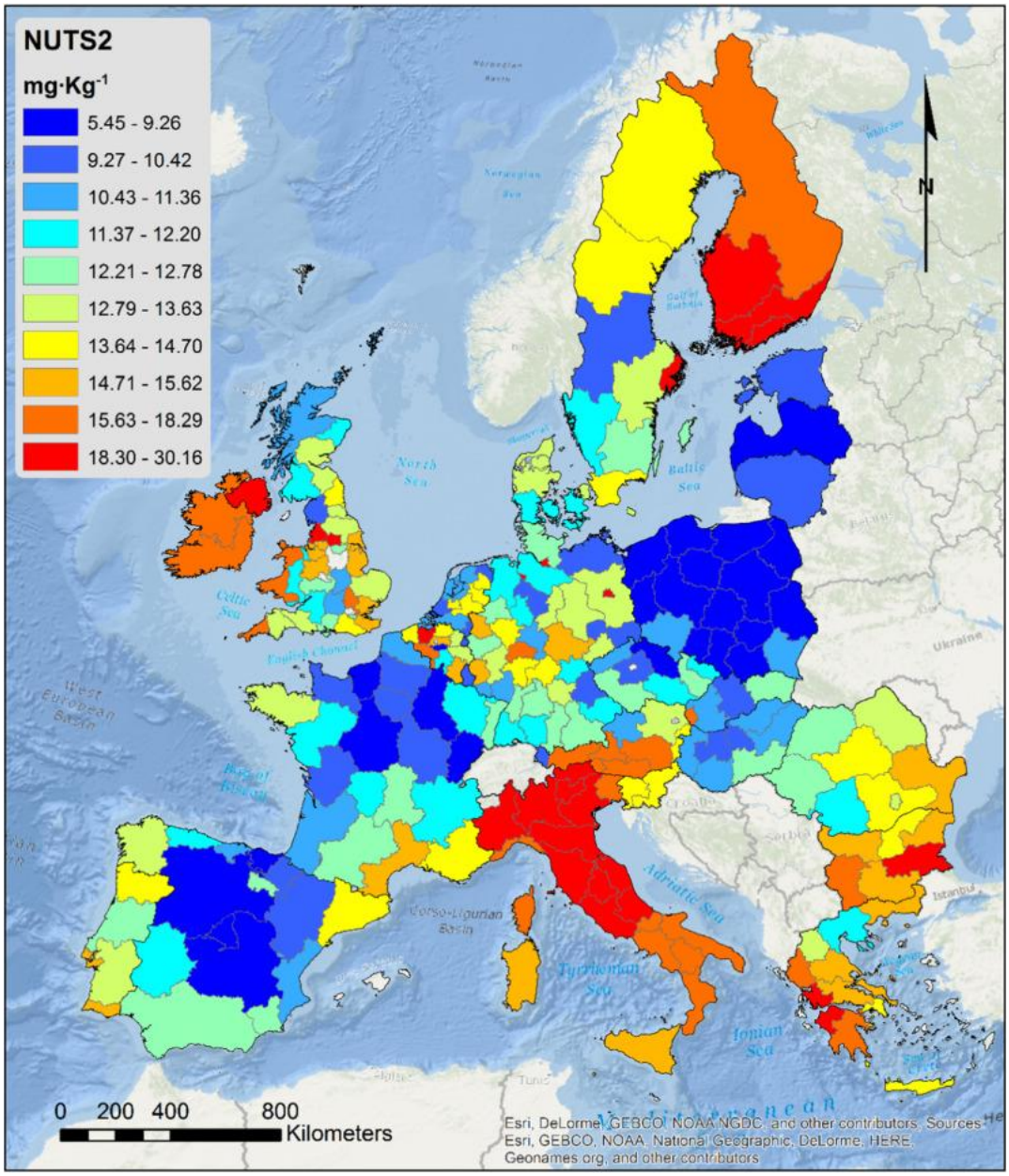

Figure 1.4 Soil copper distribution at European scale (Ballabio et al., 2018)

1.3 Main methods of groundwater remediation

The most common ex situ technology for the remediation of contaminated aquifers is that of the hydraulic barrier (pump-and-treat), which consists of the extraction of contaminated groundwater through withdrawal wells and in the treatment of the same in specific internal systems or external to the site (on/off site). The wells, located mostly transversely to the underground water flow, allow the interception of both the contaminated flow coming from upstream and the flow that has passed the line of the pumping wells but which is still inside the supply front of the barrier (or cone of influence). This remediation technology is applicable to dissolved or suspended contaminants of inorganic and organic nature. A scheme of a hydraulic barrier is shown in Figure 1.5.

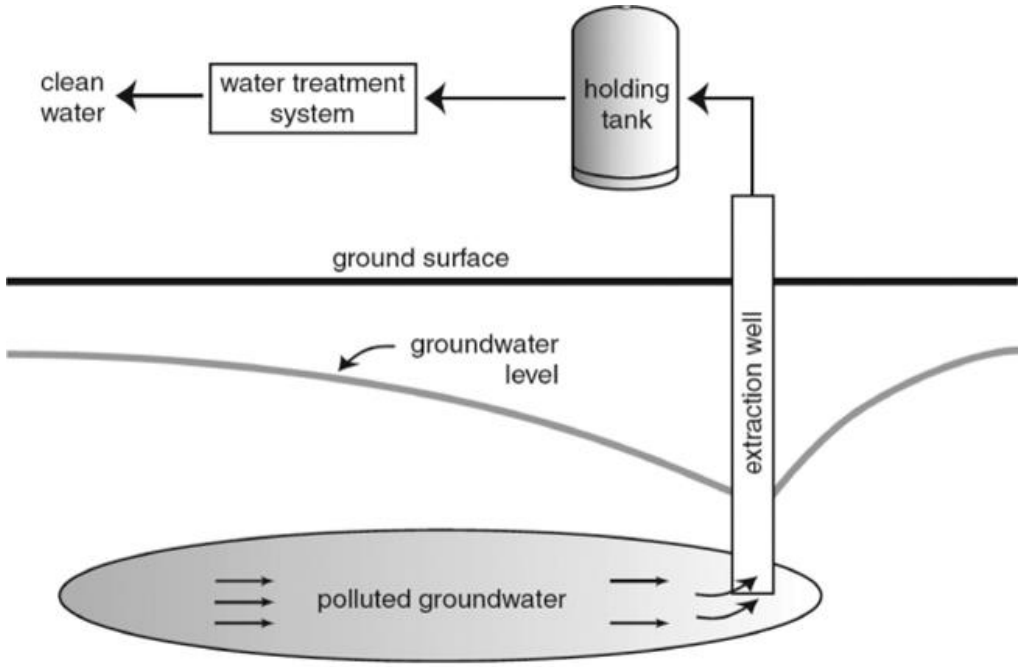

Figure 1.5 Groundwater pump and treat system (from United States Environmental Protection Agency (USEPA), A Citizen's Guide to Pump and Treat, USEPA. EPA 542-F-01-0025. Office of Solid Waste and Emergency Response, Washington, DC, 2001h.)

The most common groundwater remediation in-situ technologies are depollution by introducing air, or air and nutrients, into the saturated medium (air sparging and biosparging).

Air sparging consists in the injection of air inside the aquifer to promote the transfer of volatile organic substances from the aqueous to the vapor phase. The injected air is subsequently extracted, in the unsaturated medium above, and treated in special plants (Fig. 1.6).

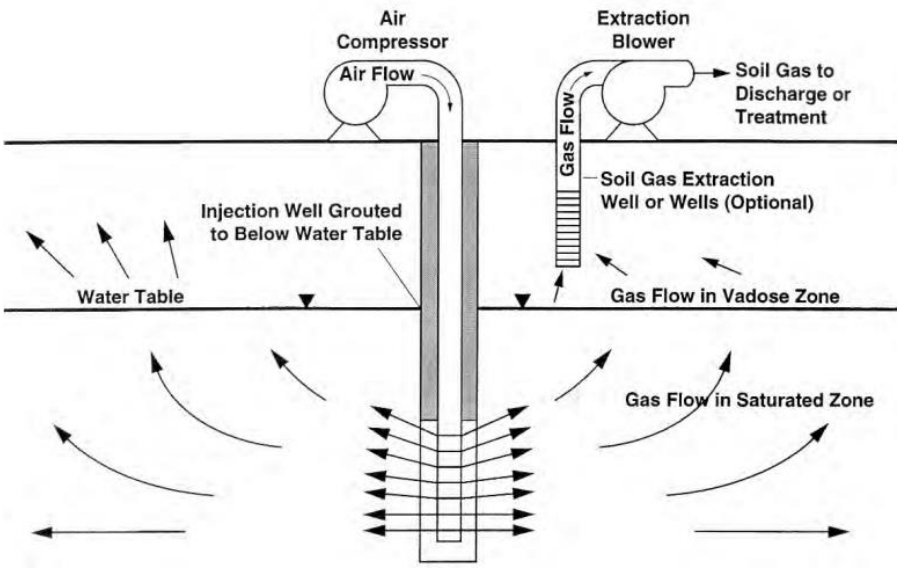

Figure 1.6 Typical in-situ air sparging (U.S. Army Corps of Engineers, 2013).

The biosparging treatment consists in the introduction of air and nutrients directly into the aquifer to favour the degradation of organic contaminants (for example medium weight petroleum substances such as diesel or gasoline) through biological processes.

An in-situ remediation technology of groundwater consists in the injection of oxidizing products (such as pure oxygen, hydrogen peroxide, potassium permanganate or ozone) into groundwater for the removal of chlorinated solvents, polycyclic aromatic hydrocarbons and mixtures petroleum (Fig. 1.7). The injection of reducing substances (such as for example zero-valent colloidal iron, hydrogen sulphide and dithionite) is instead particularly suitable for immobilizing redox-sensitive metal elements (such as chromium, uranium, thorium) or for degrading chlorinated solvents dispersed on large areas (Gorla, 2012).

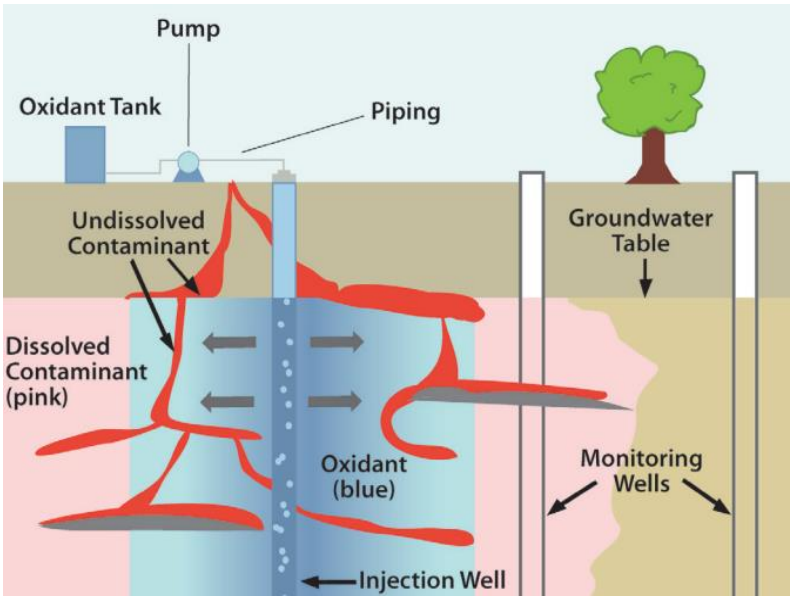

Figure 1.7 In Situ Oxidation Application (USEPA, 2012).

1.4 Working principles of a PRB

Permeable reactive barrier (PRB) is an in-situ technology for the remediation of contaminated groundwater (Tratnyek, 2002; USEPA, 2002). It consists of an engineered zone of reactive material placed in an aquifer to intercept the contaminating plume perpendicularly and remove contamination from the groundwater that passes through it (Puls et al., 1999) (Fig. 1.8).

This technology is based on the natural aquifer gradient to move the contaminated groundwater through the reactive zone. As the contaminants pass through the barrier, they react with the reactive media that either transform them into less harmful compounds or block them into the reactive zone (Gavaskar et al., 2000; Powell et al., 1998; USEPA, 1999). Different tested reactive materials can remove organic and inorganic contaminants from groundwater. Moreover, PRB reduces the exposure of workers to contaminants and allows for use of the land surface, developing the treatment underground.

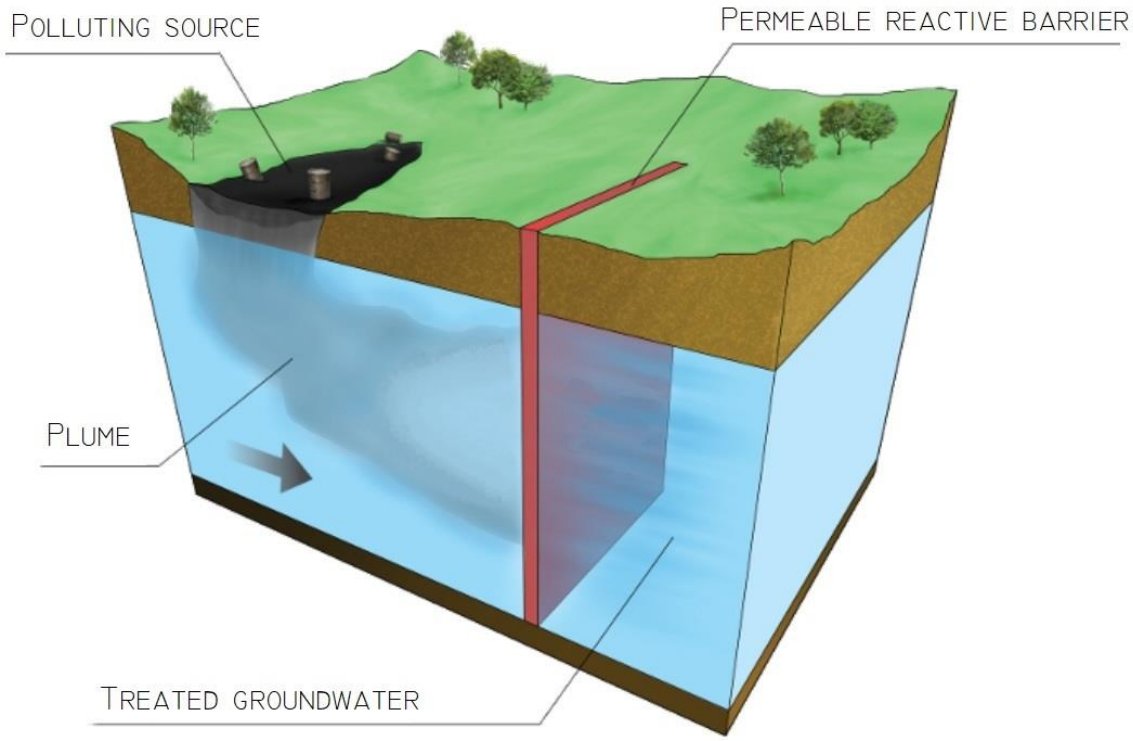

Figure 1.8 3D model of a PRB.

1.5 Configurations, dimensions and construction techniques: an overview of full and pilot scale PRB installed worldwide

1.5.1 Configurations

The purpose of the barrier design is to allow the complete capture of the contamination plume using the minimum of the reactive material. Most PRBs in use can be categorized into three types (EPA 1999): horizontal or continuous PRBs (Fig. 1.9), funnel and gate PRBs (Fig.1.10) and caisson PRBs (Fig. 1.11). Choosing the correct configuration depends on the size of the plume, accessibility and groundwater pattern. These configurations have been used for extensions up to 300 m but, as they require excavation, they are limited to depths up to 15–20 m using conventional excavation technologies.

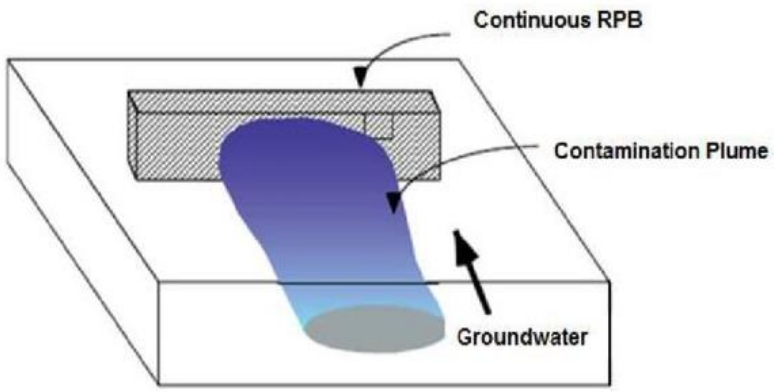

Figure 1.9 Plume capture by a continuous PRB trenched system. The plume moves unimpeded through the reactive zone (USEPA 1998).

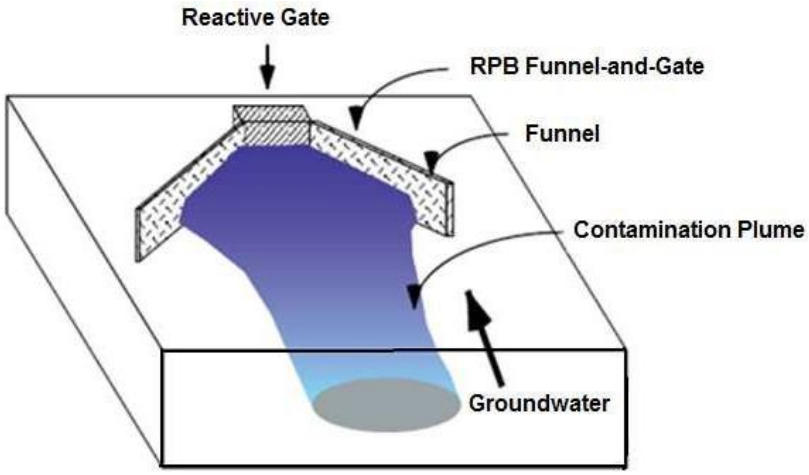

Figure 1.10 Plume capture by a funnel-and-gate system. Sheet piling funnels direct the plume through the reactive gate (USEPA 1998).

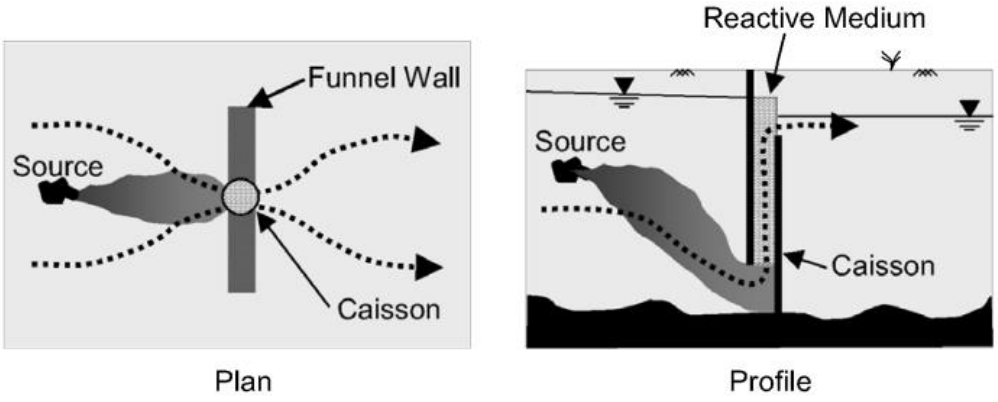

Figure 1.11 Schematic of a caisson PRB in plan and profile views (Elder & Benson, 2018).

Horizontal PRBs are the most common and consist of a trench filled with a reactive medium and located downstream of a contaminating plume and perpendicular to the water table gradient (Blowes et al. 1995). The funnel-and-gate PRB consists of a zone of reactive medium or "gate" located at the end of a non-reactive and less permeable "funnel", made up of soil-bentonite mixtures, which convey the underground water in the PRB gate (Starr and Cherry 1994, Birke et al. 2003). The width of the funnel is selected to capture the plume and the thickness and width of the gate are selected to provide sufficient residence time of the contaminants in the reactive medium. Typically, the ratio of the funnel width to the gate width is less than 6 (Day et al., 1999). The funnel and gate design has a greater impact on altering flow than groundwater at a continuous PRB.
In all configurations, the permeability of the reactive medium should be greater than that of the aquifer, to avoid deviations of the aquifer around it. PRBs are particularly convenient for groundwater remediation because they conserve water energy and are potentially cheaper than conventional pump-and-treat remediation due to lower operating and maintenance costs.

Caisson PRBs are less common and resemble a funnel-and-gate PRB in that groundwater is channelled into the PRB by a funnel. In contrast to the funnel-and-gate PRB, however, the reactive medium in the caisson PRB is located in a vertically oriented vault or tube, often referred to as a caisson (EPA 1999), flow through the reactive medium is upward rather than horizontal. The caisson has opening on its up and downgradient sides at opposite ends of the caisson. Contaminated groundwater

enters through one opening, passes vertically through the caisson PRB, and exits through the opposite opening.

GeoSiphon and GeoFlow Cells (International Patent Application filed December 19, 1997, by Westinghouse Savannah River Company) are innovative alternatives to current groundwater treatment technology. GeoSiphon cells are similar to the funnel and gate concept, except that a siphon is used to increase groundwater flow. The upgradient edge of the siphon is placed in the contaminated plume while the downgradient end can be placed in the subsurface, a surface water body, or the ground surface. GeoSiphon cells work by connecting a large diameter well to a siphon, which accelerates the flow rate between points of a natural head difference. The system is still passive, and the increased flow reduces instances of clogging due to mineral precipitates. The same types of reactive media adopted in conventional PBRs can be used (Bronstein, 2005). The world's first GeoSiphon Cell was installed at the Savannah River Site (SRS) TNX facility in July 1997, for the treatment of trichloroethylene and carbon tetrachloride contaminated groundwater (Phifer et al., 1999).

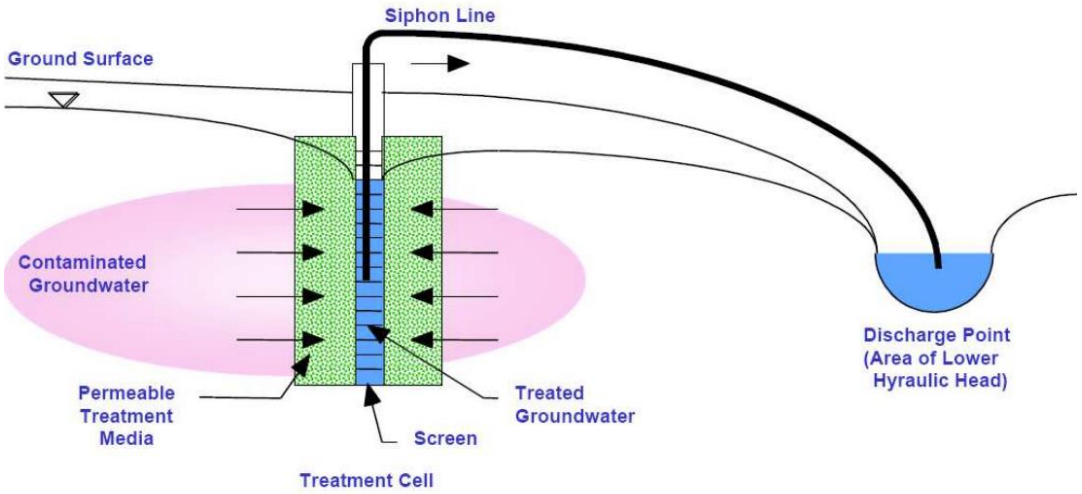

Figure 1.12 GeoSiphon configuration (Di Molfetta and Sethi., 2005)

1.5.2 Design

For a PRB to be successful, the PRB must allow contaminants to easily enter and react with the emplaced reactive media. Prior to design of a PRB, it is important to understand the groundwater flow velocity and direction, and understand the type, magnitude and location of the contamination you wish to treat. An assessment of

geochemistry is also important. This knowledge is used within the PRB design to calculate the residence time of the contamination within the PRB to ensure the contamination is properly treated prior to exiting the reactive media.

To properly design a PRB, the following should also be considered and understood:

- Good understanding of site characteristics including geology, stratigraphy, geochemistry and groundwater hydraulics
- Maximum expected groundwater plume concentrations and required treatment levels
- Maximum groundwater flow velocity
- Seasonal variability in groundwater elevations
- Depth of plume and suitable confining layer to key the PRB into

It is imperative to understand the contaminant plume shape and variability in the direction of groundwater flow over time. PRB installation techniques should then be matched with actual site conditions.

ZVI PRBs have been installed and performing in place for almost 30 years in a variety of geochemical environments. It is possible that over this length of time, mineral precipitates can form on the iron surface; this can passivate (coat) reactive sites and begin to clog the PRB. Field observations and modelling have, however, shown that in many cases this loss of porosity and permeability will occur at very low rates.

Solid organic amendments, such as mulch and leafy compost may be preferred in some instances to ZVI based on material cost savings. These organic amendments have been applied in PRBs to treat a range of contaminants that includes chlorinated solvents, acid mine drainage (containing heavy metals), nitrates and sulphates. Physically, mulches are predicted to last 15 to 30 years in the subsurface. However, in practice it appears that such “biowall” PRBs may need to be replenished every 4 to 6 years to sustain the highly reducing conditions required for effective anaerobic degradation. The replenishment strategy can involve the injection of mixtures of soluble and/or insoluble carbon substrate solutions or slurries.

The monitoring program for a PRB should be dynamic. As the PRB ages, the monitoring plan will likely require adjustments to assess variability in both hydraulic and chemical conditions.

The primary goal of any PRB design is to ensure the targeted portion of the contaminant plume is intercepted for treatment and that contaminant flow beneath, around, or above the treatment system does not occur. The second goal is to ensure that the dimensions of a PRB are adequate to achieve the contact time between contaminants and reactive medium needed for the reduction of contaminant concentrations to acceptable levels. Therefore, understanding the site-specific

hydrogeology, contaminant and reactive medium properties are critical to the design and construction of a PRB (ITRC, 2011).
The overall methodology for the application of a PRB at a given site is shown in Figure 1.13.
PRB design involves the following steps (Gavaskar et al., 2000):

- Preliminary assessment
- Site characterization
- Reactive media selection
- Treatability testing
- Modelling and engineering design
- Selection of a suitable construction method
- Monitoring plan preparation
- Economic evaluation

1.5.3 Preliminary assessment

The preliminary assessment is conducted to evaluate the technical and economic suitability of a given site for PRB application. A Preliminary Technical Assessment has the objective to specify the factors that need to be considered to determine the suitability of a site for PRB application. These factors are (Gavaskar et al., 2000):

- Contaminant Type
- Plume Size and Distribution
- Aquifer Depth
- Geotechnical Considerations
- Competent Aquitard
- Groundwater Velocity

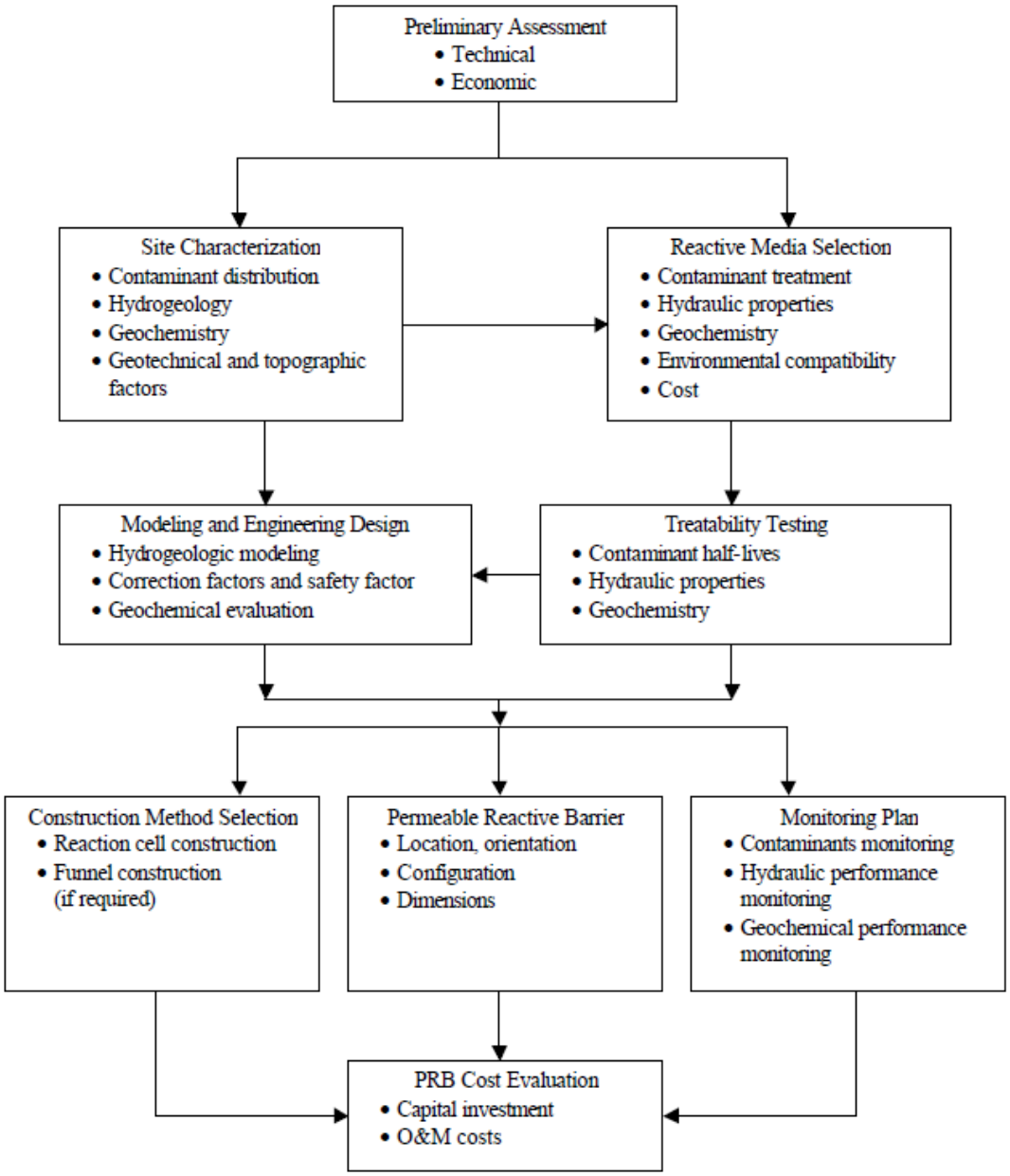

Figure 1.13 Design Methodology for a PRB Application (Gavaskar et al., 2000).

1.5.4 Site Characterization

A site characterization requires the knowledge of the following factors: soil types, depth of water, groundwater flow direction, groundwater velocity, hydraulic conductivity, porosity, depth to confining layer, and dimensions, depth and contaminants concentration of the dissolved plume. Hydrogeological investigations are essential in determining the hydrogeologic properties of the aquifer and may include: water level monitoring using pressure transducers, hydraulic conductivity testing, pump tests and tracer tests. The most significant data to be collected include variations in the depth, thickness, and water levels of different hydrostratigraphic units. This is achieved by drilling and sampling at several locations using conventional drilling or other technologies, such as cone penetrometer testing (CPT) or the use of a Geoprobe. However, at small sites, the traditional monitoring wells are likely to provide more reliable and higher resolution data. The data for hydraulic conductivity, porosity, and water levels are used to determine groundwater velocity at the site (Gupta and Fox, 1999).

1.5.5 Reactive medium selection

The choice among the possible reactive media to be used in PRB constructions is governed by the following considerations (Gavaskar et al., 2000):

- Reactivity: A medium with faster degradation rates is preferred.
- Stability: It is important that the reactive medium can maintain its reactivity.
- Availability and Cost. A cheaper medium is preferred over a more expensive medium, especially if any differences in performance are reported to be slight.
- Hydraulic Performance. The particle size of the reactive medium should be sufficient to ensure required hydraulic capture by the barrier. Moreover, the reactive medium should be a filter for the aquifer.
- Environmental Compatibility. The reactive medium should not introduce harmful by-products into the down gradient environment.
- Construction Method. Some innovative construction methods, such as jetting, may require a finer particle size distribution in the reactive medium.

The choice of the most suitable reactive medium is strictly linked to the type of contamination, whereas the main geotechnical characteristics of the medium (i.e.,

grain size curve, porosity, permeability) result from the proprieties of the aquifer. The factors that influence the choice of the grain size distribution of the reactive medium include grain size distribution, porosity, internal stability and permeability of the soil that constitutes the aquifer.
Therefore, the most important geotechnical issue regarding the choice of the grain size distribution of the medium, which has not been properly considered in the scientific literature, is the necessity for the reactive medium to satisfy the filter design criteria towards the surrounding soil.
In one-dimensional flow conditions, a filter must satisfy the following three main design criteria: internal stability, retention and permeability (Moraci et al., 2016a, 2012).
When water flows through the soil, fine particles can be washed out, leading to internal erosion (i.e., piping). Therefore, the function of a filter is to retain soil particles and to avoid the development of high internal pore pressure inside the filter (at the soil–filter interface), which can affect the draining capacity of the barrier.
Thus, a filter should be fine enough to retain loose soil particles (retention criteria) but coarse (or permeable) enough to allow seepage flow and avoid the development of high internal pore pressure (permeability criteria).
The presence of a filter (of the PRB in this case) can modify the neutral pressure and seepage flow (Giroud, J. P. Raymond, 1996; Moraci et al., 2016a). Therefore, the permeability criteria require the verification of two requirements: high internal pore pressure and flow rate. In the first case, the presence of the barrier should not increase the internal pore pressure at the soil–filter interface. The hydraulic conductivity of the barrier, in the long term, must be higher than the surrounding soil involved in the seepage. Regarding flow rate, a filter is acceptable if the relative difference between the flow rate in the soil and that in a system soil-filter is less than 10% (Moraci, 2010). In order to satisfy these two requirements, a PRB must maintain a high value of hydraulic conductivity, especially in the long term.

Another important characteristic of the granular filter is its internal stability, which is its ability to prevent the loss of its own small particles due to disturbing forces such as seepage and vibration (Moraci, 2010). It is important that this filter does not suffer appreciable variations in its particle size distribution and permeability owing to the dragging exerted by the fluid. The internal stability of a granular soil mainly depends on three factors: soil grain size distribution, soil relative density and applied hydraulic gradient. Regarding the former factor, soils that have a grain size distribution that presents a concave upward curve, a gap inside the curve (gap-

graded soils), or a broadly graded curve are generally considered to be internally unstable (Moraci et al., 2012). Three criteria are commonly used to determine the potential internal instability of a granular soil subjected to seepage: Kezdi, (1969), Sherard (1979) and Kenney and Lau (1985) criteria. Kezdi (1969) and Sherard (1979) proposed methods based on classical retention criteria for granular soils, while Kenney and Lau (1985) proposed a method based on experimental and theoretical results. Moraci et al. (2012) proposed a statistical geometrical method to evaluate the internal stability of granular soils.

1.5.6 Treatability testing

Treatability testing is conducted to evaluate the performance of the reactive medium with groundwater from a specific site for the following purposes (Gavaskar et al., 2000):

- Screening and selecting a suitable medium for the reactive cell
- Estimating the half- life of the degradation reaction
- Determining the hydraulic properties of the reactive medium
- Evaluating the longevity of the reactive medium.

Treatability testing for the screening and selection of the suitable reactive medium for the reactive cell is accomplished by batch tests. Batch experiments are generally conducted by placing the medium and the contaminated solution in septum-capped vials which are put in rotation for a short period (about one week or less).

The batch test consists in putting each of the potential reactive media in contact with the contaminated solution inside cylindrical containers (one for each sampling instant), which are subsequently placed under agitation by means of a rotary agitator (Fig. 1.14). At certain time intervals (e.g. 2, 4, 6, 8, 12, 24, 48, 72 and 96 h), one of the reactors is taken for each reactive medium, and the variation over time of the concentration of pollutants in order to obtain the kinetic constant of the reaction and therefore obtain information on the speed with which the removal of the contaminant takes place. A comparison between the values of the kinetic constants determined for the different reactive materials allows to choose the most suitable ones. The kinetic constant determined with these tests is not clearly representative of the conditions that will occur in situ as the stirring process inevitably alters some relevant processes in the real system, which can only be simulated by column interaction tests (Moraci et al., 2015).

Figure 1.14 Batch test apparatus.

Contrary to batch tests column ones can simulate the reactive medium behaviour under flow conditions. A column test is generally conducted using a column with multiple sampling ports along its length. The column is packed with the reactive medium and water is circulated in the column from bottom to top. Sampling ports are constituted of syringe needles permanently inserted into the column, with the tip at the centre of the column and allow to withdraw solution samples (Moraci et al., 2015).

1.5.7 Installation techniques

There are a variety of PRB installation techniques that have been successfully used. For shallow installations, the simplest installation technique involves opening a trench with traditional excavation equipment and placing reactive media and sand mixtures directly into the open trench. Figure 1.15 shows this technique.

When deeper placement is required (>6 to 9 m) and trench side wall collapse is a risk,

Figure 1.15 Excavation of a trench for the PRB installation.

trench boxes can be used for stability. Depending on budget, a single pass trencher can also be utilized to construct PRBs.

In permeable aquifers, groundwater control during trenching must also be considered. A common approach to prevent trench side wall collapse and to address inflowing contaminated groundwater is using biopolymer slurries. During excavation, biopolymer slurry is added to maintain the aquifer water level (thus preventing any difference in hydrostatic pressure), and when the target excavation depth is reached, reactive media is injected at the bottom of the trench thereby displacing the biopolymer slurry. For example, for the installation of the PRB in Turin, guar gum slurry was used to support the excavation that was performed using a crawler crane equipped with a hydraulic grab (Fig. 1.16). The trench was backfilled with iron and the biopolymer degraded using enzymes.

Some work sites can be more challenging for PRB installation. These locations include sites with deep plumes (>9 m), aquifers with heaving sands, or sites where the

location of above ground buildings or property lines prevent the mobilization of heavy excavating equipment. In these situations, an approach commonly used is PRB installation by high pressure ZVI slurry injection using small diameter injection rods and direct push drill rigs. ZVI slurry injections can also be completed using fracture emplacement technology.

Other PRB emplacement technologies include soil mixing equipment using mixing tools connected to excavator arms and direct placement through large diameter augers.

Figure 1.16 Crawler crane equipped and Hydraulic grab used in the excavation of a PRB in Avigliana and Buttigliera Alta (TO), 2004.

1.6 Zero valent iron

As already mentioned, the most used reactive medium in installed PRBs is the Zero Valent Iron. Zero-valent (or elemental/native) iron (Fe^0) can be found under some specific environmental and geological conditions (e.g., in some mafic and ultramafic

rocks and in meteorites). It is, however, rarely formed at the Earth's surface due to the high reactivity of elemental iron. In fact, Fe is found in the environment dominantly in two valence states the relatively water-soluble Fe(II) (ferrous iron) and the highly water-insoluble Fe(III) (ferric iron) (Cundy et al., 2008).
The ZVI used for PRB applications is recycled scrap iron coming from the manufacture of automotive parts (e.g., engine motors, brake drums, etc.). Another rare source of ZVI is molten iron, which is then granulated with high-pressure water jets. The granulated iron is sieved to a specified grain size (ITRC, 2011).
ZVI used in PRB applications should have a high fraction of iron metal (> 90%), low carbon content (< 3%), and non-hazardous levels of leachable trace metal impurities. It must be free of any surface coatings (oils or grease) that may inhibit its reactivity. The surface area of ZVI particles is particularly important because reactions occur at the iron/water interface. Reaction rates increase as the surface area of the ZVI particles increases. For PRBs constructed using excavation-based methods, the grain size range typically used is 2.0–0.25 mm, which provides an average hydraulic conductivity of about 10^{-2} cm/sec. Typically, the surface area of this coarse ZVI has a range of 0.5–1.5 m^2/g.
In recent years, the interest to emplace finer-grained fractions of 1.0 mm or less (microscale ZVI) and nanoscale iron particles using injection-based techniques is growing. Thanks to the higher surface area, nanoscale iron particles have a high reactivity but short life. They are best suited to remediation of source zones, where they can degrade a large quantity of contaminant, especially volatile organic compounds (VOCs), in a short period of time (ITRC, 2011). Microscale and nanoscale iron particles can be dispersed in a viscous suspension and injected directly into the ground at the source of contamination (Tosco et al., 2014).
Zero-valent iron (ZVI) has been used successfully to remediate groundwater contaminated by chlorinated organics) and metals (Benner et al., 2002; Blowes et al., 2000; Cantrell et al., 1995) contamination through PRB. Fe^0 used in filtration systems or Fe beds have also been proven efficient for safe drinking water provision at household level (Noubactep, 2010).

1.6.1 Typologies of ZVI

Over the past few years, ZVI nanoparticles (nZVI) have attracted extensive attention due to their high reduction potential and large specific surface area. nZVI can be directly used in wastewater treatment plants (Wang et a., 2020) or can be injected

into the subsurface for groundwater remediation (Galdames et al., 2020). In certain applications, due to the small particle size and magnetic property, these nanoparticles can easily aggregate together reducing treatment efficiency. In order to improve the dispersibility of nZVI and prolong its reactivity different approaches were proposed: i) synthesis of bimetallic nanoparticles (Fig. 1.17a) such as nZVI/Cu, nZVI/Al and nZVI/Ni tested for Cr^{6+} and Cu^{2+} removal (He et al. 2020; Ou et al., 2020); ii) coupling nZVI with a supported material (Fig. 1.17b) (Ulah et al., 2020; Qian et al., 2019), biochar is effective for Pb^{2+} (Li et al., 2020) and Cr^{6+} (Liu et al. 2020), zeolite for Cd^{2+} (Tasharrofi et al., 2020) and vermiculite for Cr^{6+} (Zhao et al., 2019). The last approach iii) is coupling nZVI with SRB: in these systems the four main ways of removing heavy metals such as Cu^{2+}, Cr^{6+}, Zn^{2+}, Pb^{2+}, and Ni^{2+} include reductive precipitation, sulfide precipitation, co-precipitation and biosorption (Dong et al., 2019).

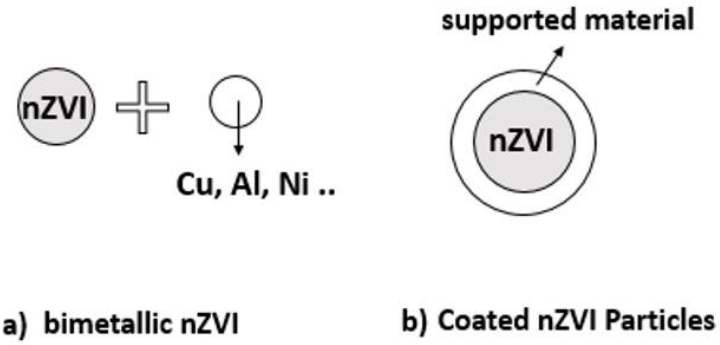

Figure 1.17 Combination of a) nZVI with nanoparticles and b) nZVI coupling with supported materials.

1.6.2 ZVI removal mechanisms

Regarding heavy metals, the possible removal mechanisms activated by ZVI depend on the type of metal to be removed and are (a) redox reactions and the processes of (b) precipitation, (c) co-precipitation, (d) adsorption and (e) size exclusion (Bilardi et al., 2020).

A redox reaction is a spontaneous electrochemical process that involves the reduction of a more electropositive species by a more electronegative metal (i.e., ZVI). The reduction process can involve direct reduction at the surface of ZVI or indirect reduction by secondary reductants – for example, aqueous Fe(II), adsorbed or structural Fe(II) and molecular (H_2) or atomic (H) hydrogen (Noubactep, 2010; Noubactep et al., 2006; Noubactep and Schöner, 2009). Direct reduction is possible when the standard redox potential of the metal ion is higher than that of ZVI

($E_0\ Fe^0/Fe^{2+} = -0.44$). According to different studies (Noubactep, 2008), if any quantitative contaminant reduction occurs in the presence of ZVI, it takes place within the matrix of corrosion products and is not necessarily a direct reduction. In fact, according to these studies, when immersed in water, ZVI is inevitably coated by an iron oxide layer. Therefore, the process of direct reduction is possible only when this layer is conductive and allows electron transfer (Noubactep, 2013).

Regarding the other removal processes, precipitation occurs as the pH of the water flowing through ZVI substantially increases, favouring the precipitation of metal hydroxides. Adsorption occurs onto the iron corrosion products; in fact, freshly precipitated, amorphous iron oxyhydroxides are known to be particularly effective adsorbents towards a range of contaminants due to their high (reactive) specific surface area (Cundy et al., 2008). Co-precipitation is a mechanism in which corrosion products, during precipitation, may entrap adsorbed contaminants in their mass (Crawford et al., 1993; Noubactep, 2010; Sridharan and Lee, 1972). Finally, the size-exclusion process concerns the formation of in situ-generated iron oxides which reduce the pore volume (PV) of the reactive medium and behave as a reactive filter in which contaminant removal occurs by self-filtration (Caré et al., 2013; Noubactep, 2013).

1.6.3 Longevity of ZVI

The main limitation of the use of ZVI in a PRB is the long-term preservation of its hydraulic and removal properties. The loss of reactivity of a PRB composed of pure ZVI alone can be attributed to the reduction of its reactive surface area, due to mineral precipitates which can cover active redox sites or cause a declining rate of electron transfer (Bilardi et al., 2013a), or to the reduction of ZVI capacity to generate new iron corrosion products which are possible adsorbent sites. Together with reactivity loss, as mentioned earlier, a possible operational problem of a ZVI PRB is the reduction of its hydraulic conductivity due to the clogging of the barrier pores. This phenomenon can be caused by precipitation of secondary minerals (e.g. calcium carbonate ($CaCO_3$), iron (II) carbonate ($FeCO_3$)) (Li et al., 2006, 2005) and of iron corrosion products (e.g. goethite (FeOOH), iron (III) oxide (Fe_2O_3), iron (II,III) oxide (Fe_3O_4)), by the accumulation of gas (e.g. hydrogen gas) (Henderson and Demond, 2007; 2011; Moraci et al., 2016a; Zhang and Gillham, 2005) and by the formation of a biofilm (when microbial activity is present). Iron corrosion products have an

expansive nature, which means that the iron oxides generated by iron corrosion are larger in volume than the original metal (Noubactep et al., 2010) and therefore contribute to reducing the initial void ratio of the filter. The potential causes of permeability reduction in the absence of biological activity and the main removal mechanism are shown in Figure 1.18.

To ensure the correct hydraulic behaviour of the barrier, at least in the short term, it should be designed to absolve the function of filter towards the soil constituting the aquifer. Its function is to prevent the migration of the fine particles of the base soil (the aquifer) and to avoid the development of high internal pore pressure inside the filter (at the soil–filter interface), which can affect the draining capacity of the barrier (Bilardi et al., 2013b; Moraci et al., 2017, 2016b). A possible solution, to limit not only ZVI reactivity loss, but also the reduction of its hydraulic conductivity in the long term, is mixing ZVI with other porous, non-expansive, inert and/or reactive granular materials in various weight or volume ratios (Bilardi et al., 2013a; Moraci et al., 2011; Moraci and Calabrò, 2010). The factors to be considered during the selection of a reactive material to be used alone or in granular mixtures with ZVI are the ability to preserve its own hydraulic conductivity and reactivity (e.g., to be highly adsorbent) over time, its commercial availability and its convenience (the use of an admixing agent allows reducing the amount of the relatively expensive ZVI required). Thus, research on cheap materials such as natural and waste materials to be used alone or in a mixture with ZVI has recently received a substantial amount of attention (Bilardi et al., 2020; Holmes et al., 2017; Khan et al., 2004; Moraci and Calabrò, 2010; Obiri-Nyarko et al., 2014; Wantanaphong et al., 2005). Moraci et al. (2015) and Madaffari et al. (2017) concluded that both pumice and lapillus are suitable admixing agents for ZVI for PRB applications. In particular, pumice and lapillus allow preservation of the hydraulic conductivity since ZVI particles are more dispersed per unit volume and the medium is less subject to clogging (Bilardi et al., 2020).

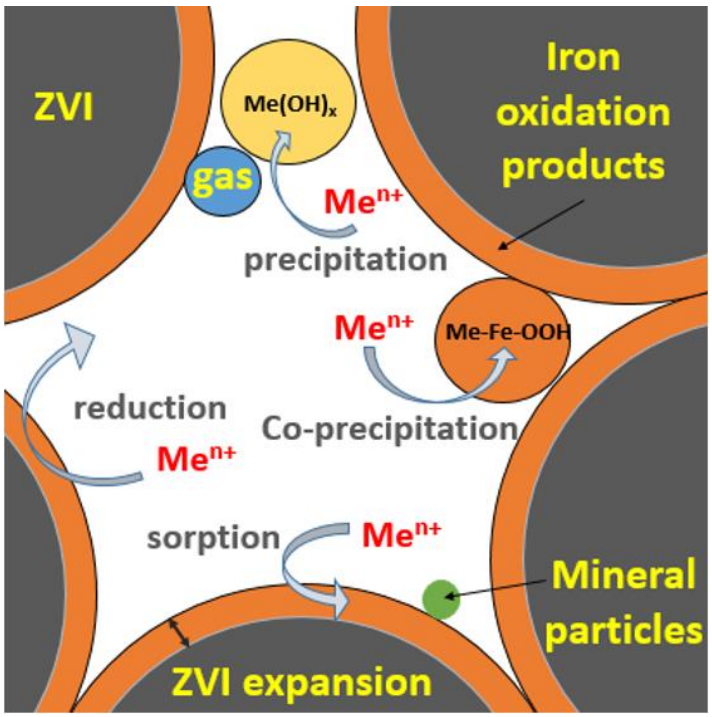

Figure 1.18 Schematic diagram of removal of heavy metals and metalloids by zero valent iron (ZVI) and of the causes of reduction in permeability (Calabrò et al., 2021).

2 MATERIALS AND METHODS

2.1 Introduction

In this chapter, the materials and methods used in the experimental activity will be described. The materials tested are Lapillus and ZVI. They have been characterized to know their physic-chemical and geotechnical properties. The materials have been observed using a scanning electronic microscope (SEM) to observe their shape and surface to obtain useful information for understanding the removal mechanisms and the processes leading to the reduction of hydraulic conductivity. The apparatus used to test the reactive and hydraulic behaviour of the granular mixtures composed of ZVI and lapillus has been described with the reagents used to prepare the synthetic contaminated solutions and the instruments necessary to evaluate the hydraulic and reactive performance of the granular mixtures.

2.2 ZVI

The Zero Valent Iron used is of the FERBLAST RI 850/3.5 type, distributed by Pometon S.p.A., Mestre, Italy. The material is made of iron (>99.74%) and the impurities include Mn (0.26%), O, S and C. (Bilardi et al., 2013). ZVI has been characterized by grain size analysis. Its grain size distribution is shown in Figure 2.1. The mean grain size (d_{50}) is about 0.5 mm and the coefficient of uniformity (U) is 2.

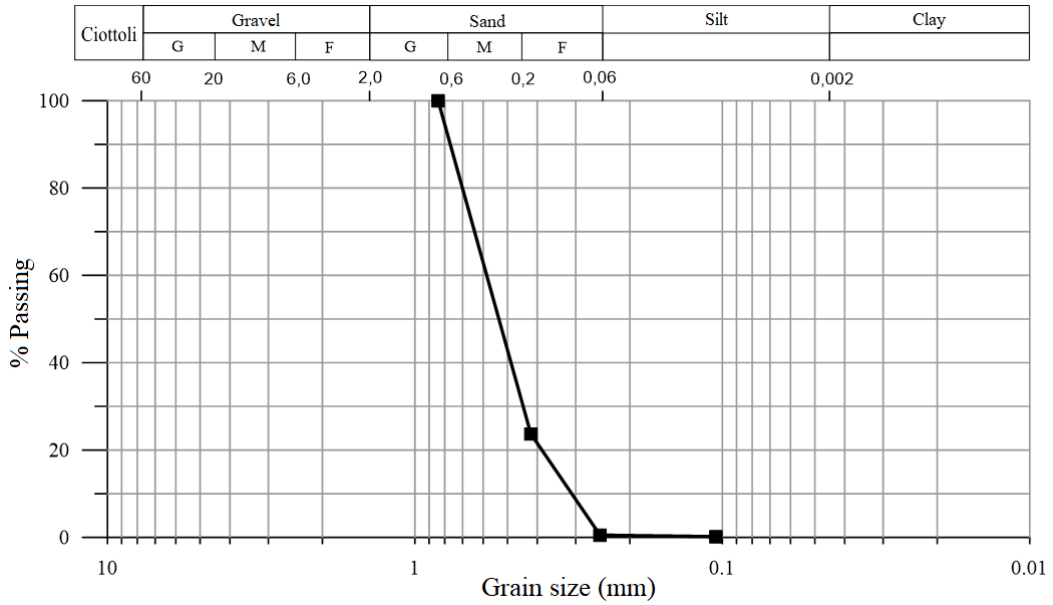

Figure 2.1 Grain size distribution of ZVI.

The used ZVI microstructure was observed using Scanning Electron Microscopy (SEM) (Fig. 2.2). ZVI samples (Fig. 2.3) were prepared for SEM observation placing them on an appropriate support and fixing them on using silver varnish. Afterwards, they were conserved under vacuum conditions. Only before placing them into the instrument a plasma using a source of Gold-Palladium (Au-Pd) was used to put some atoms on the surface of the sample to create on the surface a layer capable of conducting the electrons for a clear observation. SEM image highlights the surface of the iron free of impurities.

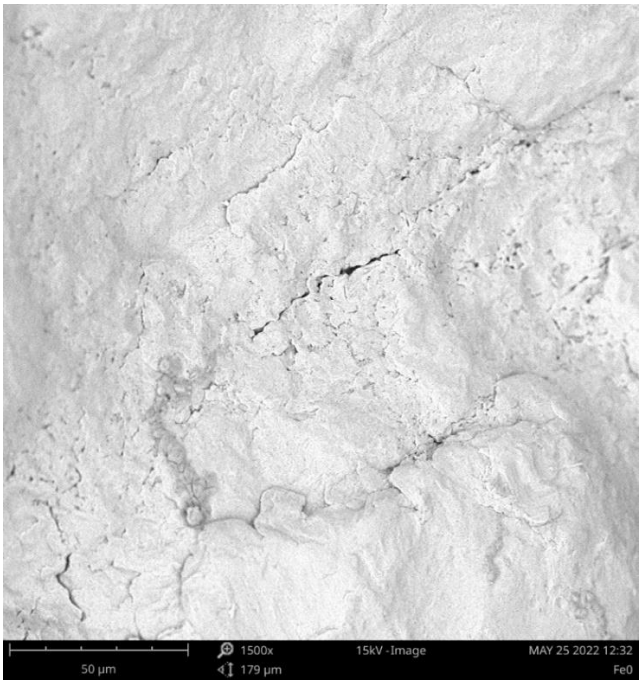

Figure 2.2 SEM image of a ZVI grain.

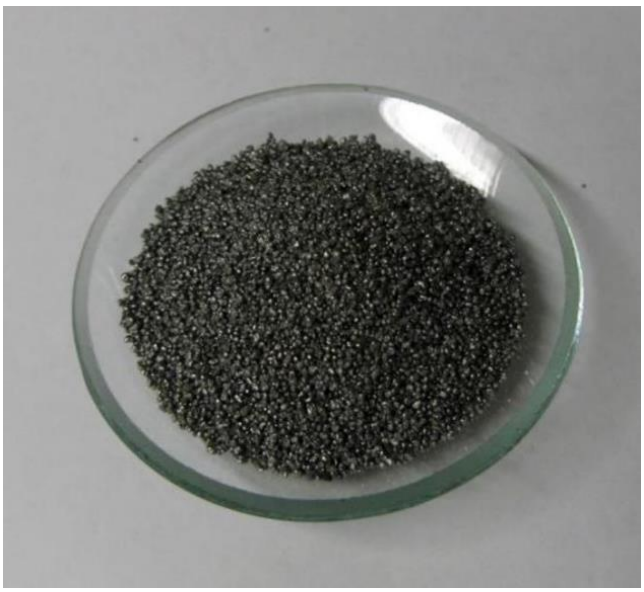

Figure 2.3 ZVI sample

2.3 Lapillus

Lapillus is a sedimentary pyroclastic material. Sedimentary rocks result from consolidation of loose materials which were created from erosion and alteration of pre-existing rocks. Pyroclastic rocks are a particular group of sedimentary rocks and are formed after volcanic products deposition in conjunction with explosive eruptions (Scesi et al., 1997). The used lapillus is a natural material distributed by SEM "Società Estrattiva Monterosi s.r.l.", Viterbo, Italy. It has granular form and a red-maroon colour (Fig. 2.4) and originated from explosive volcanic activity of the Sabatini Mountains.

Figure 2.4. Lapillus sample

It was observed with Scanning Electron Microscopy (SEM) that the lapillus was characterized by an irregular and rough surface and non-homogeneous porosity (Fig. 2.5). Moreover, the shape of the lapillus particles was highly variable.

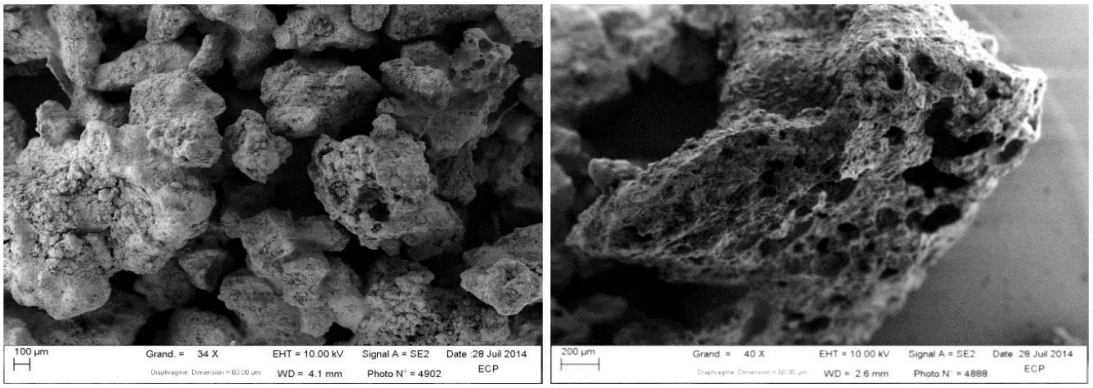

Figure 2.5 SEM pictures of Lapillus samples using an enlargement of a) 34 X and b) 40 k X

In Table 2.1 the chemical composition provided by the Società Estrattiva Monterosi is shown. Other compounds as MnO, Na_2O are present in traces, while $CaCO_2$ is absent.

Table 2.1 Lapillus chemical composition provided by SEM s.r.l..

Lapillus mineralogical composition (gr/100 gr)	
SiO_2	47
Al_2O_3	15
Fe_2O_3, FeO	7-8
MgO	5.5
CaO	11
K_2O	8
$CaCO_2$	absent
Na_2O	1
MnO	0.15

The grain size distribution of Lapillus as received is reported in Figure 2.6. The uniformity coefficient U (d_{60}/d_{10}) is equal to 10.4.

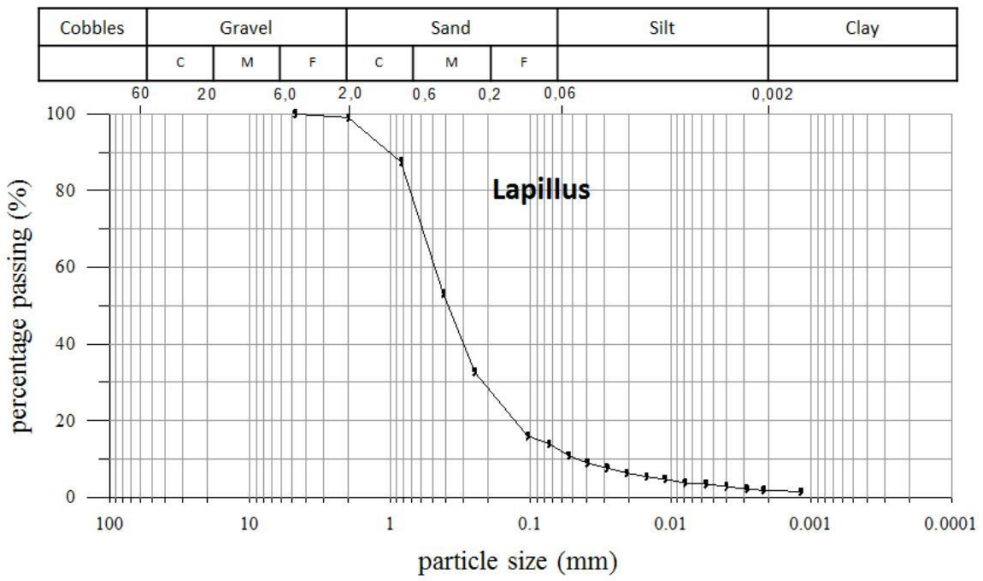

Figure 2.6 Lapillus grain size distribution (as used in column tests).

The grain size distribution of Lapillus samples used in column tests has been selected in function of that of zero valent iron and considering the internal stability filter design criteria (Moraci et al., 2012a). The Lapillus grains were washed, the retained grains on sieve No.40 (>0.42 mm) and the passing to the sieve No. 200 (<0.074 mm) were discarded to obtain a particle size distribution more similar to that of ZVI (Fig. 2.7). The coefficient of uniformity U is about 3.2 and the mean grain size (d_{50}) is approximately 0.4 mm.

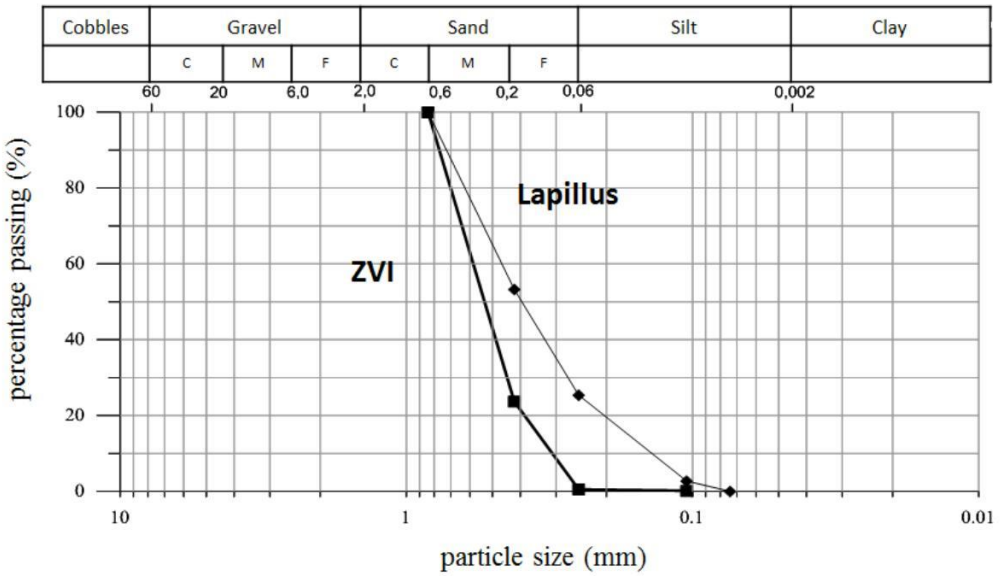

Figure 2.7 Lapillus and ZVI grain size distribution (as used in column tests).

2.4 Column test

The research activity has been developed through experimental tests at laboratory scale. Column tests can give information towards the design of a PRB and indications on how an in situ PRB will perform. Laboratory scale polymethyl methacrylate (Plexiglas) columns were used. Figure 2.8 shows the column apparatus. Columns have an internal diameter of 5 cm and height equal to 50 cm. Sampling ports are located at distance of 1.5, 3, 5, 8, 13, 18, 23, 28, 33, 38, 53.3 cm from inlet. The distance from inlet of the last sampling port (the effluent sampling port) is referred at 50 cm of reactive medium height.

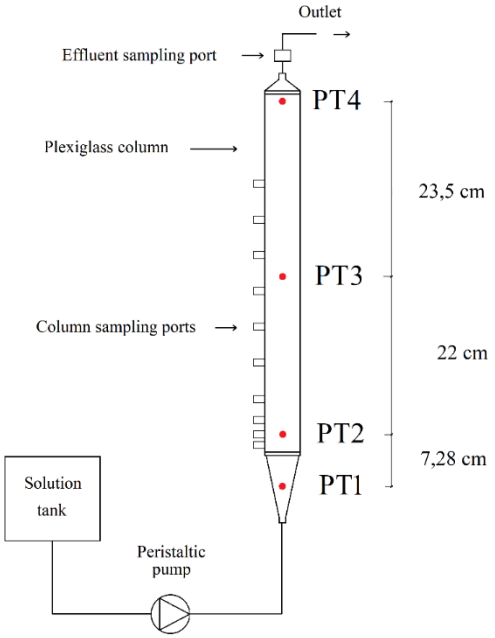

Figure 2.8 Schematic diagram of column test apparatus (PT = Pressure Transducer).

In each port a needle is inserted with the tip on the axis of the column. Sampling ports allow to determine changes in contaminant concentration and other parameters (e.g., pH) along the column length and at the outlet (Fig. 2.9).

Figure 2.9 Sampling ports.

Four pressure transducers are inserted along each column, the first located at the base of the column and the other three respectively at 3, 25 and 48.5 cm from the inlet section of the column (Fig. 2.8). The data detected by the transducers are collected through an automated system for saving the signals (Fig. 2.10); known the difference in pressure between two transducers, the permeability was calculated through Darcy's law. In particular, the difference of pressure between a first transducer located before the column inlet and a second one located at 3 cm from column inlet, allowed to determine the hydraulic conductivity of the first layer of the reactive medium. The difference of pressure between the second and the third pressure traducer, the latter located after 25 cm from column inlet, allowed to determine the hydraulic conductivity of the remaining part of the reactive medium.

Figure 2.10 Automated system for saving the signals from pressure transducers.

Column tests were conducted in up-flow mode. The contaminant solutions were pumped through the columns at a flow rate of 0,5 ml/min using multichannel peristaltic pumps (Fig. 2.11).

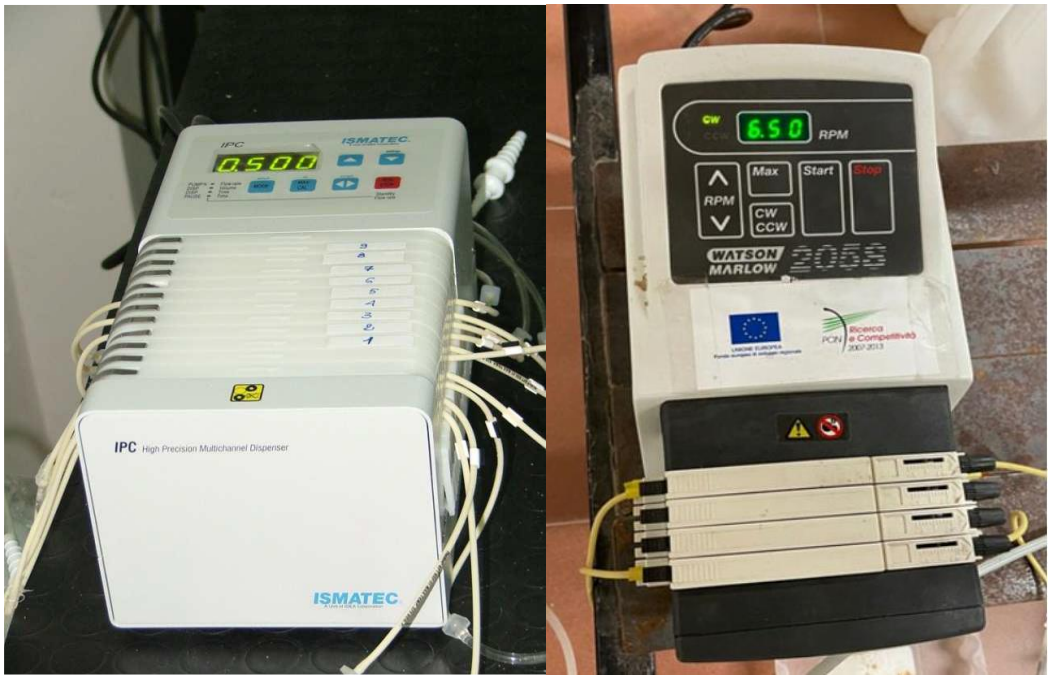

Figure 2.11 Peristaltic pumps: a) Ismatec IPC 12; b) Watson Marlow 205S.

To ensure that the column tests are sufficiently representative to be used to determine PRB design parameters, the physical, chemical and hydraulic conditions should be kept as similar as possible to those in situ. During column test design attention must be concentrated on the hydraulic conditions. The two main issues are possible channelling and wall effects associated with the use of column tests and the accurate reproduction of in situ hydrodynamic conditions. The prevention of channelling and wall effects ensures that a small column of reactive medium behaves similarly to an indefinitely large actual PRB and that the behaviour of the reactive medium is not influenced by the proximity of the column surface. According to Badruzzaman and Westerhoff 2005, these effects may be avoided if the ratio between the column diameter (D) and the mean particle size (d) is greater than 50. In the present research this ratio was about 150 for the ZVI/Lapillus mixture. Reproduction of hydrodynamic conditions is more complex in practice. According to relevant reports (Crittenden et al., 1991), the best way to comply with this criterion is to keep the experimental flow rates and Peclet numbers as similar as possible to the field values.

2.4.1 Inlet solution

The chemical composition of the synthetic solutions used for the 10 column tests, carried out in this thesis, is summarized in Table 2.2 and reported as follows. The contaminated solution of columns A, B, C, D and M (described in Chapter 3, 4 and 5) was prepared diluting Copper Nitrate (Copper(II) nitrate hydrate, purity > 99%; Sigma-Aldrich), Nickel Nitrate (Nickel(II) nitrate hexahydrate, purity > 99 %; Sigma-Aldrich) and Zinc Nitrate (Zinc(II) nitrate hexahydrate, purity > 99 %; Sigma-Aldrich) in distilled water in order to obtain a concentration of 18±1 mg/l for each metal.
The contaminated solution for columns E, F, G, H1 and H2 (see Chapters 4 and 6) also contain heavy metals with a concentration of 18 mg/l and various dissolved minerals such as $CaCO_3$ (10 mg/l) and $NaHCO_3$ (100 mg/l) as showed in Table 2.2.

Table 2.2 Composition of inlet solutions.

Column	Distilled water	Cu, Ni, Zn (18 mg/l)	Ni, Zn (18 mg/l)	$CaCO_3$ (10 mg/l)	$NaHCO_3$ (100 mg/l)
A	✓	✓	-	-	-
B	✓	✓	-	-	-
C	✓	✓	-	-	-
D	✓	✓	-	-	-
E	✓	✓	-	✓	-
F	✓	-	✓	-	✓
G	✓	-	✓	✓	✓
H_1	✓	-	-	✓	-
H_2	✓	✓	-	✓	
M	✓	✓		-	-

2.4.2 4.3.2 Specimen preparation

Lapillus and ZVI were mixed at a prefixed volumetric ratio (v.r.) and the column was filled in layers to obtain a specimen as homogenous as possible. The reactive medium is compacted by vibration with a rubber hammer hitting the upper base and sides of the column. The filling takes place through a tube that reaches the base of the column, and which is raised during filling.

2.5 ICP-OES

Atomic emission spectrometry inductively coupled to argon plasma with optical detector (ICP-OES: Inductively Coupled Plasma - Optical Emission Spectroscopy) is a technique used in order to find inorganic elements in various matrices and is currently one of the most used analytical methods for the determination of heavy metals at concentrations of the order of μg/l (e.g.: Cu, Zn, Pb, Al). This analytical technique is also widespread for the determination of macro elements such as Mg, Na K, S and Si at concentrations of the order of mg/l.

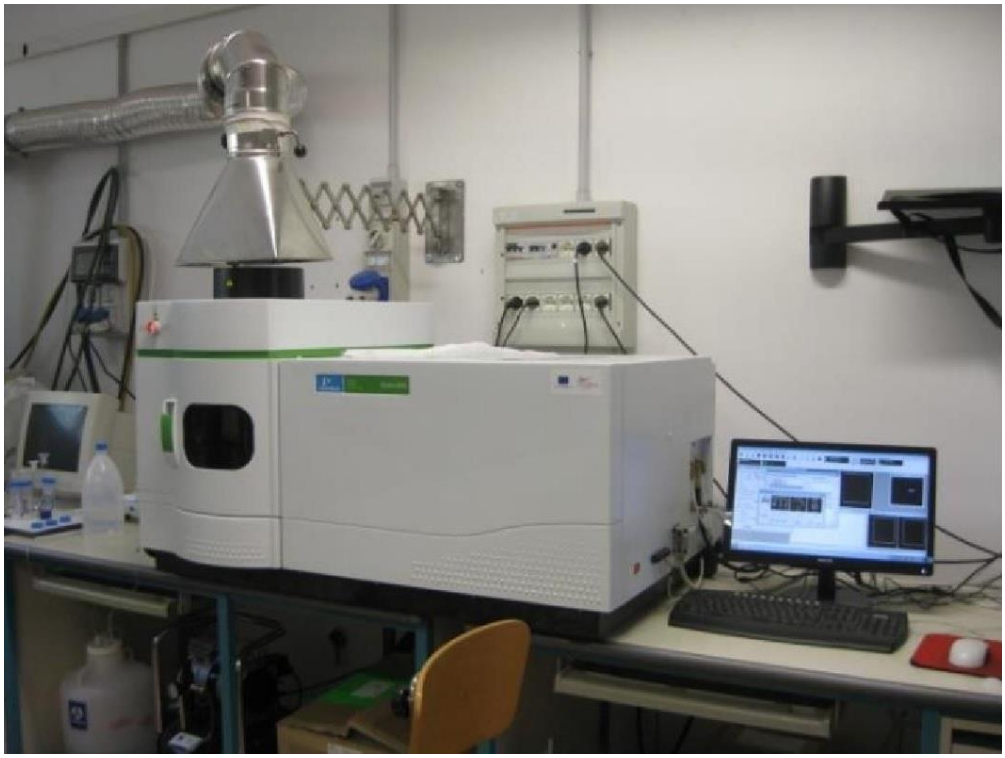

Figure 2.12 PerkinElmer Optima 8000 ICP-OES.

In inductively coupled plasma-optical emission spectrometry, the sample is transported into the instrument as a stream of liquid sample. Inside the instrument, the liquid is converted into an aerosol through a process known as nebulization. The sample aerosol is then transported to the plasma where is desolvated, vaporized, atomized, and excited and/or ionized by the plasma. The excited atoms and ions emit their characteristic radiation which is collected by a device that sorts the radiation by wavelength. The radiation is detected and turned into electronic signals that are

converted into concentration information. A representation of the ICP-OES is shown in Figure 2.12.
The instrumental system can be summarized as follows: auto-sampler for sampling, peristaltic pump for transporting the sample, nebulizer, ICP torch with argon plasma coupled to the radiofrequency generator, optical detector, software for acquisition, signal processing and integration, and software for the management of the instrumental system (Fig. 2.13).

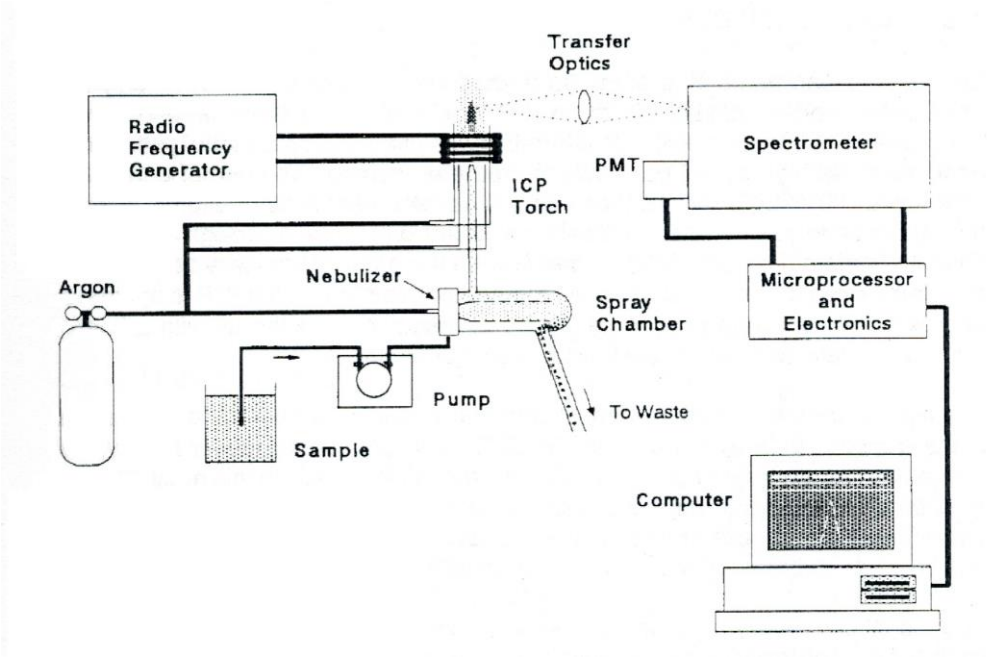

Figure 2.13 Major components and layout of a typical ICP-OES instrument

The standard solutions were prepared starting from a stock solution of 100 mg/l and diluted to obtain the concentrations necessary to construct the calibration line. The standard solutions prepared were equal to 0.5, 1 and 5 mg/l.
To carry out the analytical determination, the sample is taken automatically and transported to the pneumatic nebulizer via a peristaltic pump, the aerosol produced by the pneumatic or ultrasonic nebulizer passes through an expansion chamber and then reaches the plasma; here, following thermal excitation phenomena, the light emission spectrum is produced, composed of the characteristic lines of the elements present.

The quantitative determination of the analytes present in the sample takes place by comparing the intensity of the signals obtained on the sample, with respect to multi-element reference solutions of known concentration.

2.5.1 Aqueous sample preparation

The aqueous solution samples were taken in quantities of about 10 ml from each sampling port from top to bottom so as not to alter the flow of the column. The samples were stored in the refrigerator before conducting chemical analyses by ICP-OES.

Before the analyses they were centrifuged at 5000 rpm for 3 minutes and then diluted with distilled water to be able to fall within the measuring range of the instrument (Fig. 2.14).

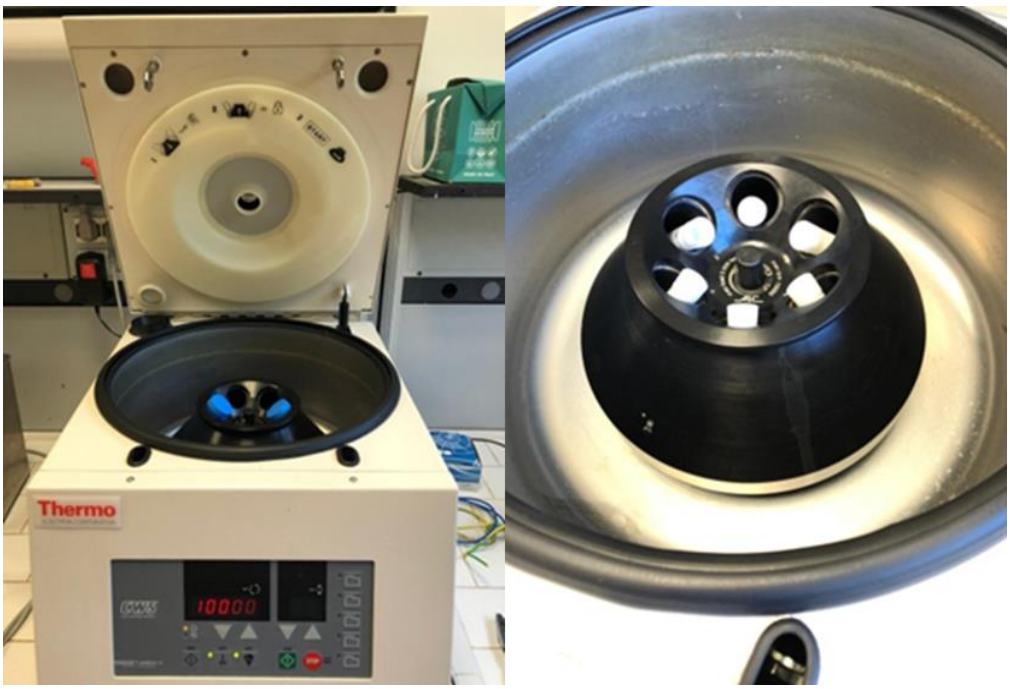

Figure 2.14 ALC-PK 121 centrifuge, internal with detail of the specimens.

3 EFFICIENCY OF MULTILAYERS PRB INFLUENCE OF THE PRE-TREATMENT ZONE IN PRBs

3.1 Introduction

In this chapter the study on the effectiveness of a multilayer configuration of a PRB has been addressed. This configuration has been studied with the objective to optimize the use of zero valent iron (ZVI) avoiding clogging phenomena due to iron corrosion.
After a panorama on the state of the art concerning the multi-PRB configuration, the results of three column tests have been analysed and discussed.

3.2 Multi-PRB: state of the art

(Singh et al., 2020) defined "multi-PRB" a sequence of two or more barriers composed of different reactive media or a single barrier composed of different layers, the latter configuration is also known as multi-layer PRBs (Lee et al., 2010; Pawluk et al., 2019; Pawluk and Fronczyk, 2015; Połoński et al., 2017; Xu et al., 2012; Ye et al., 2019). Both configurations were proposed to face a complex contamination by using different materials able to activate a removal mechanism specific for each contaminant.

Clogging phenomenon in a ZVI-PRB generally occurs at the inlet section of the barrier (ITRC, 2011; Phillips et al., 2010; Ullah et al., 2020b; Yang et al., 2016), to face this issue, a multi-layer configuration was proposed in literature and implemented in full scale PRB (Gavaskar et al., 2000; Li and Benson, 2010; Morrison, 2003). The multi-layer configuration consists of two layers with the first one containing ZVI mixed with an inert material (e.g., sand or gravel) and the second one composed of 100 % of ZVI. The first layer was called pre-treatment layer or "sacrificial pre-treatment zone" (Li and Benson, 2010) since its scope is to preserve the permeability of the reactive zone of the barrier.
An example of PRB with this configuration is at Monticello, UT, USA (Morrison, 2003) where a pre-treatment zone 0.6 m thick (13% of ZVI and 87% gravel) precedes a reactive zone, 1.2 m thick, composed of 100 % of ZVI and a third zone 0.6 m thick composed entirely of crushed gravel with the function of distribute the treated water to the aquifer. Field studies have documented the greatest loss of hydraulic conductivity within the centre of the 100-percent ZVI zone (Bartlett, 2005). Much of

the decrease was attributed to precipitation of calcium carbonate and other ZVI corrosion products (Li and Benson, 2010; Morrison, 2003).

Another site using a multi-layer PRB is at Dover Air Force Base, DE, USA where the pre-treatment zone (10% of ZVI and 90% coarse sand and 0.6 m thick) precedes the ZVI reactive zone. As in the Monticello site, the exit zone consists of 100 % coarse sand. The pre-treatment zone was installed with the aim to limit the entry of oxygen into the reactive zone and monitoring after 18 months has confirmed its reduction before entering the reactive cell. This indicates that incorporating a pre-treatment zone before the reactive cell may improve barrier longevity (Gavaskar et al., 2000).
(Li and Benson, 2010) numerically studied the efficiency of a pre-treatment zone by means of ground water flow model MODFLOW and reactive transport model RT3D. The aim of the pre-treatment layer is to create a zone where to promote secondary minerals formation due to pH and redox change before ground water enters the reactive zone. According to the results obtained by the authors, pre-treatment zones do not eliminate porosity reductions completely, as secondary minerals (e.g., $Fe(OH)_2$) still form within the reactive zone in response to iron corrosion.

The in-situ experiences described above and the modelling study revealed how a pre-treatment zone do not exclude the occurring of clogging phenomena. Therefore, a multi-layer configuration composed of granular mixtures characterized by a different degree of iron dispersion is investigated in this thesis. The logic of this configuration is to use a greater dispersion of the iron in the first layer of the barrier where the greater polluting load usually increases iron corrosion and therefore the risk of clogging phenomena (Bilardi et al., 2019). This zone should promote secondary minerals and iron corrosion products formation avoiding clogging phenomena and reduce the corrosion potential of the water entering the second layer. Whereas the minor dispersion of the ZVI in the second layer should assure greater longevity of the barrier in terms of reactivity, while ensuring the permeability necessary for groundwater flow.

3.3 Column test program

A schematic diagram of column test apparatus used to study the multilayer configuration is represented in Figure 3.1. The first multilayer configuration consists of a first layer of ZVI mixed with lapillus with a volumetric ratio (v.r.) 10:90 (called also “pre-treatment layer”), and a second layer consisting of the same ZVI/Lapillus

granular mixture in v.r. 20:80 (column B). The second multilayer configuration consists of a first layer consisting of a v.r. ZVI/Lapillus 5:95 and a second layer with v.r. ZVI/ Lapillus 20:80 (column C). The two configurations were compared with the traditional one consisting of a single layer, composed of a granular mixture ZVI/Lapillus v.r. 20:80 (Column A).

As previously described in chapter 2, the hydraulic behaviour was studied by means pressure transducers. The difference of pressure between the first and the second transducer allowed to determine the hydraulic conductivity of the first layer (or "pre-treatment layer) of the reactive medium. The difference of pressure between the second and the third pressure traducer allowed to determine the hydraulic conductivity of the remaining part of the reactive medium. The results of the three column tests were interpreted in terms of variation over time and along the thickness of the reactive medium both in the hydraulic conductivity and in the reactivity towards a multi-contaminated solution consisting of copper, nickel and zinc dissolved in distilled water.

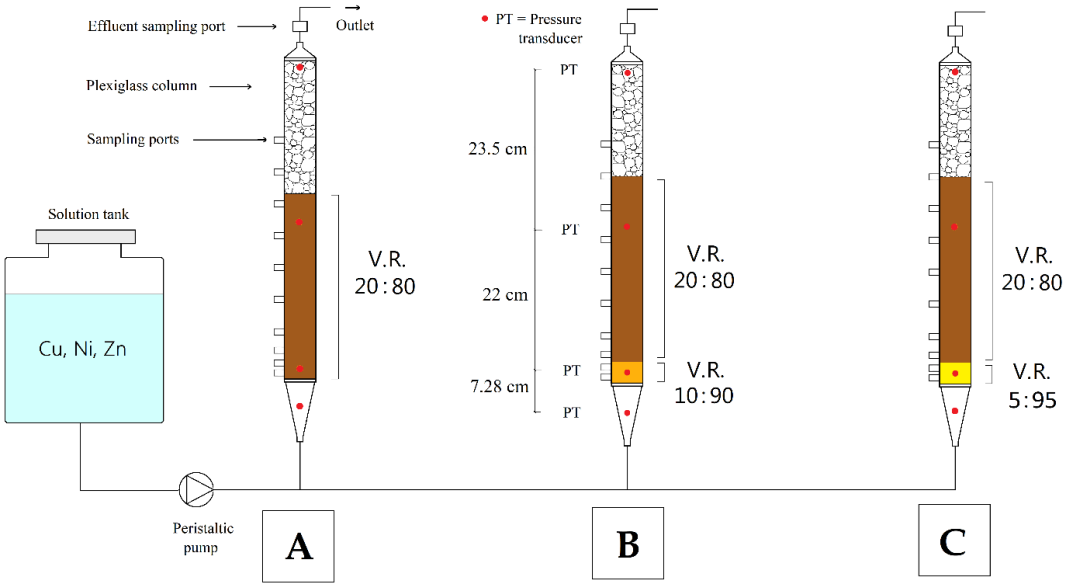

Figure 3.1 Schematic diagram of A, B and C column tests.

Table 3.1 summarizes the main characteristics of the three column tests. ZVI and lapillus were mixed at a fixed volumetric ratio.

Table 3.1 Main characteristics of column tests.

ID	A	B	C
Column fill thickness	0 - 4 cm	0 - 4 cm	0 - 4 cm
v.r. ZVI/lapillus	20:80	10:90	5:95
Column fill thickness	4 - 25 cm	4 - 28 cm	4 - 28 cm
v.r. ZVI/lapillus	20:80	20:80	20:80
Total thickness (cm)	25	28	28
Test duration (h)	3144	6360	7932
Initial porosity (%)	43.6	43.2	43.0

3.4 Results and discussion

The following paragraphs illustrate the data obtained from the three column tests in terms of reactivity and hydraulic behaviour and the results obtained from the SEM/EDX analyses.

3.4.1 Reactivity of columns A, B and C

Figure 3.2 shows the breakthrough curves (i.e., profile of the normalized concentration of the heavy metals over time) of the first 3 cm of the reactive medium thickness for the three column tests. The removal sequence Cu>Zn>Ni confirms the results observed in previous researchers (Bilardi et al., 2019, 2015). Examining copper removal (Fig. 3.2a) the time where the Italian regulatory limit (i.e., 1 mg/L) is exceeded is almost similar for columns B and C whereas it is never observed for column A, which had a shorter duration due to the excessive reduction in hydraulic conductivity. The breakthrough curves of nickel (Fig. 3.2b) and zinc (Fig. 3.2c) vary for the three columns and the greatest removal of the contaminant is observed as the iron content per unit volume increases. The complete exhaustion (i.e., $C(t)/C_0$ equal to 1) of the reactive medium towards copper has never been observed in the three columns where the removal efficiency was always greater than 70%. The complete exhaustion of the reactive medium in the first 3 cm of thickness towards nickel and zinc was instead observed only for column C.

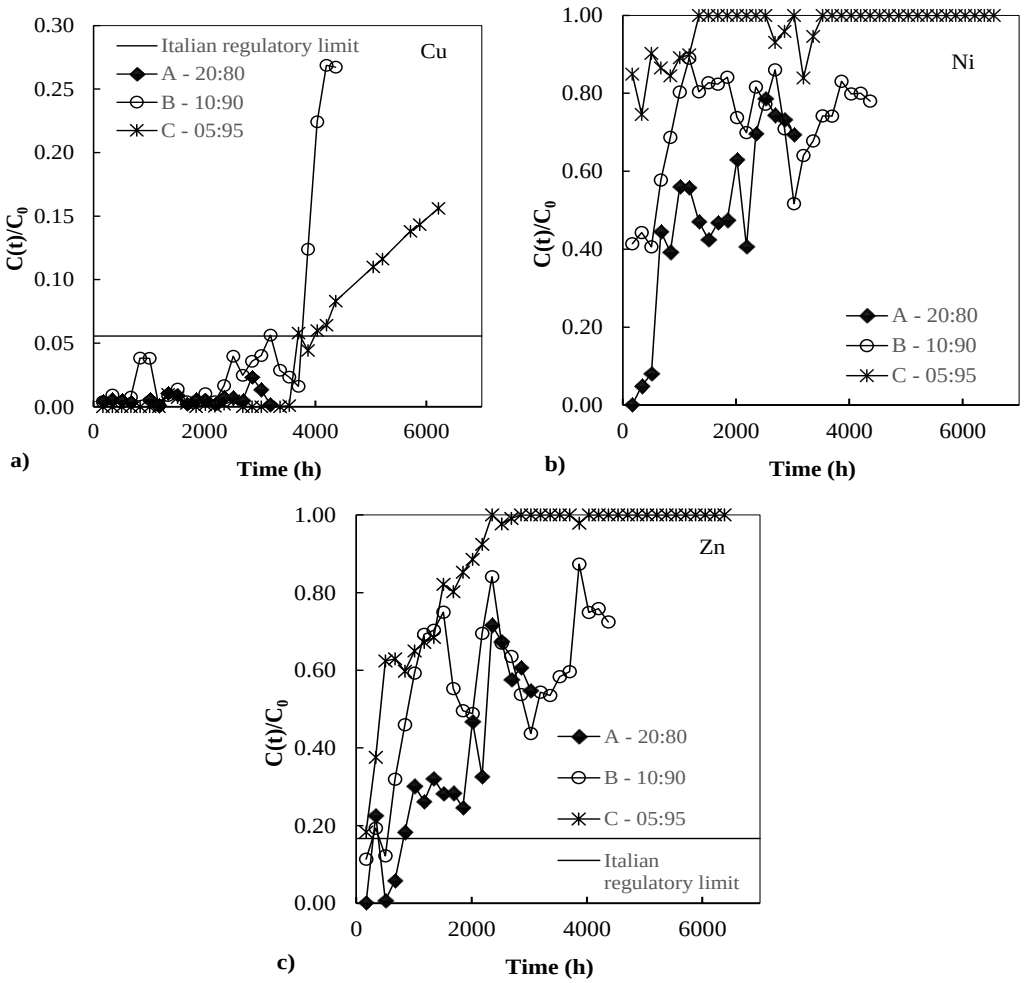

Figure 3.2 Breakthrough curves of a) copper b) nickel and c) zinc at the second sampling port (3 cm) of the reactive medium contained in columns A, B and C

Figure 3.3 shows the breakthrough curves for nickel and zinc at the sampling ports placed at a distance of 5, 8, 13, 18, 23 and 28 cm from the inlet section of column B. Considering Nickel removal (Fig. 3.3a), a thickness of almost 8 cm is necessary to remove the contaminant. The breakthrough time (i.e., the time where a rapid increase of the contaminant is observed) advances along the thickness of the reactive medium according to the process of exhaustion of the reactivity of the materials. The breakthrough time, which is the design parameter of a PRB (Bilardi et al., 2019), takes place simultaneously considering the sampling ports placed at 18, 23 and 28 cm from column inlet (Fig. 3.3a). This behaviour suggests the existence of an optimal thickness

of the barrier that in this case is 18 cm (Fig. 3.6a). The lower removal efficiency of the layers placed upstream from the inlet section could be attributed to the reduction of the reactivity of the iron particles even in the absence of contaminants as also observed in previous studies (Madaffari et al., 2017). Zinc is removed from solution better than nickel (Fig. 3.3b) and its concentration, after 26 weeks at 23 cm of thickness, is below the Italian regulatory limit (i.e., 3 mg/L). The breakthrough time observed at sampling ports located at 3, 5, 8, 13 and 18 cm linearly increases with the reactive medium thickness (Fig. 3.6b).

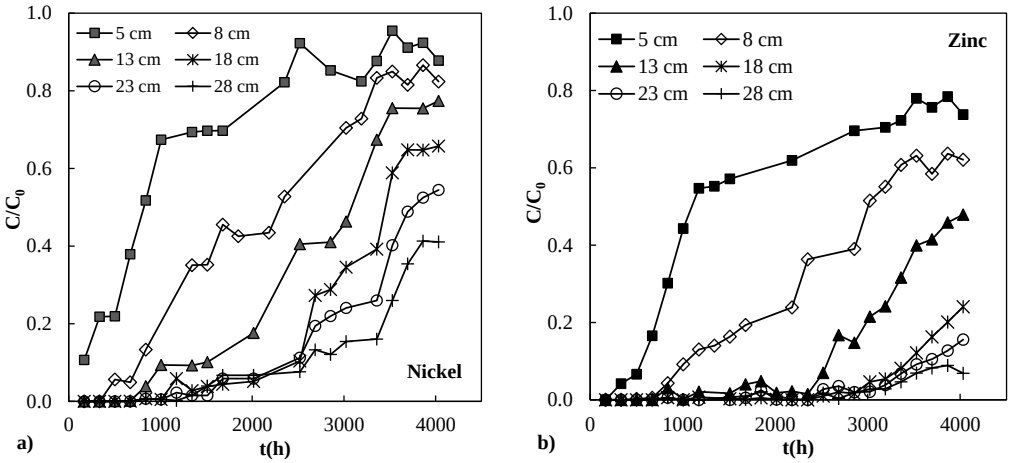

Figure 3.3 Breakthrough curves of a) nickel and b) zinc at the sampling ports placed at a distance of 5, 8, 13, 18, 23 and 28 cm from the inlet section of column B.

Figure 3.4 shows the breakthrough curves of nickel (Fig. 3.4a) and zinc (Fig. 3.4b) derived from column test C. The exhaustion of the reactive medium towards nickel removal (Fig. 3.4a), occurs in shorter times than in column A. This behaviour is linked to the lower iron content per unit volume present in the first 4 cm of the reactive medium thickness. This rapid depletion of the reactivity is highlighted by the proximity of the breakthrough curves which, for some thicknesses of the reactive medium, tend to overlap (e.g., sampling ports located at 13 and 18 cm or at those located at 23 and 28 cm from column inlet) as can be observed in Figure 3.6. The breakthrough curves referred to zinc (Fig. 3.4b) are more spaced and an optimal thickness of 23 cm can be identified (Fig. 3.6b).

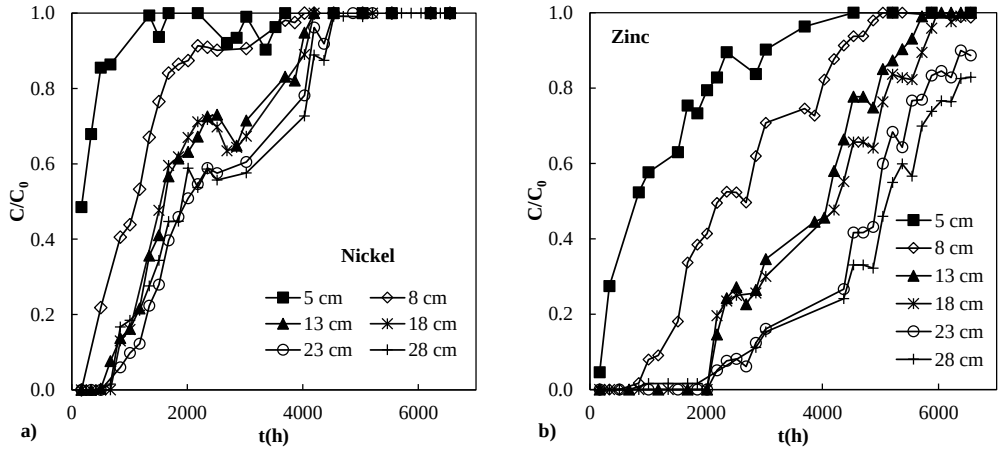

Figure 3.4 Breakthrough curves of a) nickel and b) zinc at the sampling ports placed at a distance of 5, 8, 13, 18, 23 and 28 cm from the inlet section of column C.

Figure 3.5 shows the breakthrough curves of nickel (Fig. 3.5a) and zinc (Fig. 3.5b) derived from column test A. Due to the higher iron content per volume unit, in the first 4 cm of barrier thickness, the breakthrough time for nickel (Fig. 3.5a) is observed starting from the 5 cm thickness of the reactive medium. As observed for columns A and C, neglecting the hydraulic behaviour, an optimal thickness of the reactive medium, in this case equal to 13 cm, can be identified (Fig. 3.6a). Regarding Zinc removal, its concentration, after 17 weeks at 23 cm of the reactive medium thickness, is below the Italian regulatory limit (i.e., 3 mg/L). The breakthrough time observed at sampling ports located at 3, 5, 8 and 13 cm linearly increases with the reactive medium thickness (Fig. 3.6b).

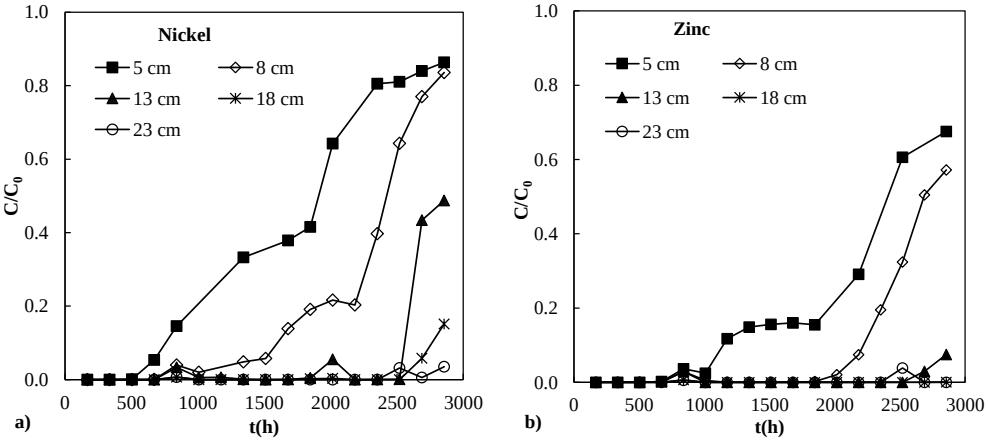

Figure 3.5 Breakthrough curves of a) nickel and b) zinc at the sampling ports placed at a distance of 5, 8, 13, 18 and 23 cm from the inlet section of column A.

From a comparison of the breakthrough time profile over the reactive medium thickness (Fig. 3.6) it emerges that the presence of the pre-treatment zone negatively affects nickel removal and do not allow increasing the barrier longevity. Indeed, column A would have required the substitution of the reactive medium due to the excessive permeability reduction, columns B and C would have required the substitution of the reactive medium due to a rapid depletion of the reactivity. On the contrary, regarding zinc and copper removal a pre-treatment zone can increase barrier longevity with a moderate increase of the barrier thickness.

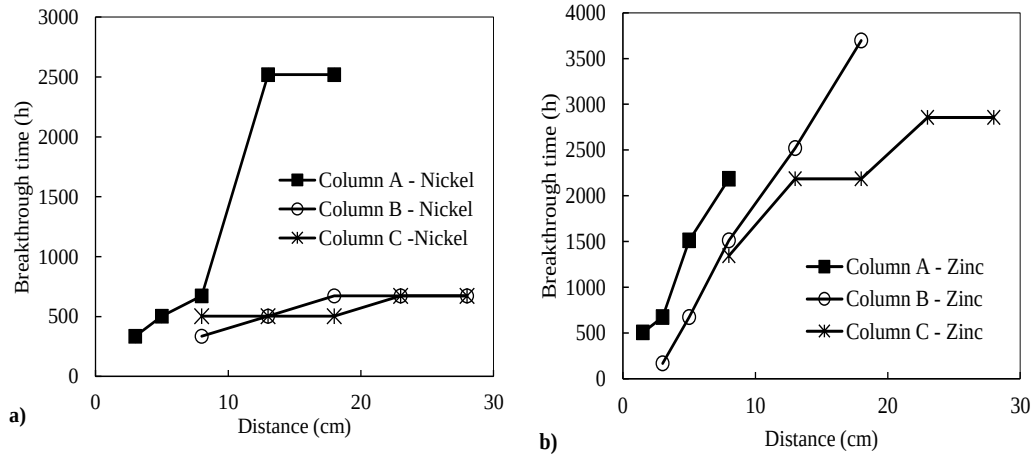

Figure 3.6 Breakthrough times (h) vs. column distance (cm) for a) nickel and b) zinc.

To show more clearly the influence of the pre-treatment zone on the reactive behaviour of a ZVI-based mixture, the results of the three columns were compared in Figures 3.7 and 3.8 for nickel and zinc at 18 and 23 cm of reactive medium thickness, respectively. Considering 18 cm of reactive medium thickness (Fig. 3.7a), a substantial difference between the reactive behaviour of column C with that of columns A and B towards nickel removal is observed. Although, this difference reduces passing from 18 to 23 cm of column length (Fig. 3.8a), it is possible to state that a content of iron < 20 % in volume in the first centimetres of the reactive medium can greatly influence the reactivity towards nickel. Regarding zinc, the reaching of the Italian regulatory limit at 18 cm of reactive medium thickness happens after 2000 and 3700 hours passing from test C to test B, respectively. This difference between the breakthrough times reduces considering 23 cm of column thickness (Fig. 3.7b and 3.8b). In particular, the limit is reached after 3000 hours for column test C and it is touched after 4000 hours for column test B. For column A, the limit was not reached in the investigated period (17 weeks). Therefore, in terms of zinc removal, the iron content in the first centimetres of reactive medium thickness seems to reduce its influence as the thickness of the reactive medium increases.

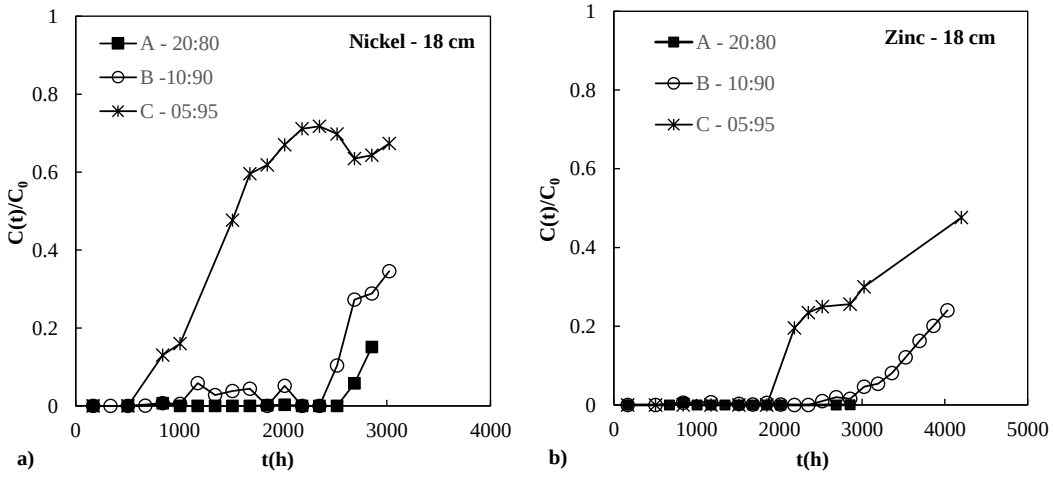

Figure 3.7 Breakthrough curves of a) nickel and b) zinc at 18 cm for columns A, B and C.

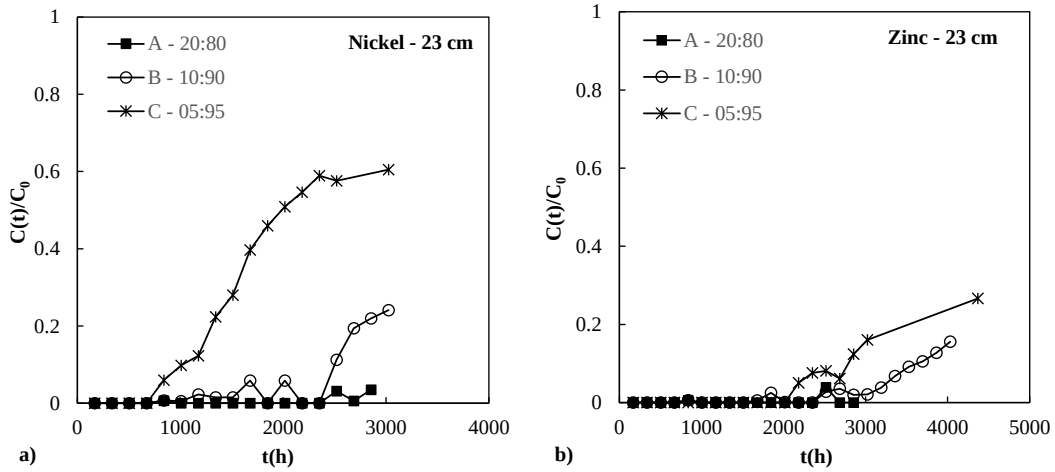

Figure 3.8 Breakthrough curves of a) nickel and b) zinc at 23 cm for columns A, B and C.

During column tests, measures of pH and E_h were conducted on the aqueous samples withdrawn from the sampling port located at the outlet. Figure 3.9 shows the profile of pH (Fig. 3.9a) and E_h (Fig. 3.9b) of the three columns over time (h). It can be observed that pH profile of columns A and B is very similar and it decreases over time, whereas pH is almost constant for column C. E_h profile shows the same trend observed for pH. pH increases and E_h decreases respect to the inlet solutions observed at the beginning of the tests are due to ZVI oxidation by constituents present in water, so it can be stated that this effect is more relevant as the iron mass increases.

In column C the pre-treatment zone influences the pH and E_h profile.

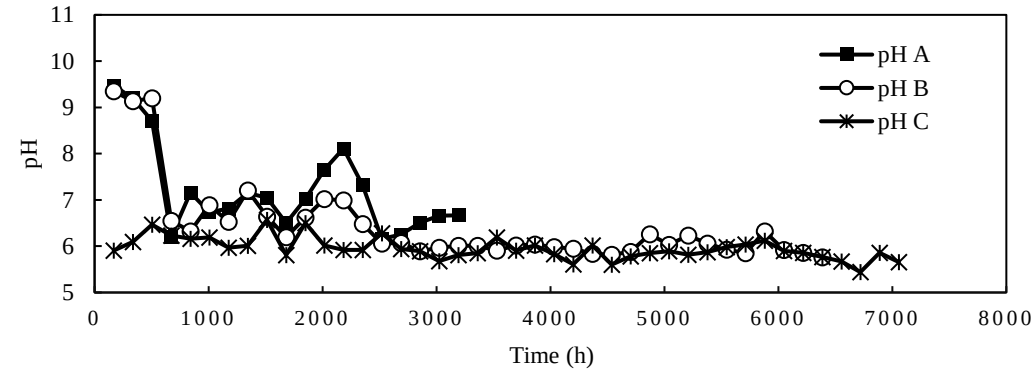

a

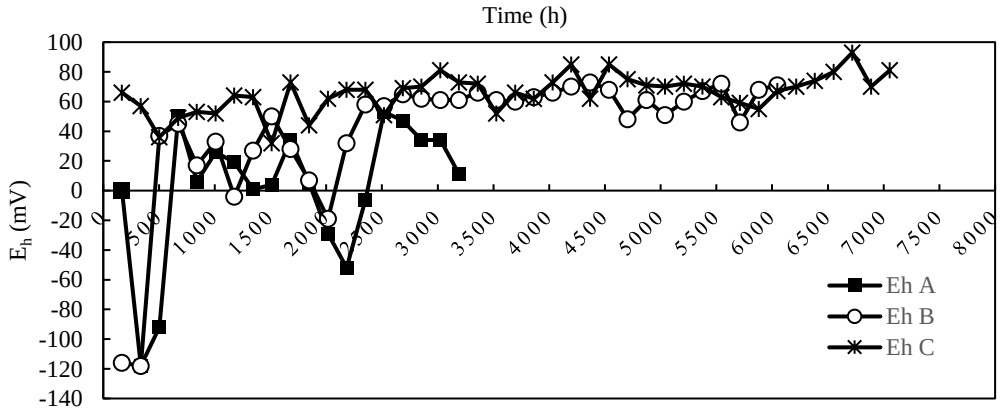

b

Figure 3.9 pH and E_h values vs. time (h) for column tests A, B and Cs.

3.4.2 Hydraulic conductivity of columns A, B and C

Figure 3.10 shows the hydraulic conductivity profile of the first (0-3 cm) and second layer (3-24 cm) of the three column tests. Considering the first layer (Fig. 3.10a) the hydraulic conductivity decreases after 200 and 1000 hours for columns A and B respectively whereas it is constant for column C until 3000 hours and subsequently a slight increase is observed. With reference to the second layer (Fig. 3.10b) the hydraulic conductivity decreases after 1600 hours for column A, slightly decreases after 4200 hours for column tests B, whereas remains constant for column test C. Following the reduction of the permeability of column A, a drastic reduction in the volume of water exiting the column was observed.

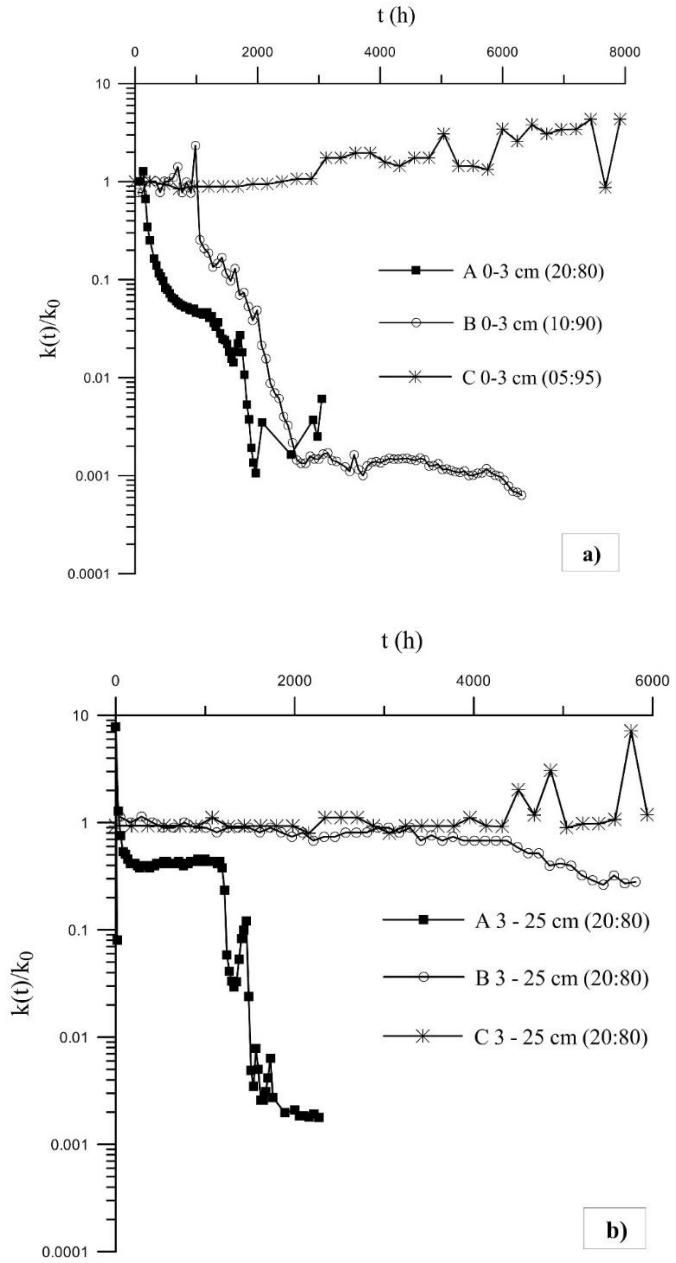

Figure 3.10 Hydraulic conductivity profile of a) the first (0-3 cm) and b) second (3-25 cm) layer of the reactive media contained in columns A, B and C.

As expected, column A is the one that showed the worst hydraulic behaviour indeed a quick and progressive reduction of the hydraulic conductivity starting from column inlet is observed. Therefore, considering the examined condition of flow rate and water composition, the iron content per unit volume is too high to assure the correct operation of the barrier.
The hydraulic conductivity profile of the first layer of column B is the same of the one observed in column A but translated for longer times due to the less iron content per unit volume. This strong similarity of the hydraulic conductivity profile of the first layer of columns B and A suggests a very precise kinetics of iron corrosion under the same boundary conditions (flow rate and water composition).

In column C, the corrosion process does not lead to the reactive medium clogging thanks to the greater dispersion of the iron particles in the first layer. Since the permeability in column C remains always constant, it is possible to hypothesize that a decline in reactivity corresponds to a lower formation of iron corrosion products (responsible for nickel and zinc removal) responsible for reducing the porosity of the medium. This statement can be confirmed observing the reactive behaviour of the "pre-treatment" zone (Fig. 3.2) towards Nickel and Zinc whose removal is mainly attributed to iron corrosion products.

Indeed, the formation of iron corrosion products that caused the permeability reduction observed in columns B and A is likely responsible of a residual removal of nickel and zinc (Fig. 3.2b and 3.2c). Vice versa, in column C where permeability is constant, the reactive medium after 2000 hours is completely exhausted towards nickel and zinc removal (Fig. 3.2b and 3.2c). In the light of these findings, heavy metal removal must take place before the formation of iron corrosion products can cause a considerable reduction in the hydraulic conductivity. The long duration of test C (at least 8 months) without any reduction in hydraulic conductivity suggests a strong slowdown in the corrosion process linked to the reduction of its reactivity.

Examining columns B and C it is possible to state that a "pre-treatment" layer can preserve the hydraulic conductivity of the subsequent layer. The different hydraulic behaviour of the second layer of the three column tests, which is in all cases the ZVI/lapillus mixture at the same volumetric ratio, is necessarily due the presence of the first layer or "pre-treatment" zone that changes the chemical composition of the water flow entering the second layer. As pointed out by (Hu et al., 2020) the solution chemistry influencing iron corrosion rate includes the presence of dissolved O_2

(probably consumed in the pre-treatment zone) and contaminants whose removal starts from this zone. Another important concept pointed out by the same authors (Hu et al., 2020) is that corrosion rate is not linear the non-linear nature of the corrosion kinetics implies a decrease in iron efficiency.
The fluctuations in permeability values over time with reference to the slight increase observed in the first layer of column C could be attributed to a probable gas venting.

3.4.3 SEM/EDX analysis of columns A, B and C

Figure 3.11 shows the images of columns A, B and C before disassembly, the presence of iron corrosion products can be clearly seen starting from the inlet section of the column. Some some areas of the mixture have a reddish or green color, corresponding respectively to iron oxide and copper oxide. Even the solution up to the area containing gravel is colored and the walls stained by a thin layer of oxides.

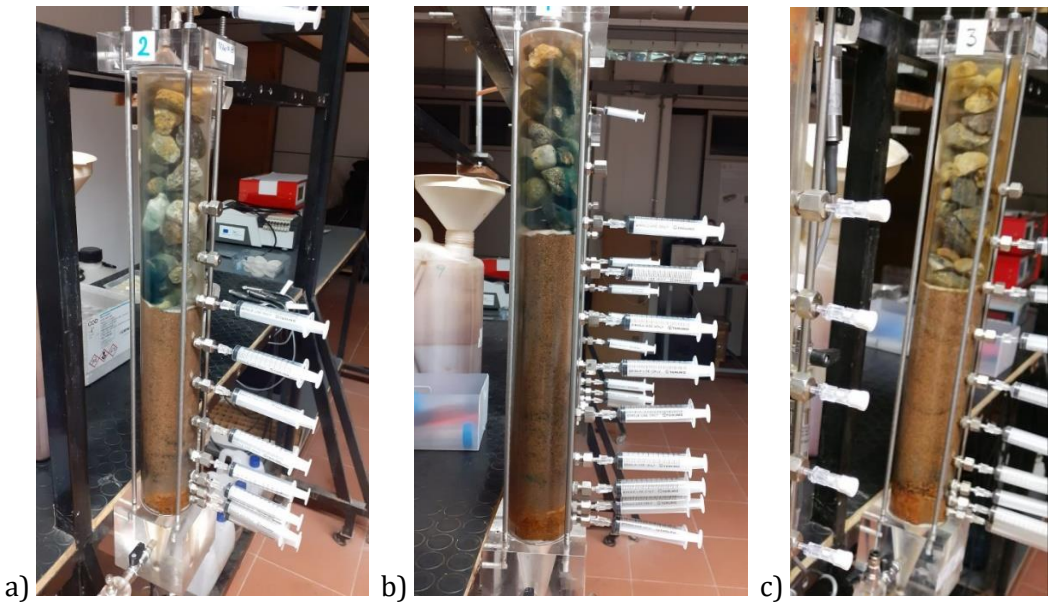

Figure 3.11 Images of a) column A, b) column B and c) column C before disassembly.

Figure 3.12 shows the material inside column A after disassembly (Fig. 3.12a) and a part of extracted material (Fig. 3.12b). Brown areas representing lapillus and grey areas representing iron, form Figure 3.12b it is clear the aggregation/cementation among particles.

a)  b) 

Figure 3.12 ZVI/lapillus mixture inside column A after disassembly (Fig. 3.10a) and after extraction (Fig. 3.10b).

SEM image of the reacted surface of the ZVI/lapillus granular mixture takes from the inlet of column A (Fig. 3.13a) revealed the presence of copper under two different shape. Trapezoidal copper crystals (point 1 of Fig. 3.13a) whose EDX analyses revealed the presence of 48.3 % of O, 45 % of Cu and 6.8 % of S (weight percent). The trapezoidal shape of deposited copper was revealed also by (Komnitsas, 2007). In Figure 3.13b copper can be found as bulbous formation. EDX analyses performed at point 2 revealed the presence of 94 % of Cu, 4.2 % of Fe and 1.9 % of O (weight percent).

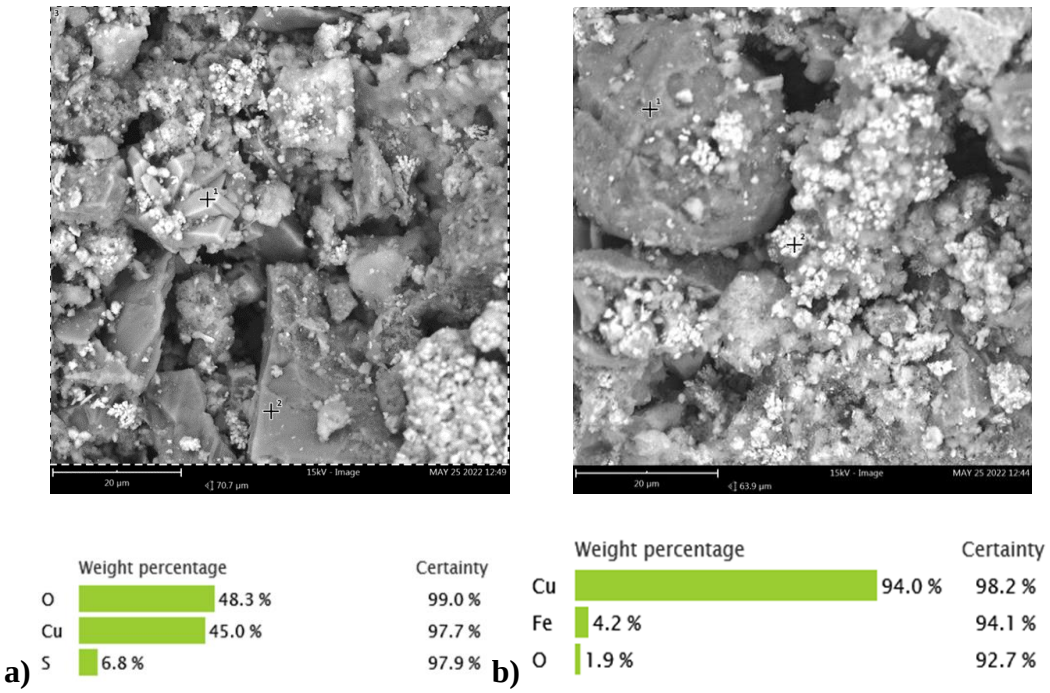

Figure 3.13 SEM images of ZVI/lapillus mixture taken from column A and EDX analysis (a) point 1 showing trapezoidal metallic copper and (b) point 2 showing a bulbous formation of copper.

Figure 3.14 shows the SEM images of the ZVI/lapillus granular mixture taken from column A (Fig. 3.14a) and column B (Fig. 3.14b). From EDX analyses performed on point 1 of both figures it is possible to suppose the presence of iron corrosion products having a spongeous nature. Furthermore Figure 3.14a shows the presence of zinc most likely incorporated within iron corrosion products.

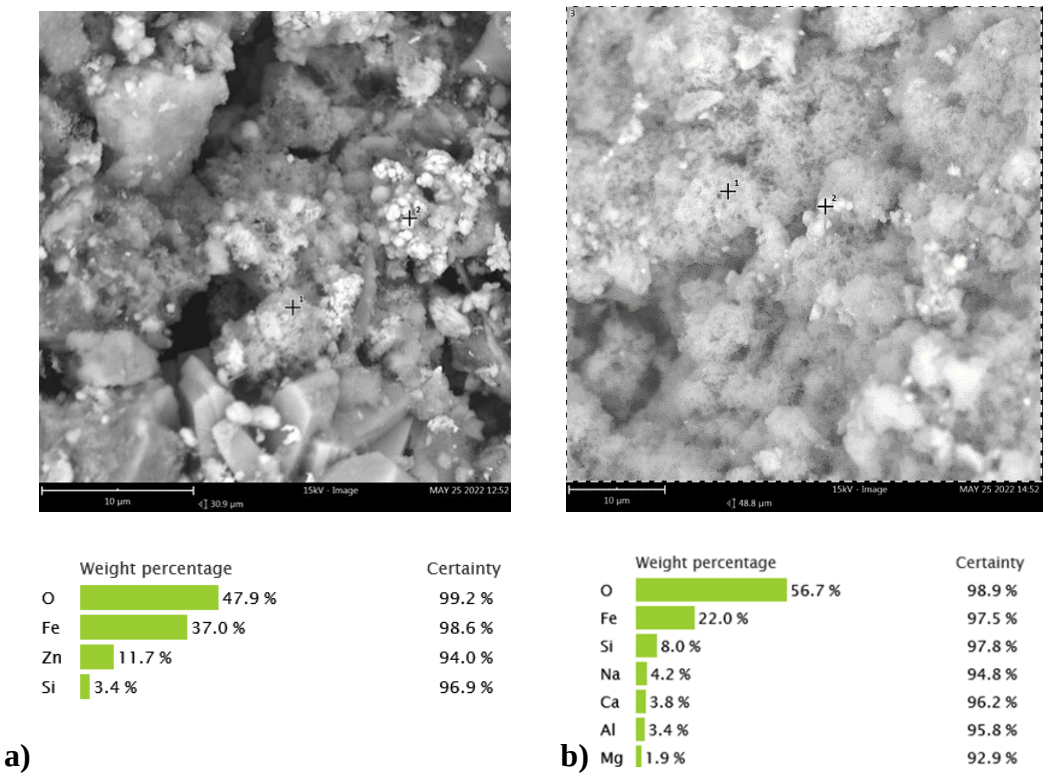

Figure 3.14 SEM images of ZVI/lapillus mixture taken from a) column A and b) column B showing the spongeous nature of iron corrosion products and EDX analyses on point 1.

Nickel was found mostly together with zinc, iron and oxygen as shown from SEM/EDX analyses of the granular mixture ZVI/lapillus taken from column B inlet (Fig. 3.15). Image depicted in Figure 3.15a suggests a spongeous nature of the precipitates whereas at higher magnification (Fig. 3.15b) is clear the presence of precipitates having a bulbous formation and containing copper, as shown previously, and a filamentous structure of precipitates containing Fe, O, Zn, Ni and Cu.

a)

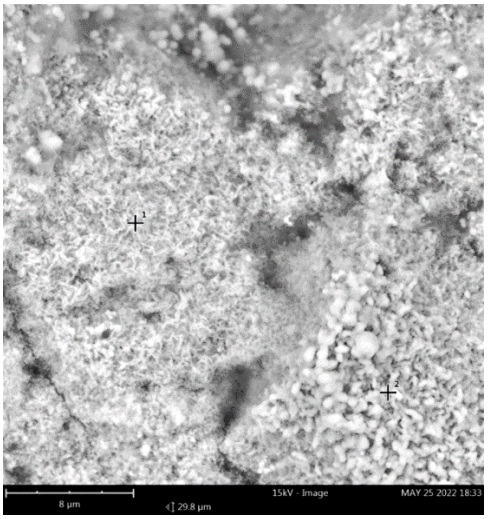

Point 1

	Weight percentage	Certainty
O	39.4 %	99.0 %
Fe	36.2 %	98.5 %
Zn	9.7 %	93.5 %
Si	4.3 %	97.2 %
Ni	3.8 %	91.7 %
Al	2.5 %	95.5 %
Cu	2.4 %	85.1 %
K	1.7 %	95.0 %

Point 2

	Weight percentage	Certainty
Fe	62.8 %	98.0 %
O	23.4 %	97.7 %
Zn	8.0 %	88.7 %
Ni	4.3 %	88.1 %
Si	1.6 %	91.1 %

b)

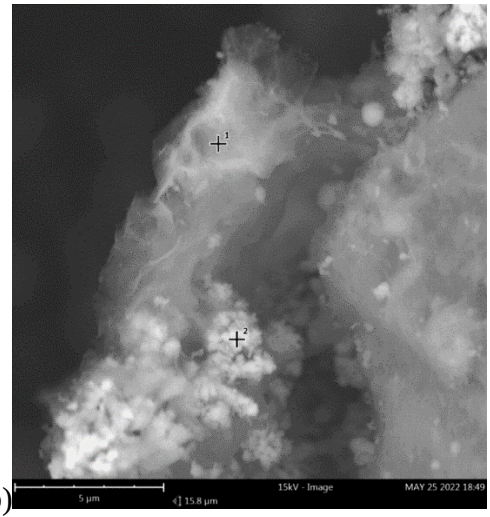

Point 1

	Weight percentage	Certainty
Fe	33.3 %	96.0 %
Zn	29.5 %	91.4 %
O	19.0 %	95.9 %
Cu	6.3 %	79.2 %
Ni	4.6 %	79.7 %
Si	4.1 %	92.2 %
Al	3.2 %	89.6 %

Point 2

	Weight percentage	Certainty
Cu	69.3 %	95.2 %
Fe	20.4 %	94.3 %
O	10.3 %	93.2 %

Figure 3.15 SEM/EDX analysis of ZVI/Lapillus granular mixture taken from column B.

SEM/EDX analysis of the ZVI/lapillus mixture taken from column C (Fig. 3.16) reveal the presence of precipitates containing copper having a bulbous formation, as previously observed in columns A or B, and precipitates of Fe and O (probably iron corrosion products) containing copper, nickel and zinc.

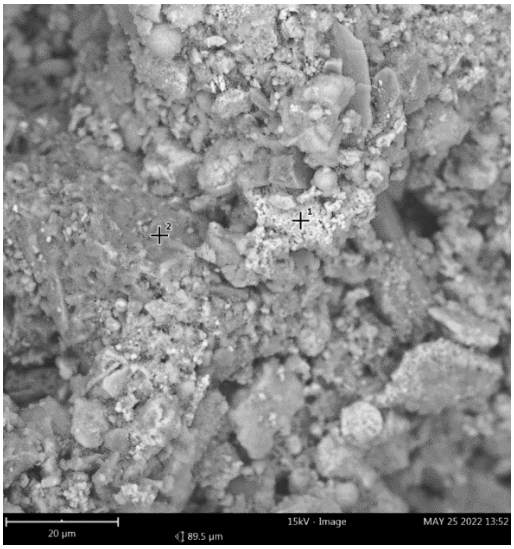

Point 1

	Weight percentage	Certainty
Cu	93.5 %	98.0 %
Fe	4.6 %	93.4 %
O	1.9 %	91.7 %

Point 2

	Weight percentage	Certainty
O	31.1 %	97.4 %
Fe	26.1 %	96.3 %
Zn	12.9 %	85.9 %
Si	8.4 %	96.4 %
Ni	7.7 %	86.7 %
Ca	6.8 %	95.5 %
Al	3.5 %	92.9 %
Mg	3.4 %	91.8 %

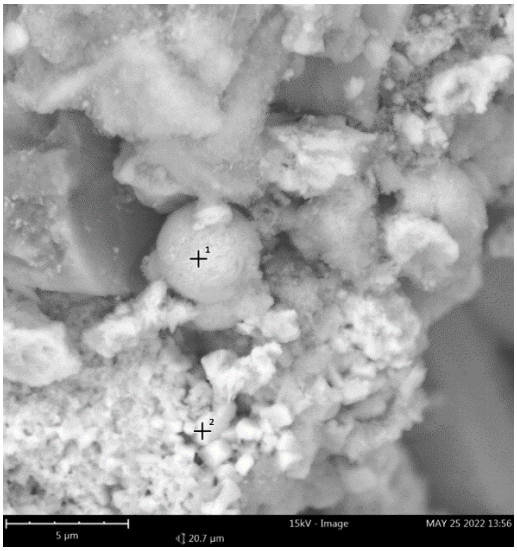

Point 1

	Weight percentage	Certainty
Cu	84.1 %	98.0 %
O	10.2 %	96.7 %
Fe	5.7 %	94.5 %

Point 2

	Weight percentage	Certainty
Cu	100.0 %	97.9 %

Figure 3.16 SEM/EDX analysis of ZVI/Lapillus granular mixture taken from column C

3.5 Conclusions

In this chapter the behaviour of a multilayer PRB configuration composed of two layers of a granular mixture of ZVI and lapillus each characterized by a different degree of iron dispersion has been investigated. The objective of the first layer, named “pre-treatment layer” where ZVI particles are more dispersed, is to avoid the clogging phenomenon, which generally occurs at the barrier inlet. To explore the effectiveness of this multi-layer configuration three column tests have been performed. Two columns were filled with a first layer 4 cm thick and consisting of a ZVI/lapillus granular mixture with a volumetric ratio of 10:90 (column B) or 5:95

(column C) and with a second layer having a volumetric ratio equal to 20:80. A third column filled with a single layer of the 20:80 ZVI/lapillus mixture was used as benchmark (column A). The columns were permeated with a multi-contaminated solution of copper, nickel and zinc.

Regarding the reactive behaviour, the presence of the pre-treatment zone is not beneficial in terms of nickel removal since it involves a rapid depletion of the barrier reactivity. Whereas in terms of zinc and copper removal, the pre-treatment zone can assure the simultaneous removal of the two contaminants with a moderate increase of the barrier thickness.

When the PRB filling material revealed a short reactive lifetime, as in case of Nickel, it was possible to identify an optimal thickness of the barrier for the three column tests. In these cases, an increase in the thickness of the reactive medium does not correspond to a significant removal of the contaminant.

Regarding the hydraulic behaviour, in column A the iron content per unit volume was too high to assure the correct operation of the barrier and a quick and progressive reduction of the hydraulic conductivity starting from column inlet was observed. The hydraulic conductivity profile of the first layer of column B was the same of the one observed in the first layer of column A but translated for longer times. This strong similarity of the hydraulic conductivity profile suggested a very precise kinetics of iron corrosion.

In column C, the “pre-treatment” layer has not undergone any reduction in hydraulic conductivity and has allowed preserving the hydraulic conductivity of the subsequent layer assuring the correct hydraulic behaviour of the barrier. The long duration of test C (at least 8 months) suggested a strong slowdown in the corrosion process most likely linked to the reduction of its reactivity. Indeed, in the first centimetres the reactive medium reached the complete exhaustion of its reactivity. On the contrary, the formation of iron corrosion products that caused the permeability reduction observed in the first centimetres of columns A and B was likely responsible of the modest removal of contaminants. This behaviour confirms the role of corrosion products in the removal of nickel and zinc.

Column A was interrupted due to the excessive reduction of hydraulic conductivity. The material extracted from the column has showed the aggregation/cementation among particles.

SEM images of column A, B and C revealed the presence of copper in the form of trapezoidal crystals or in the form of a bulbous formation, the presence of iron corrosion products having a spongeous nature and the presence of nickel and zinc most likely incorporated within iron corrosion products.

4 INFLUENCE OF THE GEOCHEMICAL PARAMETERS ON THE EFFICIENCY OF THE ZVI/LAPILLUS GRANULAR MIXTURES

4.1 Introduction

The reactive and hydraulic performance of a PRB composed of ZVI is strictly related to iron corrosion process in turn influenced by the groundwater chemical composition. Therefore, this study explores the effect of $CaCO_3$ on the reactive and hydraulic performance of a ZVI/lapillus granular mixture at volumetric ratio equal to 10:90 on the simultaneous removal of Cu, Ni and Zn. Moreover, the single effect of $NaHCO_3$ and the combined effect of $CaCO_3$ and $NaHCO_3$ on the reactive and hydraulic performance of a ZVI/lapillus mixture (v.r. 10:90) for the simultaneous removal of Ni and Zn is investigated.

4.2 State of the art and research purposes

The chemical composition of groundwater plays a significant role on the behaviour of a PRB composed of ZVI. Various geochemical constituents, such as natural organic matter, carbonate species and hardness can have a significant impact on the long-term hydraulic and reactive behaviour of the barrier fill material (Jeen et al., 2008; Liang et al., 2000; Liu et al., 2009).

The influence of geochemical constituents on the ZVI performance was studied with reference to the removal of hexavalent chromium (Liu et al., 2009; Lo et al., 2006; Pratt et al., 1997), chlorinated hydrocarbons (Gong et al., 2020; Xin et al., 2018), Uranium (Wang et al., 2019; Zhang et al., 2015), arsenic (Mak et al., 2009), and selenium (Shan et al., 2018).

(Jeen et al., 2008) found as the addition of dissolved calcium carbonate flattened the pH profile along the thickness of ZVI packed into a column. Alkalinity (HCO_3^-) could also exert an influence on ZVI reactivity by stabilizing the solution pH and forming carbonate minerals (Mak et al., 2009). (Lo et al., 2006) found that the coexistence of Ca^{2+} and HCO_3^- determines a decrease of Cr(VI) removal capacity, whereas (Mak et al., 2009) found that in the same geochemical conditions the removal rate of arsenic increases.

According to Gui et al., 2008 the presence of $CaCO_3$ slows down the pH increase caused by the corrosion of Fe and the reduction of Cr(VI), keeping the corrosion potential relatively low and improving the reactivity of Fe towards Cr(VI).

Based on the examined scientific literature, the influence of the Ca^{2+} and HCO_3^- in the hydraulic and reactive behaviour of ZVI/lapillus granular mixtures have not been addressed. For this purpose, four long-term column experiments were conducted. Column M was permeated with a solution containing Cu, Ni and Zn; Column E was permeated with a solution containing Cu, Ni, Zn and $CaCO_3$ dissolved in distilled water; the other two columns were permeated with a solution containing Ni and Zn and $NaHCO_3$ (column F) or $CaCO_3$ and $NaHCO_3$ (column G). Column results were interpreted in terms of reactive and hydraulic behaviour along the reactive medium thickness and over time.

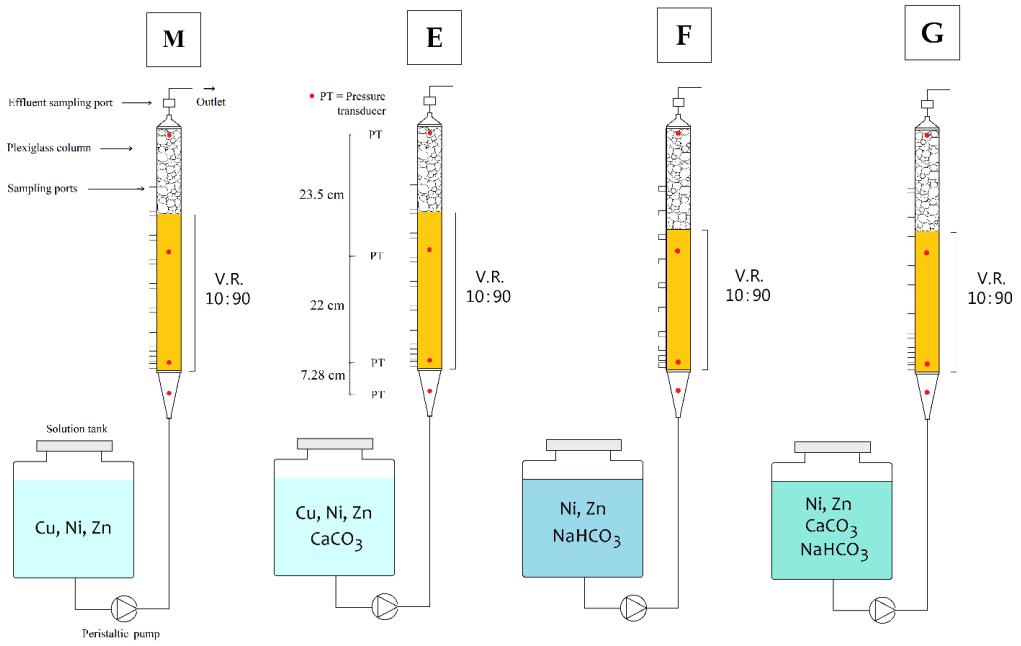

Figure 4.1 M, E, F, G column test apparatus.

Tables 4.1 and 4.2 summarizes the main characteristics of the three column tests. ZVI and lapillus were mixed at a fixed volumetric ratio.

Table 4.1 Main characteristics of M, E, F, G column tests.

ID	M	E	F	G
v.r. ZVI/lapillus	10:90	10:90	10:90	10:90
Total thickness (cm)	29	29	28	28
Test duration (h)	3492 (in progress)	7584 (in progress)	7584 (in progress)	7044 (in progress)
Initial porosity (%)	42.9	42.9	42.9	42.9

Table 4.2 Composition of inlet solutions.

ID	Distilled water	Cu, Ni, Zn (18 mg/l)	Ni, Zn (18 mg/l)	$CaCO_3$ (10 mg/l)	$NaHCO_3$ (100 mg/l)
M	✓	✓		-	-
E	✓	✓		✓	-
F	✓		✓	-	✓
G	✓		✓	✓	✓

After about three days from the beginning of the test in the part of the columns filled with gravel the presence of gas bubbles is clearly visible. The production of these gas bubbles is related to the iron corrosion process. If the gas is vented, it doesn't influence the permeability of the reactive medium.

Figure 4.2 Presence of gas bubbles at the beginning of the test.

Figure 4.3 shows the breakthrough curves for column M related to Ni (Fig. 4.3a) and to Zn (Fig. 4.3b). Results related to copper have not been shown because it was completely removed from the first sampling port up to eight weeks. From Figure 4.3a, it can be observed as the minimum thickness necessary to removal nickel is equal to 13 cm. Due to the progressive exhaustion of the reactive medium the breakthrough time occurs at 18 cm after two weeks and at 23 cm after three weeks. The Ni concentration is lower than its regulatory limit at 28 cm after 8 weeks. Regarding Zn (Fig. 4.3b), 8 cm are necessary to remove the contaminant, whereas the regulatory limit has never been reached at 13 cm in the studied period (8 weeks).

Figure 4.4 shows the breakthrough curves for column E related to Cu (Fig. 4.4a), Ni (Fig. 4.4b), Zn (Fig. 4.4c). Copper concentration exceeds the regulatory limit at 1.5 cm

of reactive medium thickness from the beginning of the test, whereas it is completely removed until 3 cm after 12 weeks and after 5 cm for all test duration. Regarding Ni, the minimum thickness necessary to removal nickel is equal to 13 cm. In this case a rapid exhaustion of the reactive medium can be observed. Regarding Zn (Fig. 4.4c), a minimum thickness of 8 cm is necessary to remove the contaminant from solution. Due to the progressive exhaustion of the reactive medium the breakthrough time occurs at 13 cm after three weeks, 18 cm after four weeks, 23 and 28 cm after six and eight weeks.

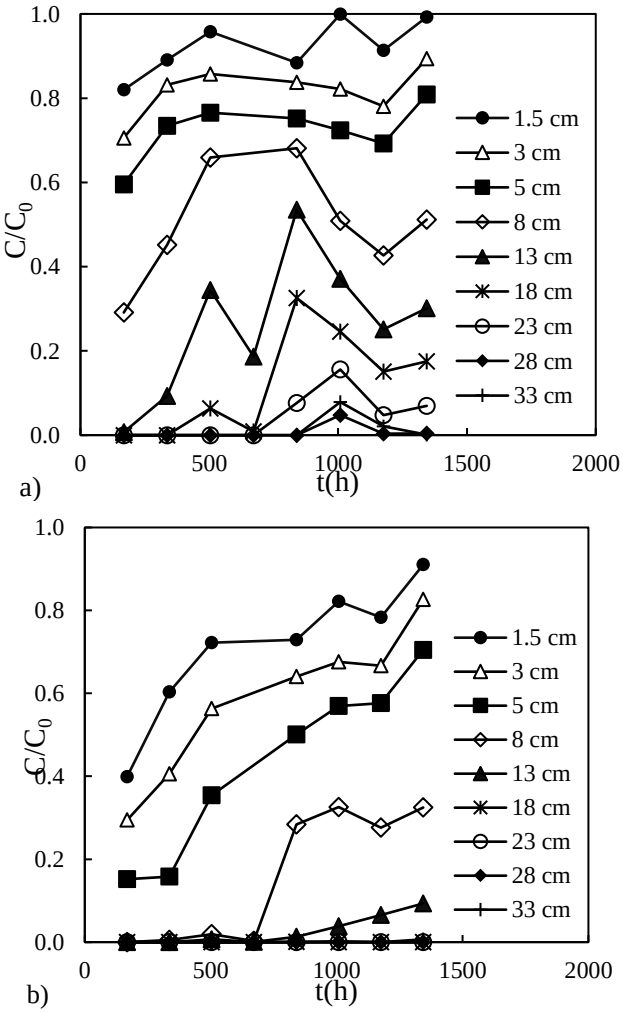

Figure 4.3 Breakthrough curves of a) nickel and b) zinc at the sampling ports placed at a distance of 1.5, 3, 5, 8, 13, 18, 23, 28 and 33 cm from the inlet section of column M.

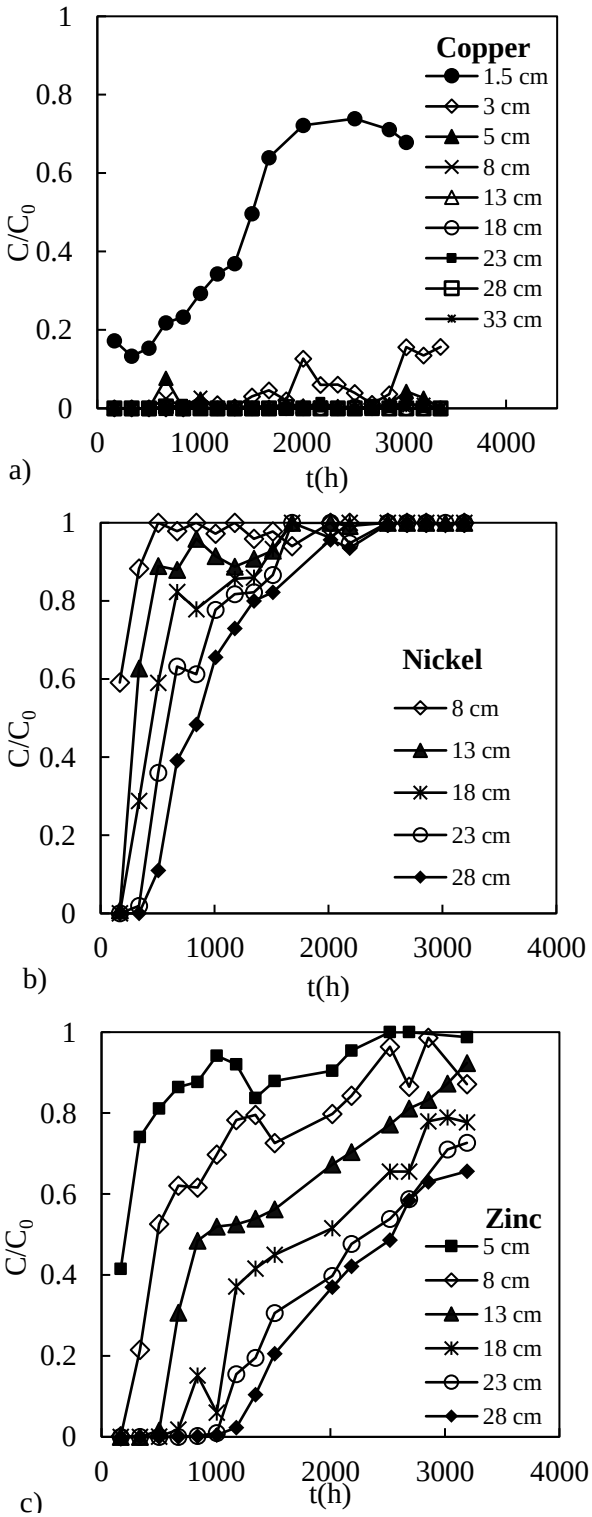

Figure 4.4 Breakthrough curves of a) copper, b) nickel and c) zinc at different sampling ports of column E.

Figure 4.5 shows the comparison of the breakthrough curves of Cu at the sampling ports equal to 1.5 cm (Fig. 4.5a) and 3 cm (Fig. 4.5b) for the columns E and M. As observed in Figure 4.5a, Cu removal is affected by the presence of $CaCO_3$ and therefore it has not been completely removed.

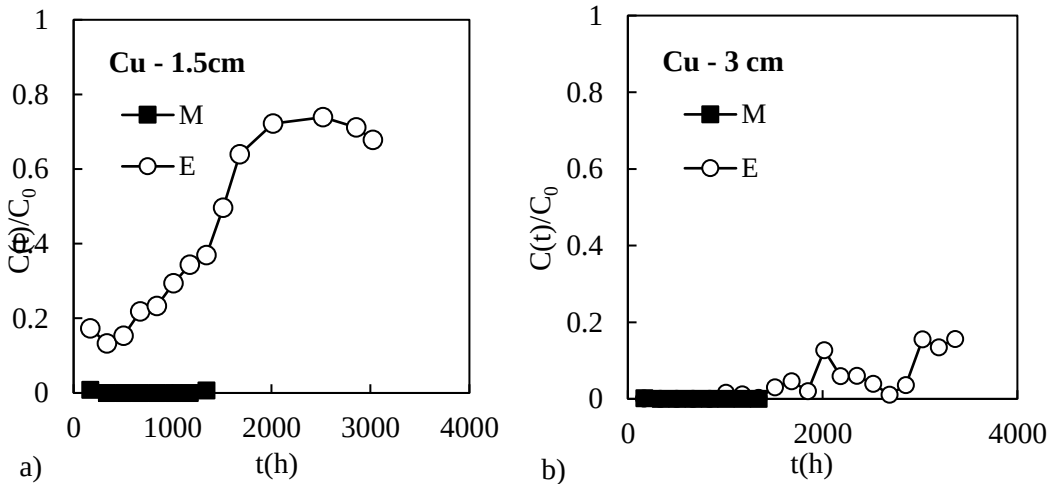

Figure 4.5 Breakthrough curves of Cu at a) 1.5 cm and b) 3 cm for columns E and M.

Figure 4.6 shows the comparison of the breakthrough curves of Ni at the sampling ports equal to 8, 13, 18, 23, 28, 33 cm (Fig. 4.5 a,b,c,d,e,f) for the columns E and M. As observed for Cu, Ni removal is negatively affected by the presence of $CaCO_3$. Therefore, the presence of $CaCO_3$ decreases the removal capacity of the reactive medium. A similar result was obtained by Zhang et al. (2015), who have found that the presence of the dissolved Ca^{2+} and carbonate decreases U(VI) onto nZVI.

Figure 4.7 shows the comparison of the breakthrough curves of Zn at the sampling ports equal to 3, 5 8, 13, 18, 23, 28, 33 cm (Fig. 4.7 a,b,c,d,e,f,g,h) for the columns E and M. As noted for the other two contaminants, the presence of $CaCO_3$ decreases the removal capacity of the reactive medium towards Zn.

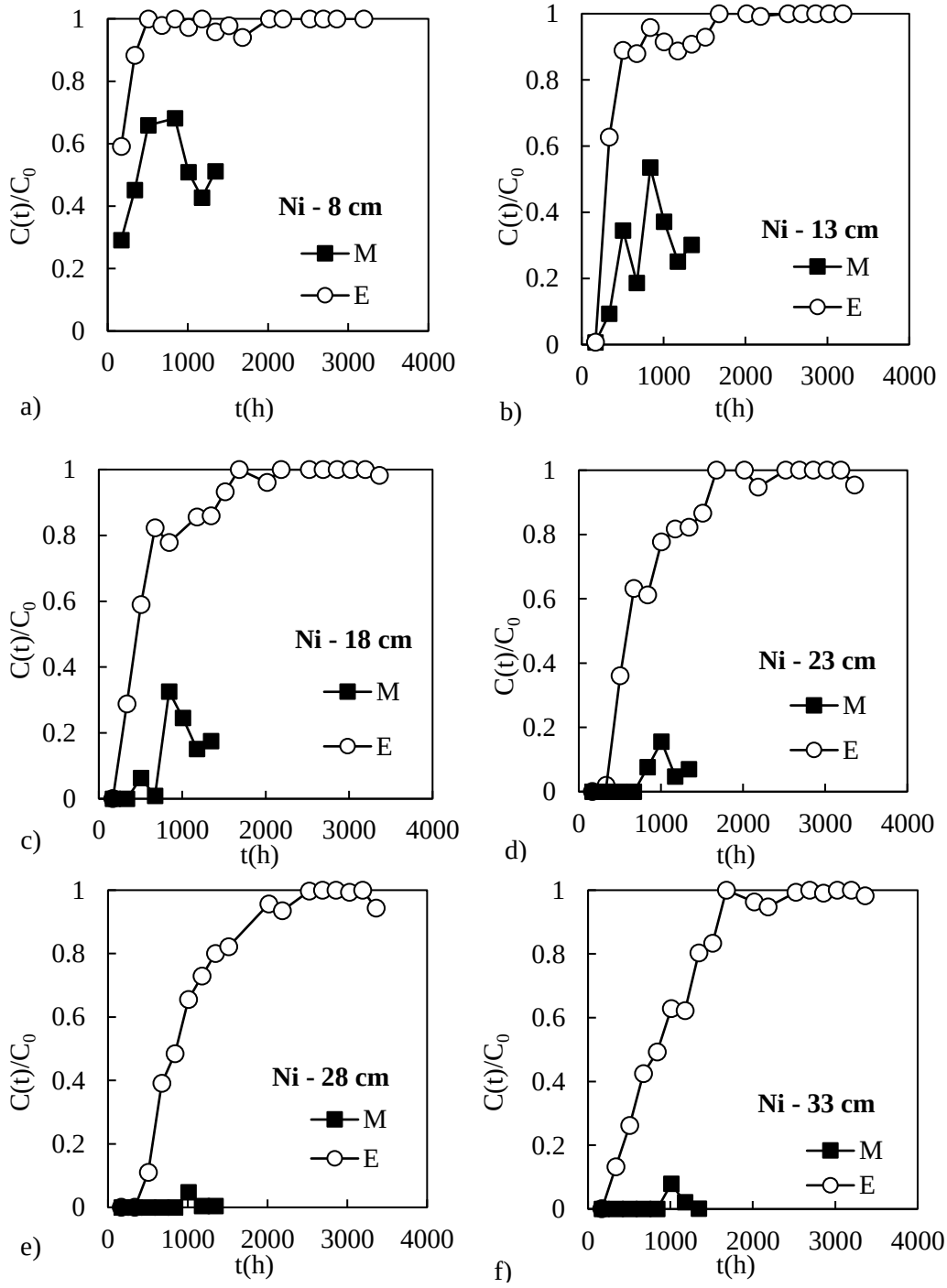

Figure 4.6 Breakthrough curves of Ni at a) 8 cm, b) 13 cm, c) 18 cm, d) 23 cm, e) 28 cm and f) 33 cm for columns E and M.

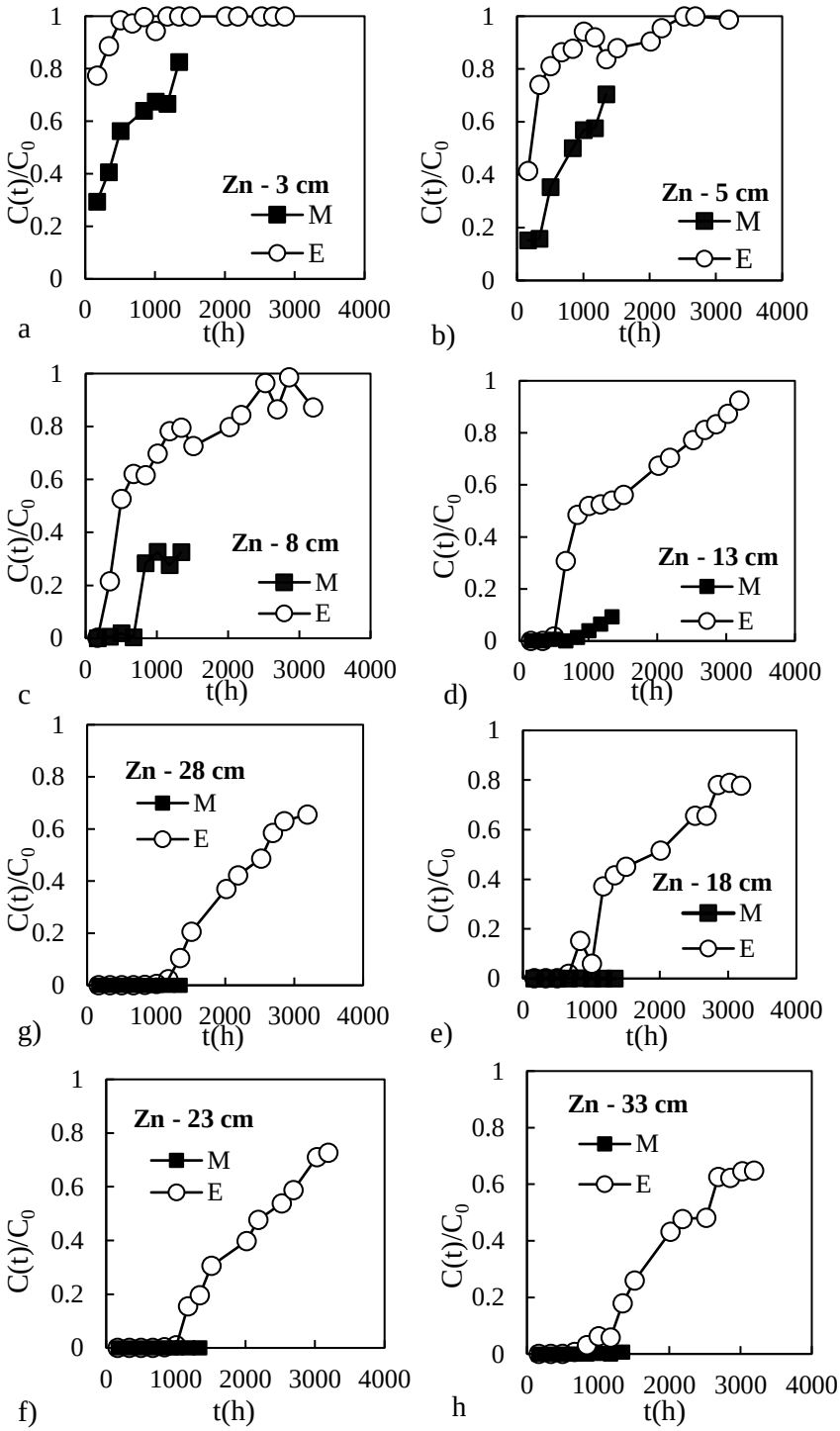

Figure 4.7 Breakthrough curves of Zn at a) 3 cm, b) 5 cm, c) 8 cm, d) 13 cm, e) 18 cm, f) 23 cm, g) 28 cm and h) 33 cm for columns E and M.

Figures 4.8 and 4.9 show the profile of pressure over time for columns M and E respectively. The two figures show the pressure detected at three different measuring ports located at the base of the column (Channel 1) and at 3 (Channel 2) and 25 cm (Channel 3) from the inlet section of the columns (see schematic diagram of Fig. 2.8). The pressure detected in the first channel of column M starts to increase after about 2500 hours. Whereas the pressure in the first channel of column E starts to increase after about 6000 hours.

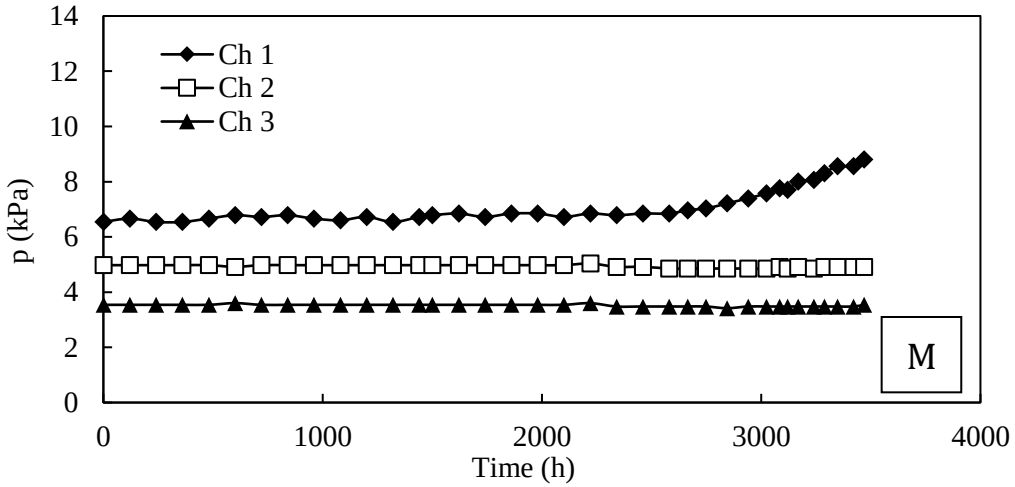

Figure 4.8 Pressure (kPa) detected at Channels 1, 2 and 3 vs. time (h) for column M.

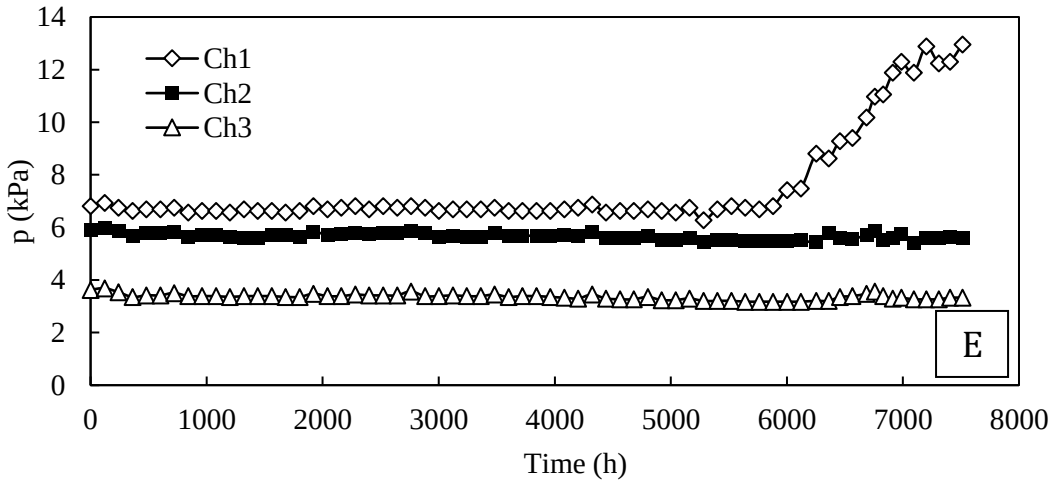

Figure 4.9 Pressure (kPa) detected at Channels 1, 2 and 3 vs. time (h) for column E.

Figure 4.10 compares the two reactive media in terms of hydraulic behaviour. In particular, the normalized permeability calculated in the first 3 cm of the reactive medium thickness is diagrammed as function of time. The presence of $CaCO_3$ retards the hydraulic conductivity reduction in a mixture containing 10% by volume of ZVI. If the formation of iron corrosion products is considered the main cause of hydraulic conductivity reduction, it is possible to state that a greater production of iron corrosion products enhances contaminants removal but can decrease the hydraulic conductivity of the reactive medium.

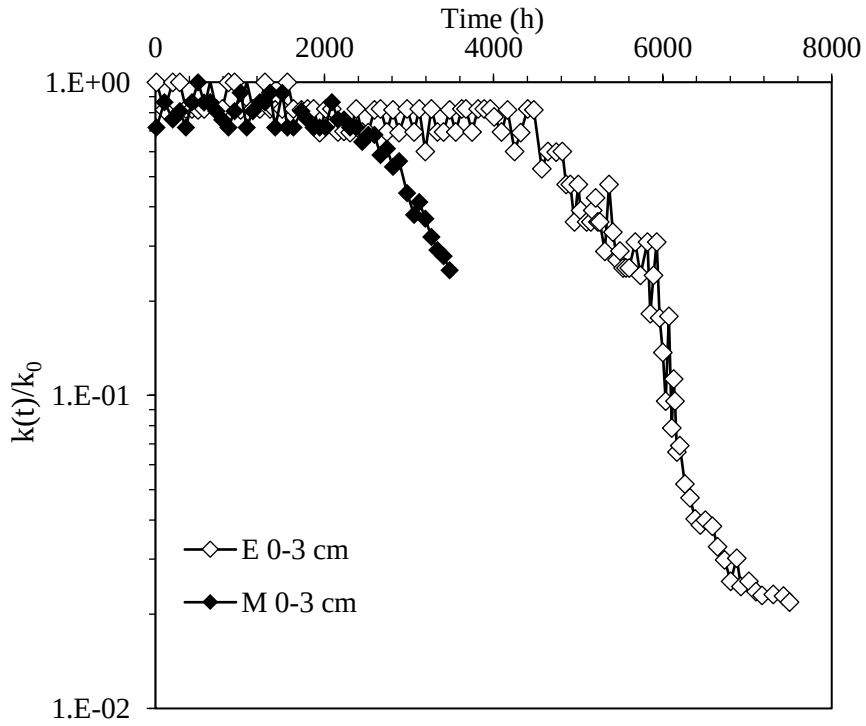

Figure 4.10 $k(t)/k_0$ profile over time for columns M and E.

Figure 4.11 shows the breakthrough curves for column F related to Ni (Fig. 4.11a) and to Zn (Fig. 4.11b). From Figure 4.11a, it can be observed as the minimum thickness necessary to removal nickel is at least 5 cm. The breakthrough occurs at 13 cm after 840 hours whereas it is never observed for the sampling ports located after 13 cm of the reactive medium thickness. Zn is completely removed at the first sampling port for four weeks and at the second or third sampling port after 5 weeks,

whereas the regulatory limit has never been reached in all the sampling ports located after 5 cm in the studied period (18 weeks) (Fig. 4.11b).

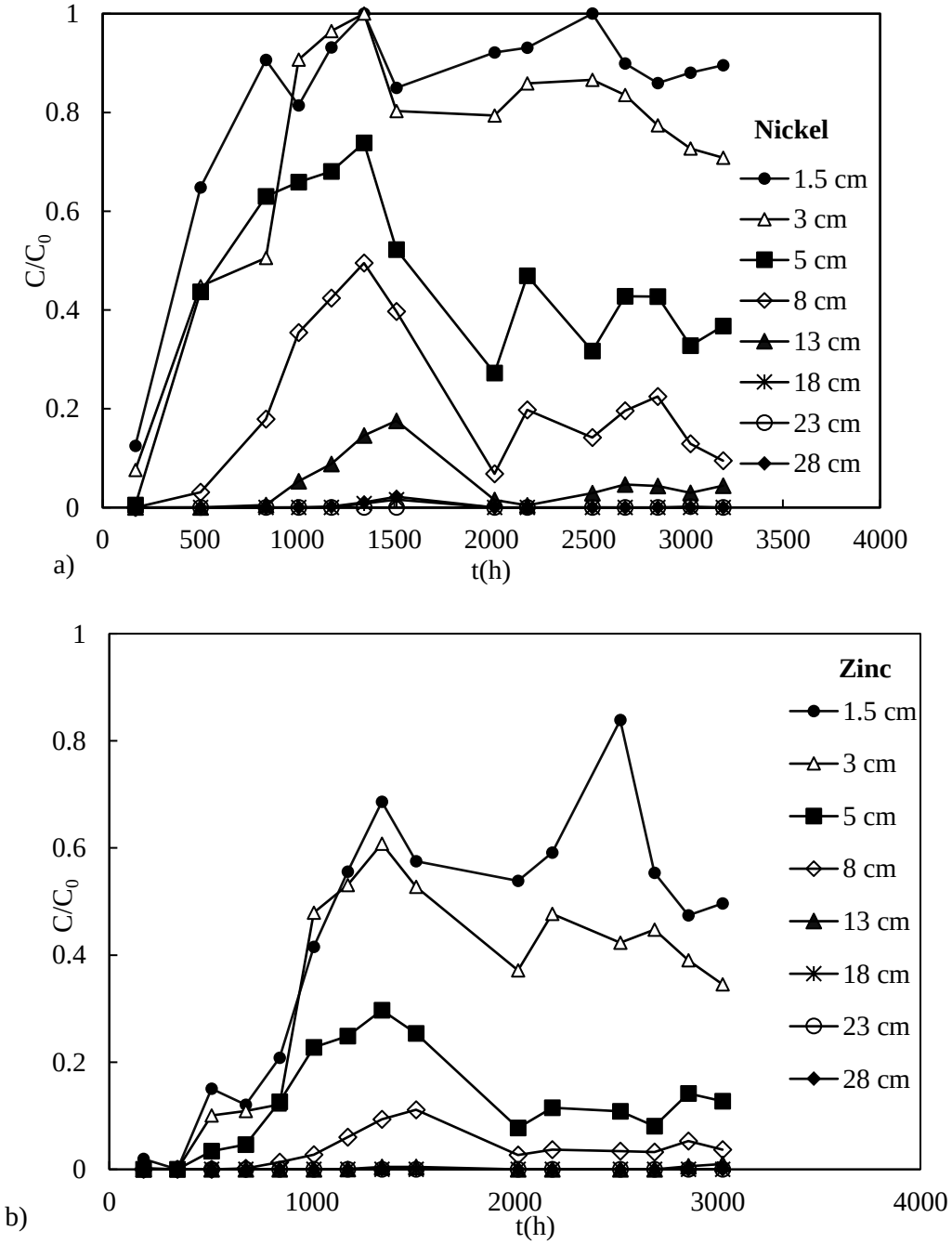

Figure 4.11 Breakthrough curves of a) nickel and b) zinc at different sampling ports of column F.

Figure 4.12 shows the breakthrough curves for column G related to Ni (Fig. 4.12a) and to Zn (Fig. 4.12b). From Figure 4.12a, it can be observed as the minimum thickness necessary to removal nickel is 5 cm. The breakthrough occurs at 8 cm after 504 hours and at 13 cm after hours 1844 hours whereas it is never observed for the sampling ports located after 23 cm of the reactive medium thickness. Regarding Zn, a thickness of 3 cm is necessary to remove the contaminant, breakthrough occurs at 5 cm after 2016 hours, whereas the regulatory limit has never been reached in all the sampling ports located at 13 and 23 cm in the studied period (18 weeks) (Fig. 4.12b).

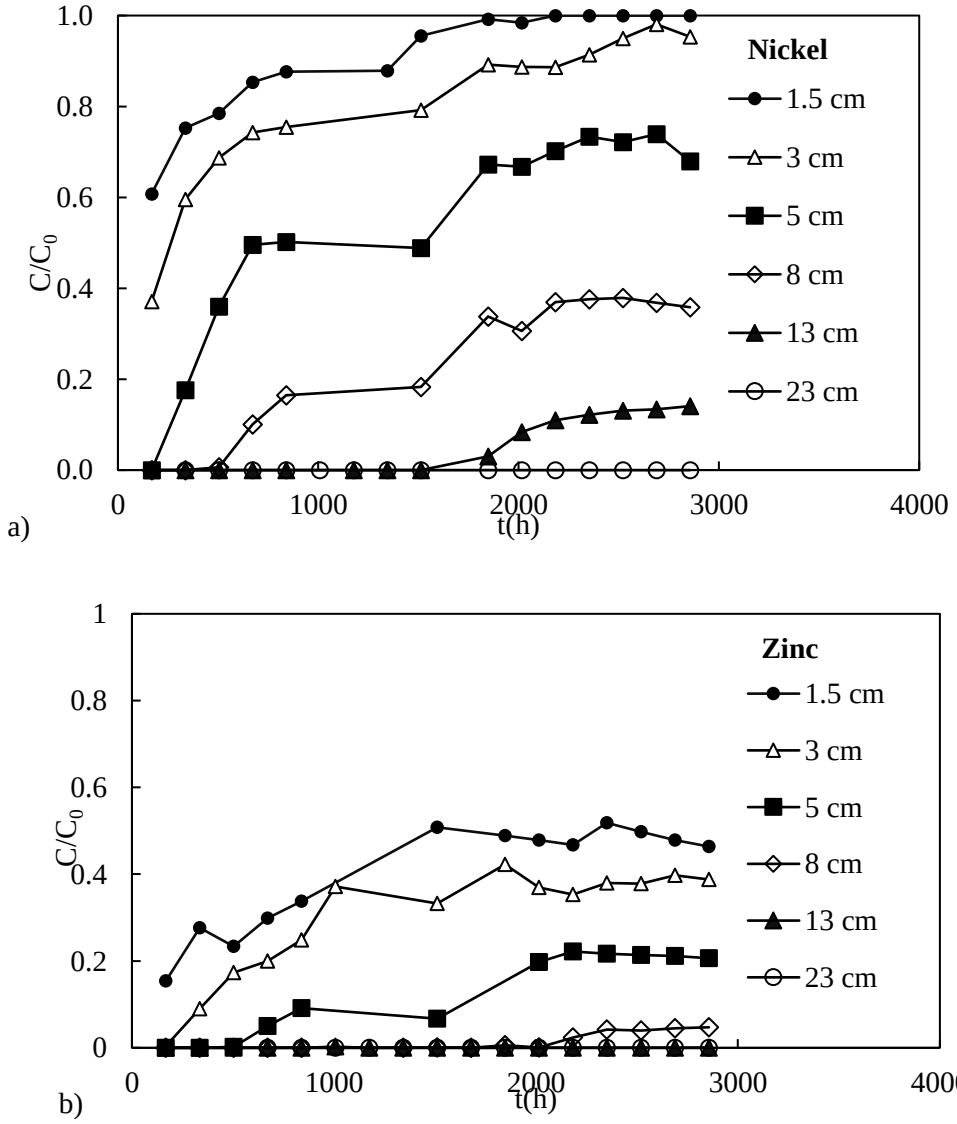

Figure 4.12 Breakthrough curves of a) nickel and b) zinc at different sampling ports of column G.

Figures 4.13 show the relative concentration calculated at the sampling ports located at 18 and 23 cm for Ni and Zn for column F. The breakthrough time for Ni occurs at the same time for the two sampling ports after about 3800 h. Zn concentration is below regulatory limit for the two sampling ports for all test duration.

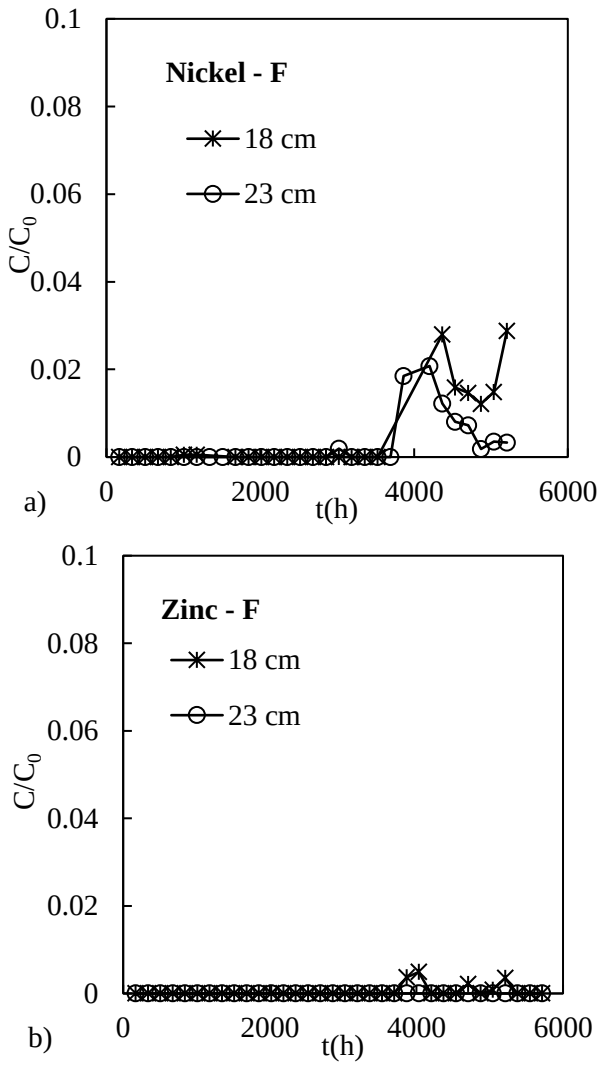

Figure 4.13 Breakthrough curves of a) nickel and b) zinc at 18 cm and 23 cm for column F.

Figure 4.14 show the relative concentration calculated at the sampling ports located at 23 cm for Ni and Zn for column G. Ni and Zn are removed for all test duration with a removal efficiency greater than 99%.

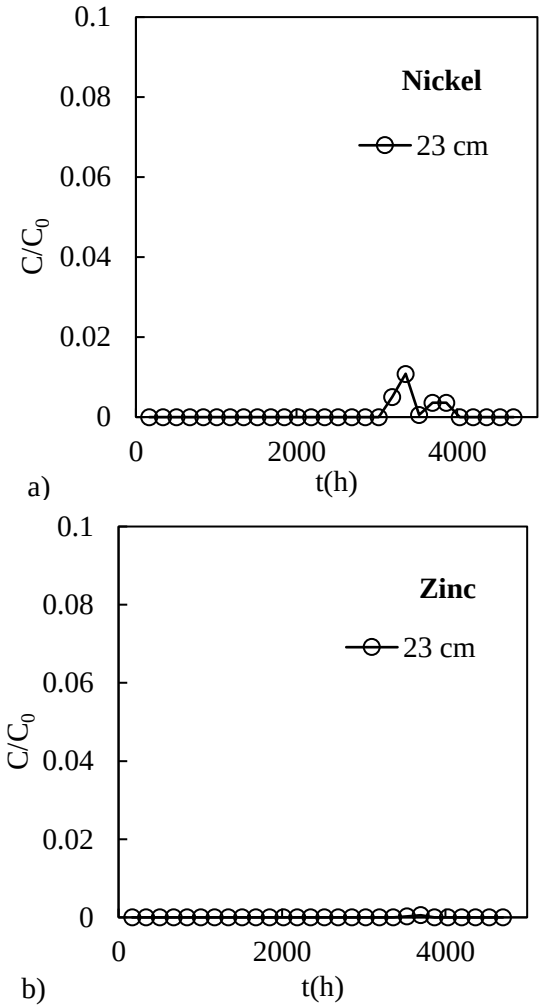

Figure 4.14 Breakthrough curves of a) nickel and b) zinc at 23 cm for column G.

Figures 4.15 and 4.16 show the comparison between columns F and G towards Ni and Zn removal respectively. It can be observed that the difference between the two columns is negligible.

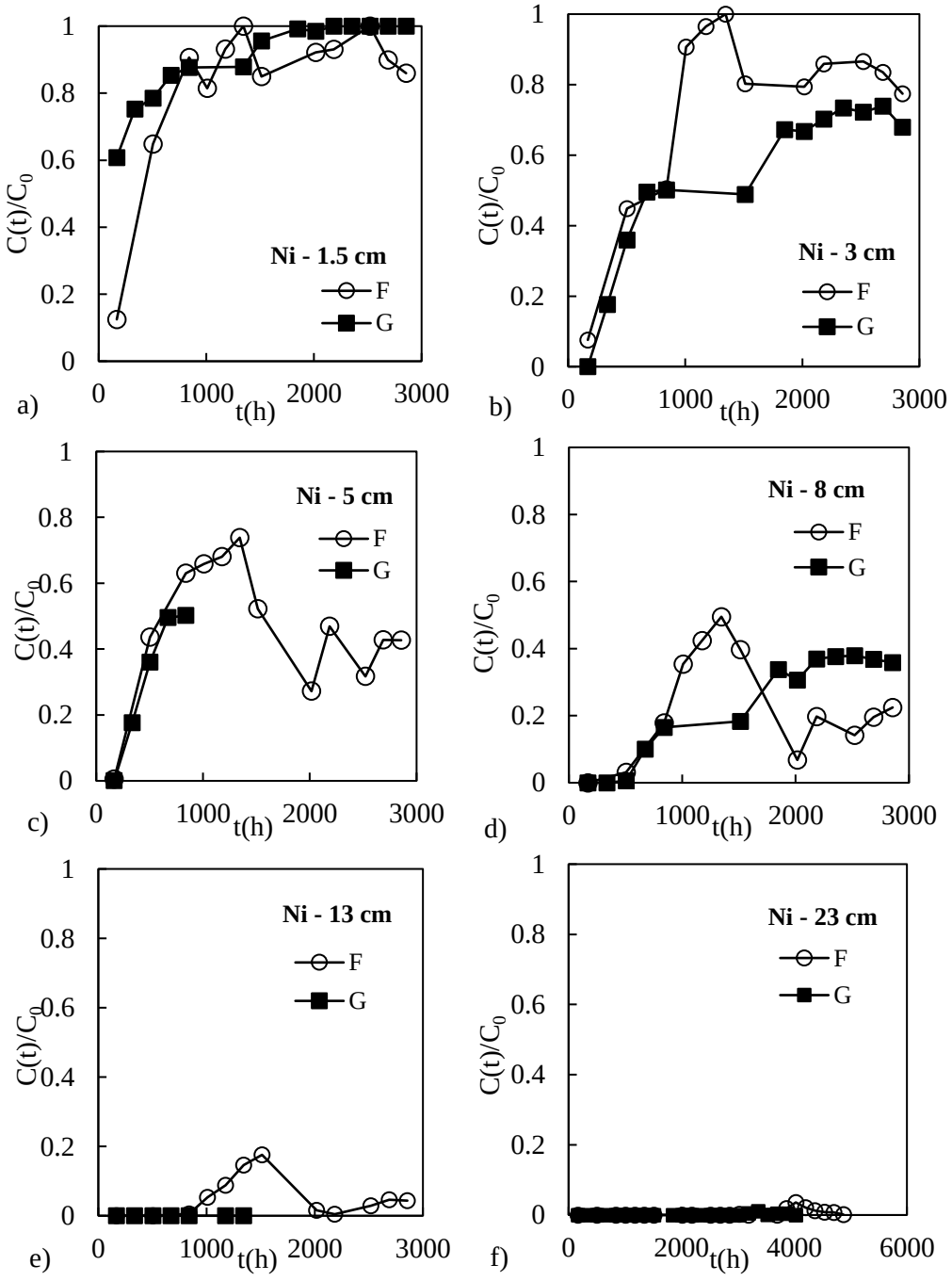

Figure 4.15 Breakthrough curves of Ni at a) 1.5 cm, b) 3 cm, c) 5 cm, d) 8 cm, e) 13 cm and f) 23 cm for columns F and G.

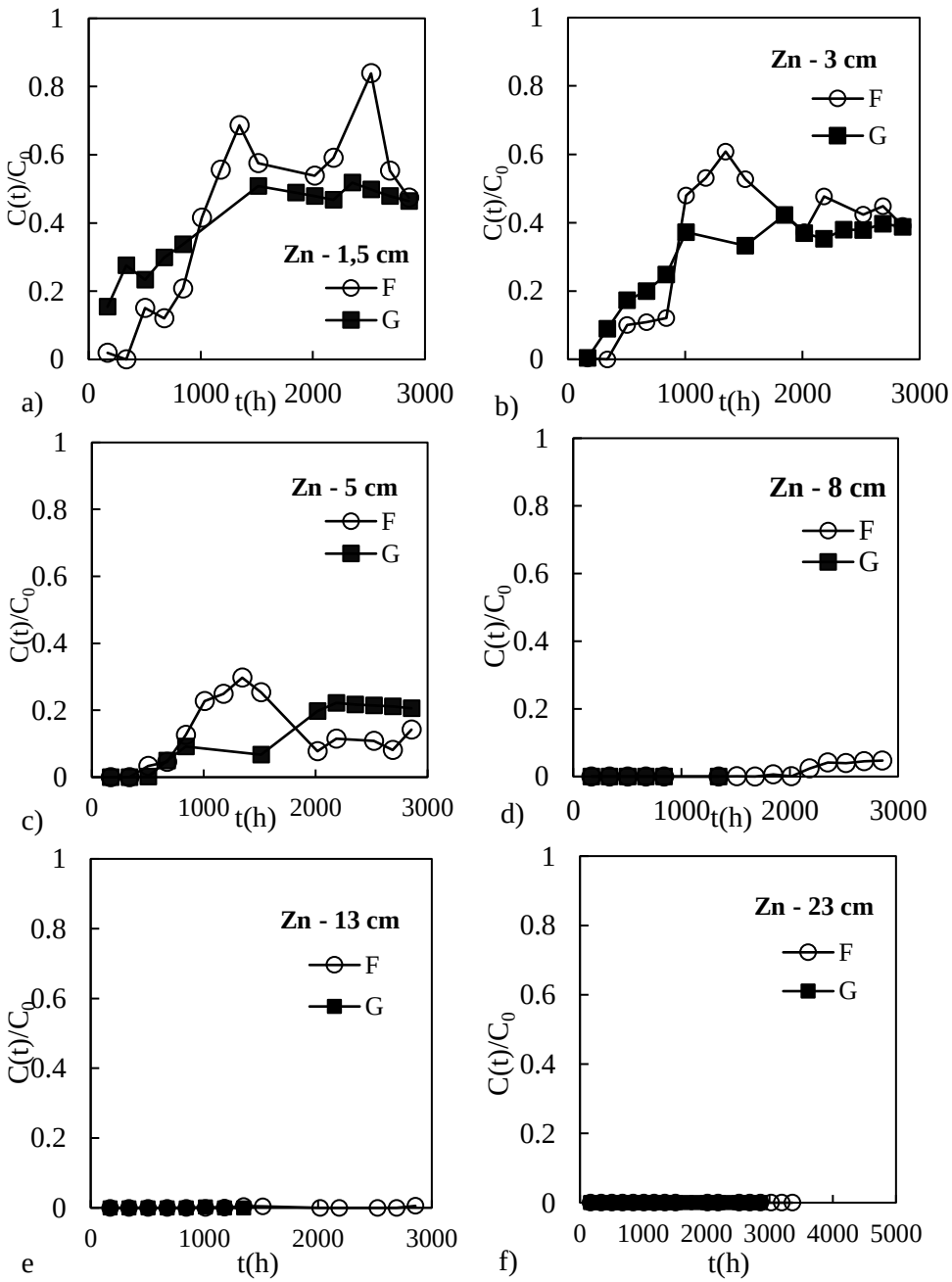

Figure 4.16 Breakthrough curves of Zn at a) 1.5 cm, b) 3 cm, c) 5 cm, d) 8 cm, e) 13 cm and f) 23 cm for columns F and G.

Figures 4.17 and 4.18 show the profile of pressure over time for columns F and G respectively. The two figures show the pressure detected at three different measuring ports located at the base of the column (Channel 1) and at 3 (Channel 2) and 25 cm (Channel 3) from the inlet section of the columns (see schematic diagram of Fig. 2.8). The pressure detected in the first channel of column F starts to increase after about 6000 hours. Whereas the pressure in the three channels of column G remains constant.

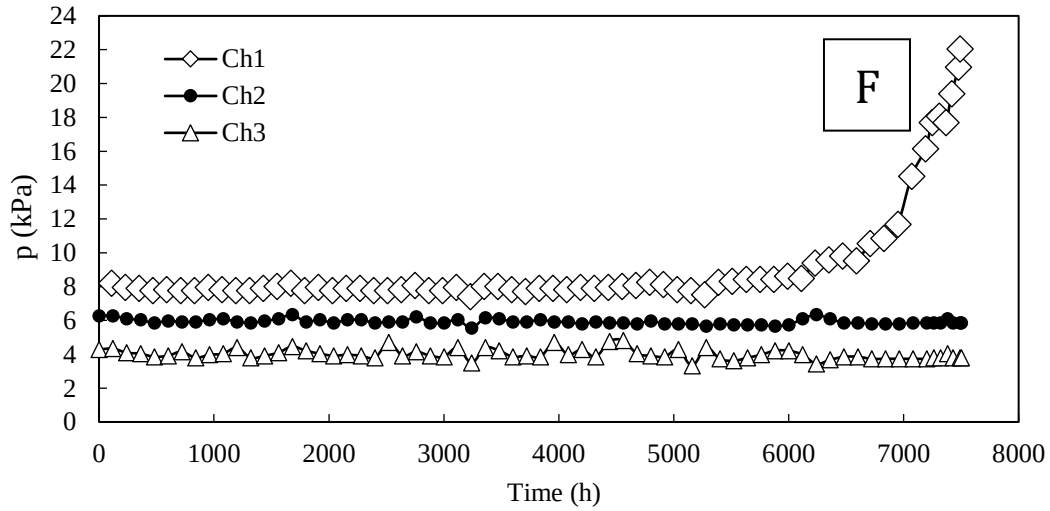

Figure 4.17 Pressure (kPa) detected at Channels 1, 2 and 3 vs. time (h) for column F.

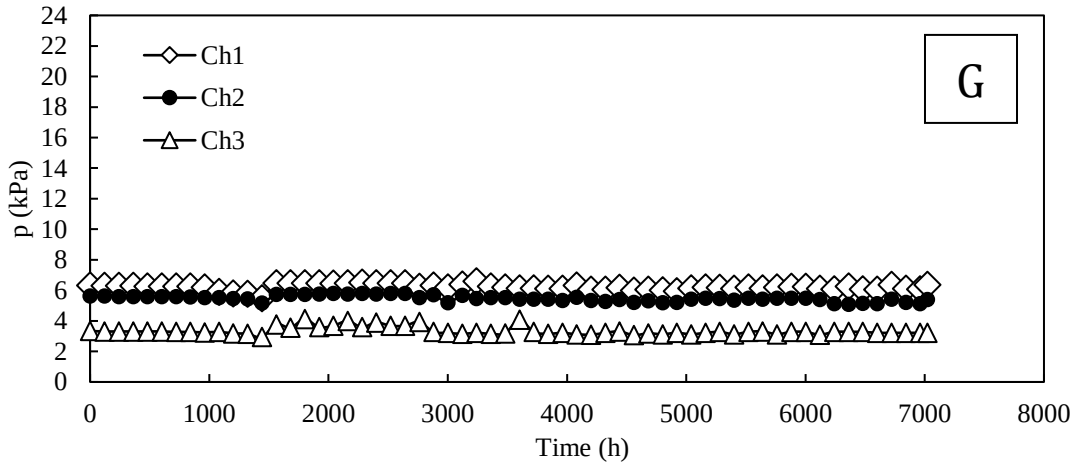

Figure 4.18 Pressure (kPa) detected at Channels 4, 5 and 6 vs. time (h) for column G.

Figure 4.19 compares the two reactive media in terms of hydraulic behaviour. In particular, the normalized permeability calculated in the first 3 cm of the reactive medium thickness is diagrammed as function of time. It can be observed that the values of $k(t)/k_0$ decrease by an order of magnitude in column F between approximately 5000 and 8000 hours of testing, while those relating to column G remain almost constant up to approximately 7000 hours and then undergo a slight reduction.

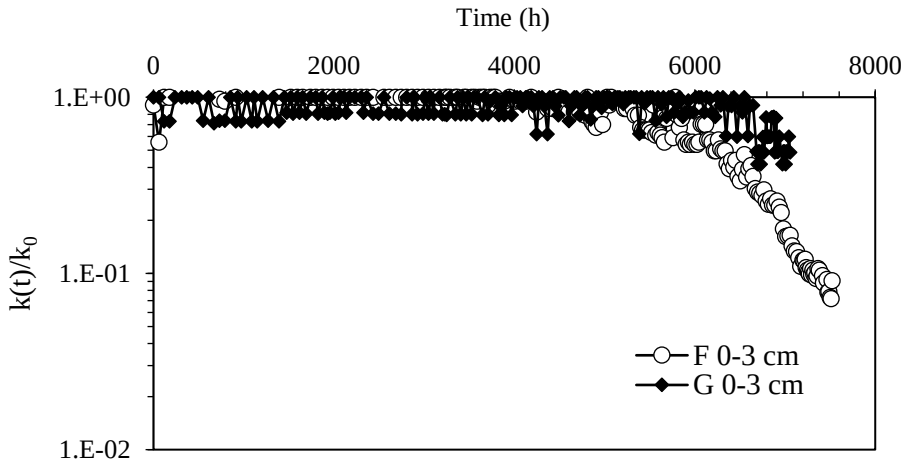

Figure 4.19 $k(t)/k_0$ profile over time for columns F and G.

Figure 4.7 shows the images of columns M, E, F and G during operation. The presence of iron corrosion products can be clearly seen starting from the inlet section of the column.

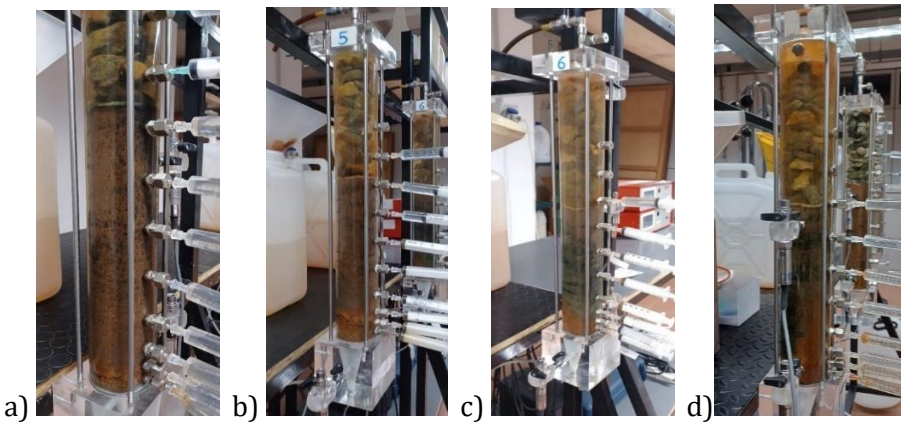

Figure 4.20 Images of a) column M, b) column E, c) column F and d) column G.

4.3 Conclusions

This chapter examined the results obtained from four long-term column experiments. Column M was permeated with a solution containing Cu, Ni and Zn; Column E was permeated with a solution containing Cu, Ni, Zn and $CaCO_3$ dissolved in distilled water; Column F and G were permeated with a solution containing Ni and Zn as contaminants, and $NaHCO_3$ (Column F) or $CaCO_3$ and $NaHCO_3$ (column G) as mineral compounds.

In solutions contaminated by Cu, Ni and Zn (Columns M and E) the removal sequence observed was Cu>Ni>Zn. Column M showed no sign of exhaustion towards copper starting from the first sampling port located at 1.5 cm thickness of the reactive material for all test duration (8 weeks). The reactive medium showed its exhaustion towards Ni and Zn removal along its thickness but was able to guarantee a concentration of the two contaminants below the regulatory limit at the outlet of the column. The reactive medium contained in column E showed its exhaustion towards Cu only in the first sampling port and a rapid exhaustion along its all thickness for Ni and Zn removal. A comparison between the two columns revealed as $CaCO_3$ negatively affected the removal of the three contaminants. In terms of hydraulic behaviour, both columns showed a reduction of the hydraulic conductivity at the inlet of the reactive medium, but the presence of $CaCO_3$ delayed this reduction.

The removal efficiency towards Ni and Zn calculated in Columns F and G was greater than the removal efficiency calculated in columns M and E. This behaviour was attributed to the absence of copper in the solutions used in columns F and G. The removal efficiency was greater than 90% for Ni and 99% for Zn at the outlet of column F and greater than 99% for both contaminants at the outlet of column G. The difference among the breakthrough profiles of Ni and Zn, observed in each sampling port of columns F and G, can be considered negligible. Therefore, the influence of $CaCO_3$ on the removal of Ni and Zn is negligible. In terms of hydraulic behaviour, the hydraulic conductivity after 7000 hours reduced of one order of magnitude in column F and it is slightly reduced for column G. Currently, the two columns cannot be compared because the two tests are still in progress.

5 EFFECTIVENESS OF LAPILLUS IN THE REMOVAL OF HEAVY METALS

5.1 Introduction

In this chapter, the efficacy of the lapillus in the removal of Cu, Ni and Zn is discussed. Column tests conducted by (Madaffari et al., 2017) and (Bilardi et al., 2020) demonstrated that lapillus was not completely inert towards the nickel removal but showed a removal capacity probably related to its chemical composition (presence of metal oxides) and to the high specific surface (due to surface roughness), which influenced the adsorption process. In particular, (Madaffari et al., 2017) performed a column test using an initial concentration of Nickel equal to 50 mg/L, whereas (Bilardi et al., 2020) used an initial concentration of Nickel equal to 10 mg/L. With a lower concentration of Nickel, the removal efficiency of lapillus significantly increased and for this reason, the authors (Bilardi et al., 2020) suggested that pure lapillus could be efficiently used as a reactive medium in the technology of PRB in cases of low concentrations of this metal. Moreover, batch tests conducted by (Bilardi et al., 2020) showed that lapillus is reactive not only towards nickel but also towards copper and zinc in single contaminated solutions. As batch tests can provide information on the reactivity in the short term of a material and cannot simulate the real boundary condition of a PRB, in this chapter it was performed a column test (Column D) using a pluri-contaminated solution of Cu, Ni and Zn at initial concentration of 18 mg/L. Data were interpreted in terms of removal efficiency towards the tricontaminant solution and in terms of hydraulic behaviour. SEM-EDX analysis have been performed on the material extracted from the column at the end of the column test in order to study the atomic composition of the material and grain morphology. Moreover, a comparison of the results derived from columns D and M is carried out.

5.2 Column test program

Figure 5.1 shows the column test carried out in order to investigate the performance of lapillus. The column was filled of lapillus for the entire length (i.e., 50 cm) and was fed with the contaminated solution at a flow rate equal to 0.5 mL/min (Fig. 5.2). The main characteristics of the test are summarized in Table 5.1.

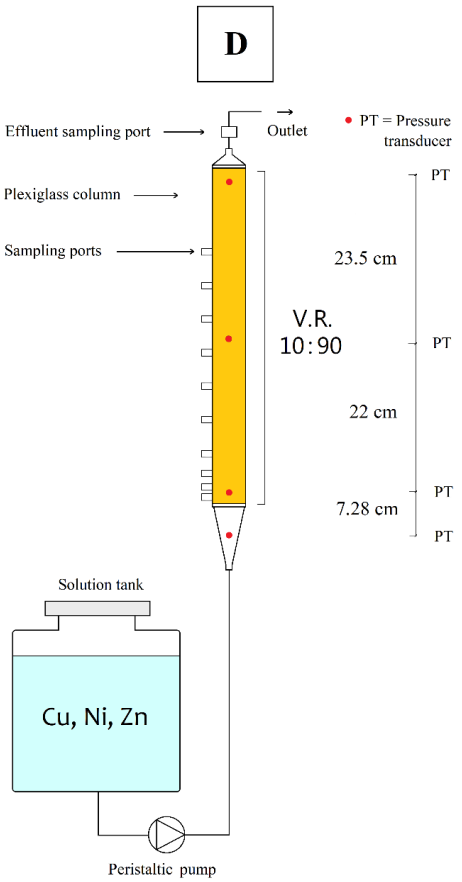

Figure 5.1 Schematic diagram of column test conducted using lapillus.

Table 5.1 Main characteristics of column tests.

ID	D
Reactive medium	Lapillus
Total thickness (cm)	50
Test duration (h)	4788
Initial porosity (%)	42.3

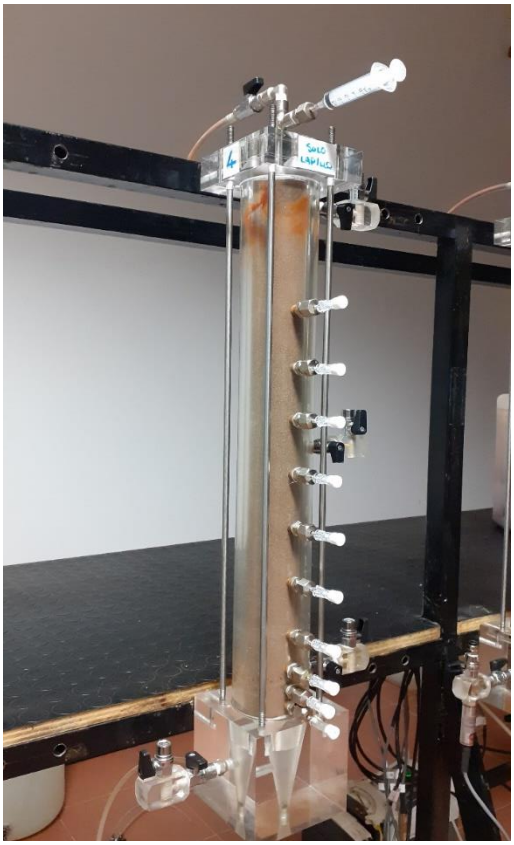

Figure 5.2 Column D.

5.3 Results and discussion

Figure 5.3 shows the relative concentration (C/C_0) of copper (Fig. 5.3a), nickel (Fig. 5.3b), and zinc (Fig. 5.3c) over distance for the column test conducted using lapillus. The volcanic material is selective in the removal of the three metals according to the following sequence Cu>Zn>Ni. Copper is completely removed from solution until 1344 hours at 38 cm of reactive medium thickness (Fig. 5.3a). Nickel is removed only in the short time (i.e., until 336 h) at 28 cm of column thickness, subsequently the reactive medium is completely exhausted (Fig. 5.3b). Zinc is removed until 672 hours at 50 cm of lapillus thickness (Fig. 5.3c) and subsequently as observed for nickel, is not able to remove the contaminant.

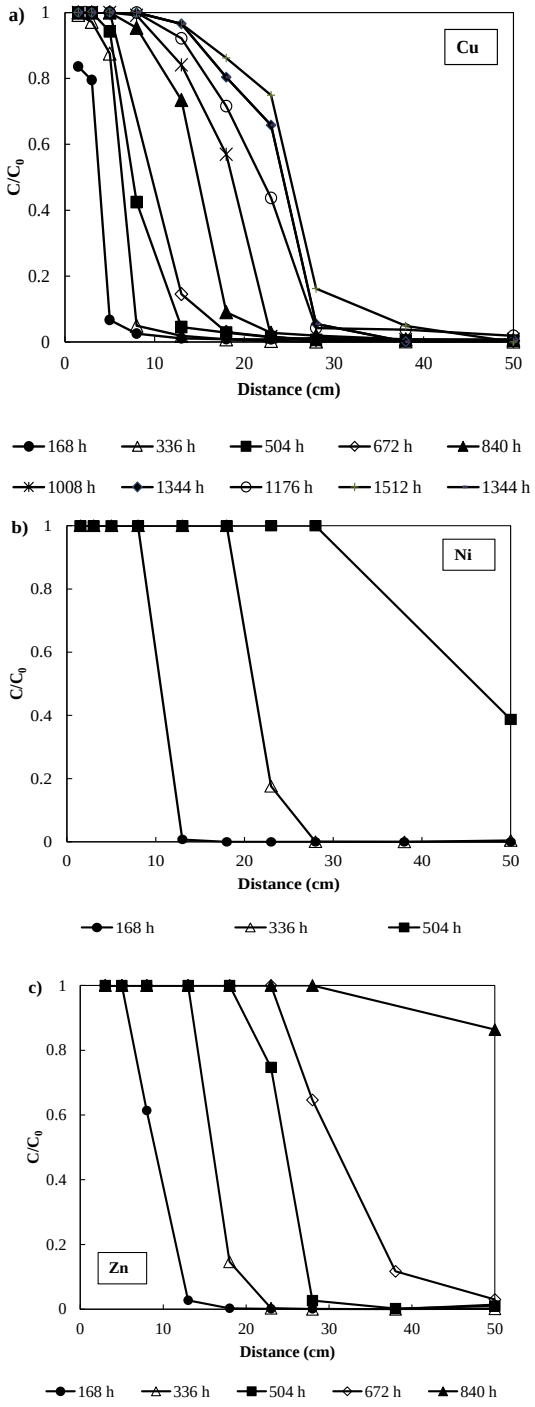

Figure 5.3 Normalized concentration (C/C_0) of a) copper, b) nickel and c) zinc as function of column distance (cm) for lapillus.

Figure 5.4a shows the breakthrough curves of copper, Figure 5.4b shows the breakthrough times as function of column distance. It can be clearly observed how the contamination front propagates linearly as the thickness of the lapillus increases.

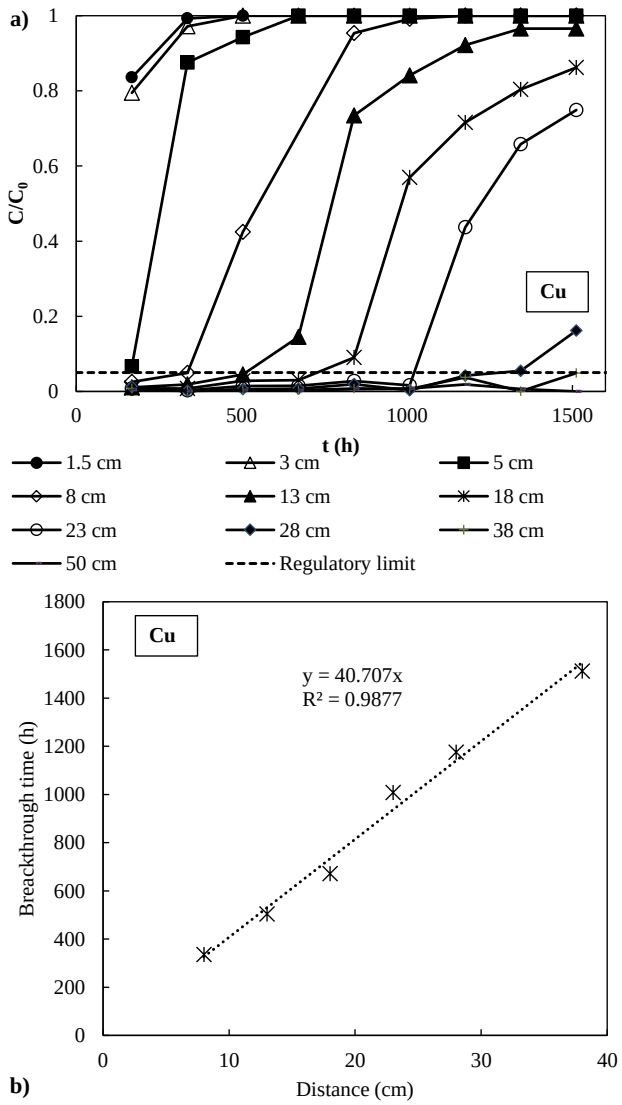

Figure 5.4 a) Normalized copper concentration (C/C_0) for different sampling ports as function of time (h) and b) breakthrough times (h) as function of column distance (cm) for lapillus column test.

The reactive medium shows a rapid exhaustion towards nickel, so there are not sufficient data to evaluate the trend of the breakthrough times with the thickness of the reactive medium.

As done for copper, Figure 5.5a shows the breakthrough curves of zinc whereas Figure 5.5b shows the breakthrough times as function of column distance.

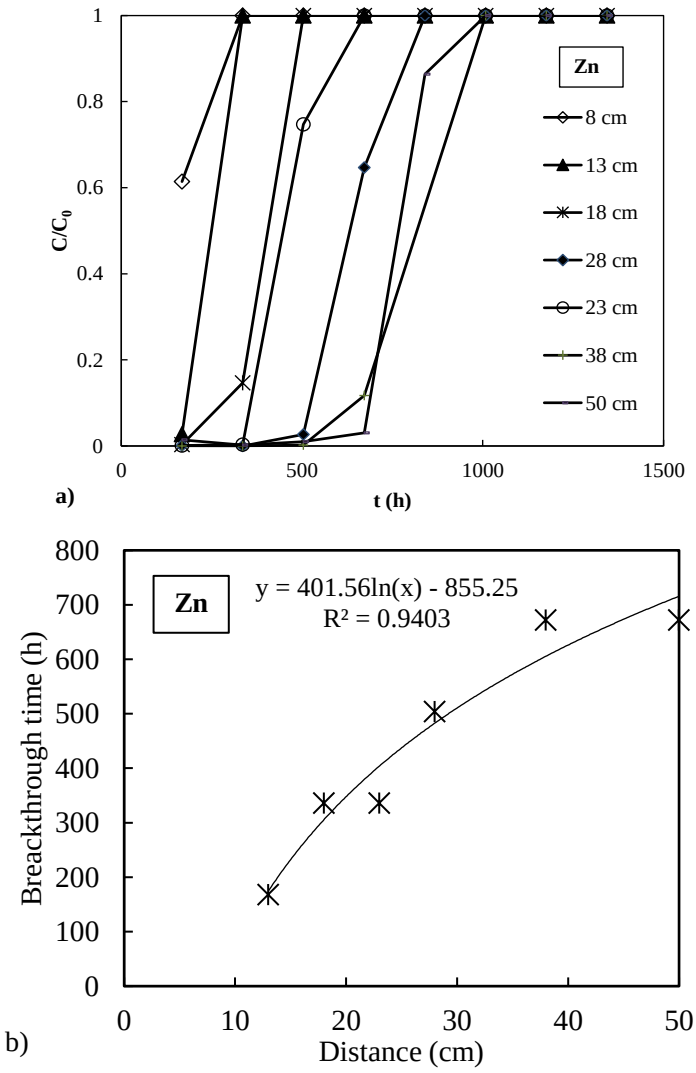

Figure 5.5 a) Normalized zinc concentration (C/C_0) for different sampling ports as functions of time (h) and b) breakthrough times (h) as function of column distance (cm) for lapillus column test.

Contrary to what is observed for copper, the breakthrough times do not increase linearly with the thickness of the reactive medium. This behaviour could be due to the occupation of the lapillus adsorption sites by copper.

In general, the rapid exhaustion of the lapillus towards nickel and zinc could be linked to the strong affinity of the lapillus towards copper that reduces the availability of adsorption sites.

The measurements of pH and potential of the solution at the outlet provided the results shown in Figure 5.6, plotted as a function of time. The pH is slightly acidic and remains between 6 and 7 for the entire test duration; the fluctuations of the values are more marked from 0 to 2000 hours.

The values of E_h increase during the test until they reach a stable value of about 70 mV.

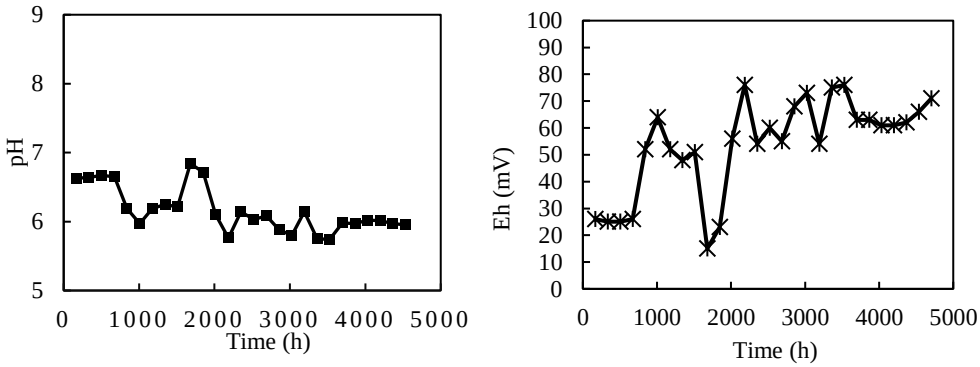

Figure 5.6 pH and E_h values in function of time for column D at port 9 (33 cm).

Figure 5.7 shows the permeability profile as function of the time for column D. As expected, the permeability remains constant for all test duration.

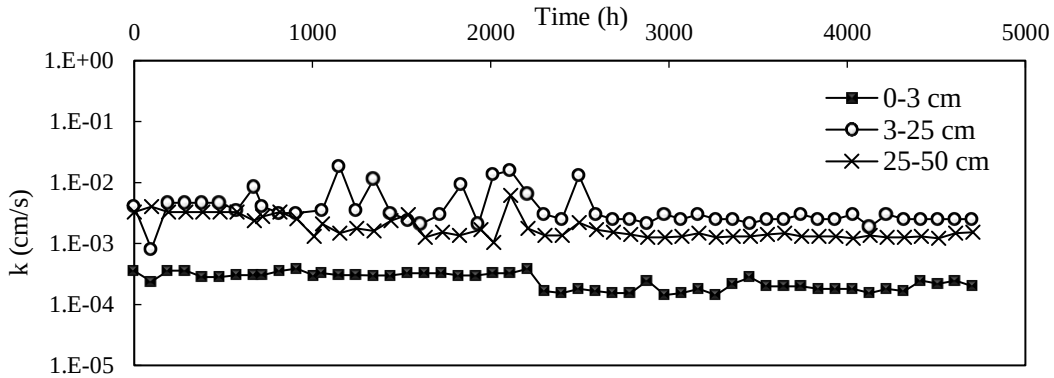

Figure 5.7 Permeability (cm/s) as function of time (h) for column D.

Figure 5.7 shows SEM image of the virgin lapillus (Fig. 5.7a and 5.7c), of the lapillus extracted from column (Fig. 5.7b and 5.7d) together with the atomic composition derived from EDX analysis conducted on the region depicted in Figure 5.7d (Fig. 5.7e).

a) b)

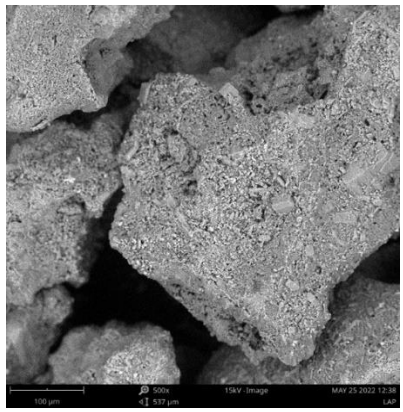

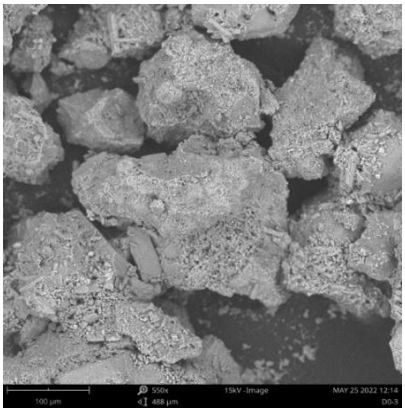

c)

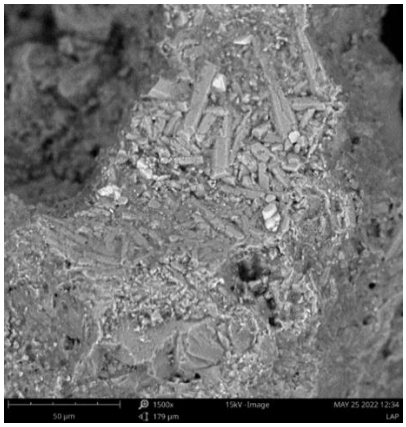

d)

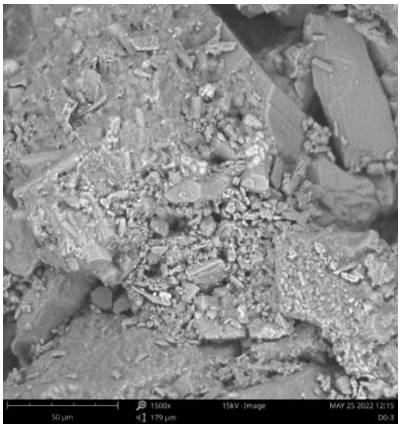

e)

	Weight percentage	Certainty
O	55.6 %	98.7 %
Si	14.7 %	98.4 %
Al	10.4 %	98.0 %
Fe	5.8 %	94.5 %
Cu	3.7 %	87.3 %
Ca	3.4 %	96.0 %
Zn	2.3 %	75.6 %
Na	1.6 %	90.4 %
K	1.4 %	93.1 %
Mg	1.3 %	91.6 %

Figure 5.8 SEM image of a) virgin lapillus (500x magnification) b) exhausted lapillus (550x magnification), c) virgin lapillus (1500x magnification), d) exhausted lapillus (1500x magnification); e) Atomic composition (weight %) of lapillus extracted from column referred to SEM image at 1500x magnification.

With reference to morphology, there is no clear difference between virgin and exhausted material. EDX analysis shows the presence of copper and zinc, the absence of nickel could be due to the lower removal efficiency for nickel compared to the other two metals.

From Figure 5.8 to 5.10 the efficiency of lapillus is compared with the ZVI/lapillus 10:90 granular mixture (Column M). The addition of 10% by volume of ZVI mixed with lapillus allows to considerably increase the longevity in terms of reactivity of a PRB.

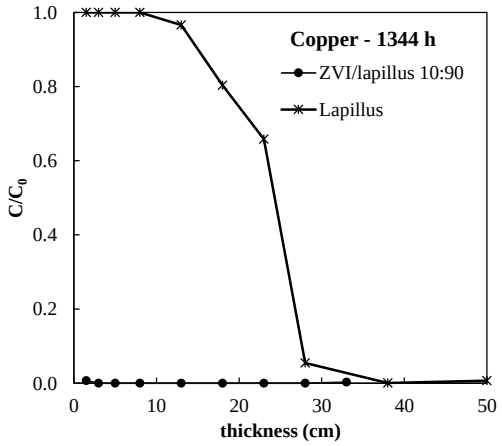

Figure 5.9 Normalized copper concentration (C/C_0) as function of thickness (cm) for the ZVI/lapillus 10:90 granular mixture and lapillus after 1344 hours.

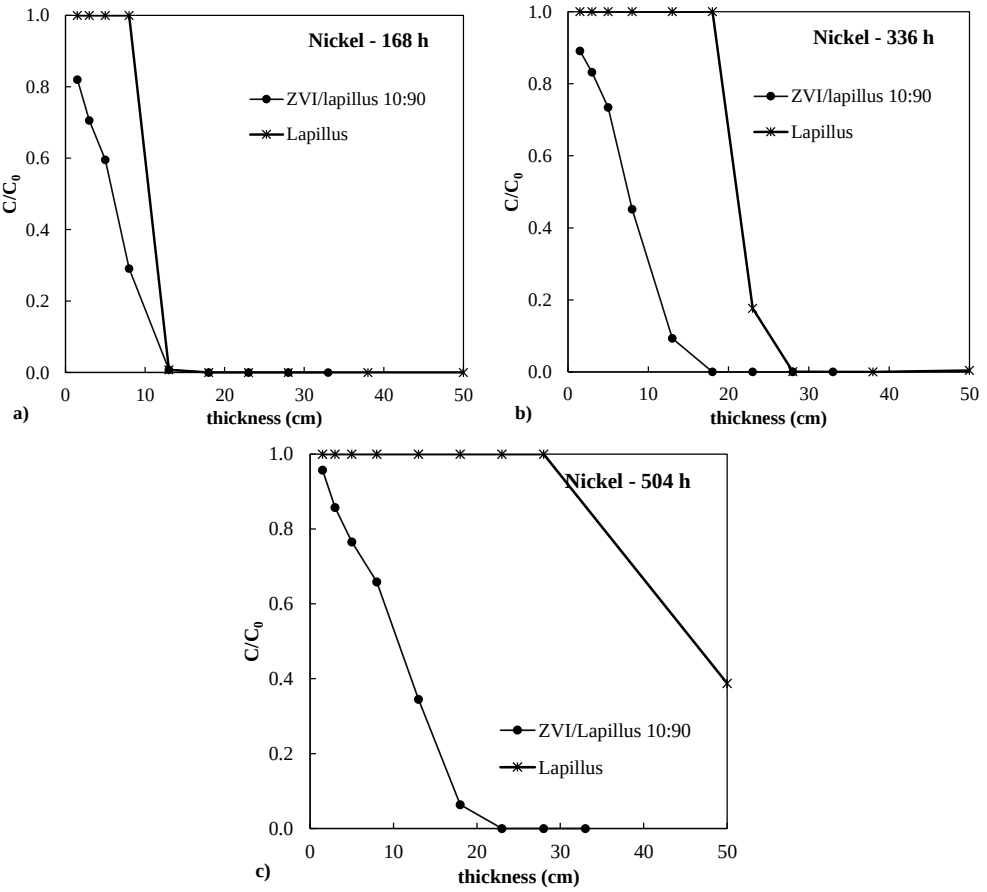

Figure 5.10 Normalized nickel concentration (C/C_0) as function of thickness (cm) for the ZVI/lapillus 10:90 granular mixture and lapillus after a) 168 h, b) 336 h and c) 504 h.

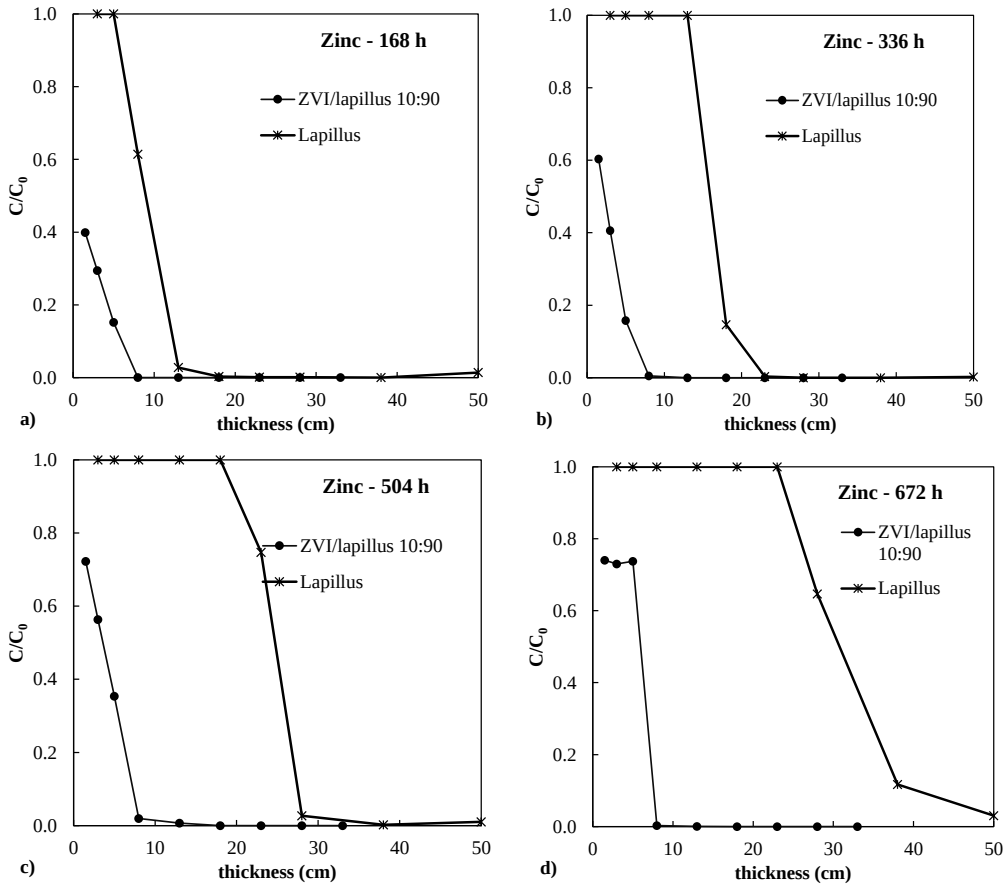

Figure 5.11 Normalized zinc concentration (C/C_0) as function of thickness (cm) for the ZVI/lapillus 10:90 granular mixture and lapillus after a) 168 h, b) 336 h, c) 504 h and d) 672 h.

6 REMOVAL EFFICIENCY OF ZVI/LAPILLUS MIXTURE AFTER AGING WITH NON-CONTAMINATED WATER

6.1 Introduction

Madaffari et al. (2017) observed that the removal capacity of a granular mixture containing ZVI is not constant along the reactive medium thickness. In particular, the authors showed that the mass of removed nickel was significantly higher near the inlet and that the ZVI located in the upper part of the column has shown a lower removal capacity. Therefore, it was hypothesized that the ZVI present in this part of the column is consumed in the reactions with water and with other constituents possibly present in the solution also in absence of the contaminant that was removed upstream.

Therefore, the aim of the study presented in this chapter is to show the efficiency of a ZVI/lapillus granular mixture aged with non-contaminated water. For this purpose, a mixture at volumetric ratio equal to 10:90 has been permeated with a non-contaminated water for 23 weeks (Column H_0); subsequently the mixture has been permeated with a pluri-contaminated solution (Column H_1) in order to evaluate the performance of ZVI corroded with water. The performance of the aged reactive medium has been compared with the performance of a virgin reactive medium in the same test conditions. The results were interpreted in terms of removal and hydraulic efficiency.

6.2 Column test program

Figure 6.1 shows the column test program presented in this chapter.

A ZVI/lapillus mixture at volumetric ratio equal to 10:90 was permeated in a first phase (Column H_0) with a solution of distilled water and $CaCO_3$ (10 mg/l) for 23 weeks. In a second phase (Column H_1), the reactive medium, aged with the above mentioned non-contaminated solution, was permeated with a tricontaminant solution with Cu, Ni and Zn in presence of $CaCO_3$. The flow rate used was equal to 0.5 ml/min. The characteristics of the two columns are summarized in Table 6.1.

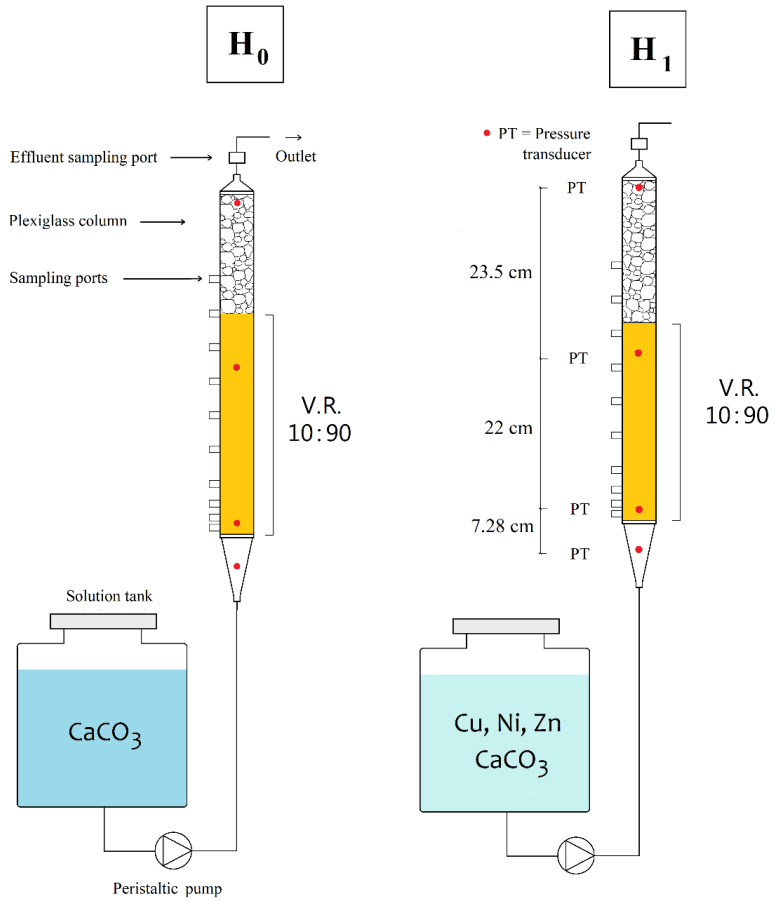

Figure 6.1 Schematic diagram of H_0 -H_1 column test.

Table 6.1 Main characteristics of H_0 -H_1 column tests.

ID	H_0	H_1
v.r. ZVI/lapillus	10:90	10:90
Total thickness (cm)	29	29
Test duration (h)	3864	840 (in progress)
Initial porosity (%)	42.9	

A comparison of the results obtained for column H with those obtained from columns E and M was made, with reference to permeability (Fig. 6.6) and relative concentrations of Cu, Ni and Zn (Fig. 6.2-5). The chemical composition of the contaminating solutions used for the three tests is compared in Table 6.2.

Table 6.2 Composition of inlet solutions.

ID	**Distilled water**	**Cu, Ni, Zn (18 mg/l)**	**$CaCO_3$ (10 mg/l)**
M	✓	✓	-
E	✓	✓	✓
H_0	✓	-	✓
H_1	✓	✓	✓

Figure 6.2 shows the trend over time of the relative concentrations of the three contaminants for the H_1 column at 5 cm (6.2a) and 33 cm (6.2b) from the base. The copper is almost completely removed at 5 cm. At the same thickness, the nickel concentration is nearly unchanged from the initial concentration; at 33 cm, the relative concentration of nickel rapidly increases over time with an approximately parabolic trend. However, the nickel concentrations at the outlet exceed the regulatory limit (CSC = 0.02 mg/l) right from the test beginning. Zinc is only minimally available at 5 cm but its presence at 33 cm is strongly reduced. The relative concentration of zinc at 5 and 33 cm increases linearly over time, but its absolute concentration remains below the regulatory limit (CSC = 3.0 mg/l) at 5 and 33 cm for the entire time window.

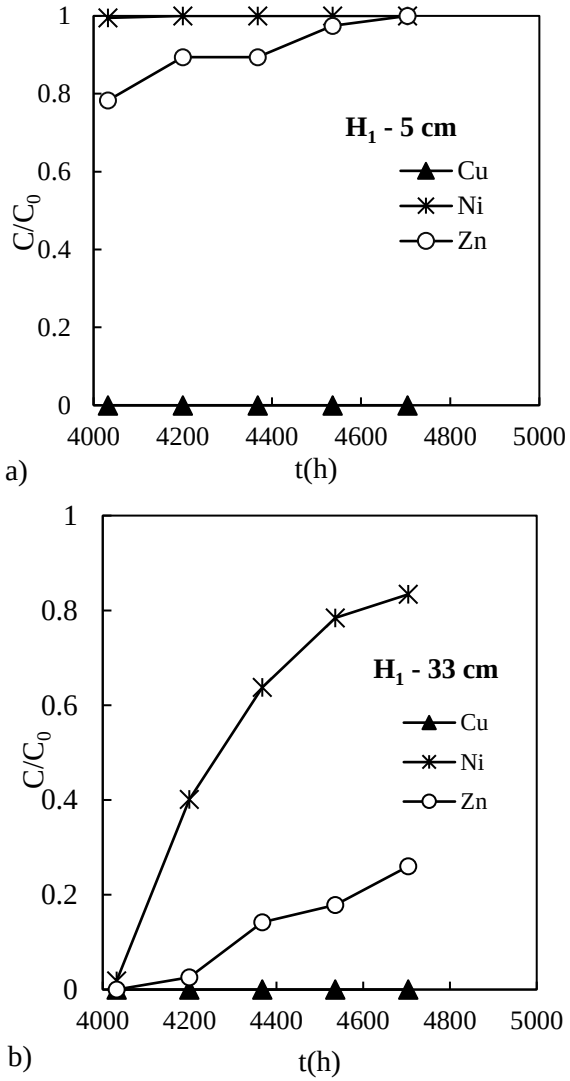

Figure 6.2 Cu, Ni and Zn relative concentrations as a function of time for column H_1 at a) 5 cm and b) 33 cm.

Figure 6.3 compares the relative Cu concentration values over time for columns M, E and H_1 at two sampling ports located at 5 (Fig. 6.3a) and 33 cm (Fig. 6.3b) from column inlet. It can be observed as the reactive medium aged with water does not reduce the removal capacity of ZVI towards copper.

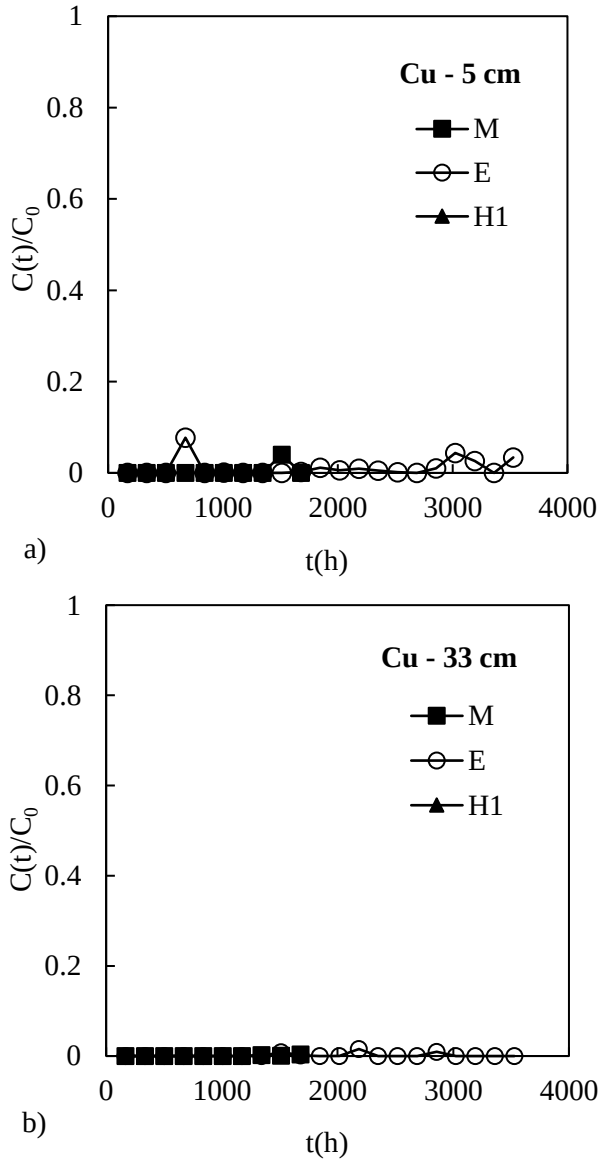

Figure 6.3 Relative Cu concentration for columns M, E and H_1 at a) 5 cm and b) 33 cm.

Figure 6.4 compares the relative Ni concentration values over time for columns M, E and H1 at two sampling ports located at 5 (Fig. 6.4a) and 33 cm (Fig. 6.4b) from column inlet. It can be observed as the reactive medium aged with water strongly reduce the removal capacity of ZVI towards nickel.

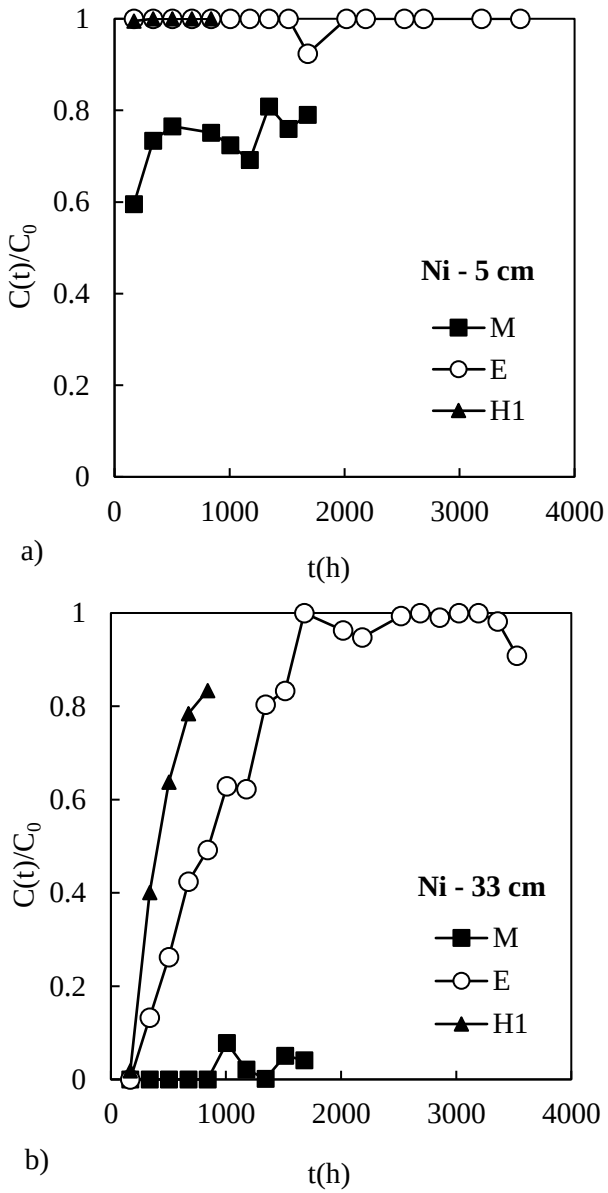

Figure 6.4 Relative Ni concentration for columns M, E and H_1 at a) 5 cm and b) 33 cm.

Figure 6.5 compares the relative Zn concentration values over time for columns M, E and H1 at two sampling ports located at 5 (Fig. 6.5a) and 33 cm (Fig. 6.5b) from column inlet. It can be observed as the reactive medium aged with water strongly reduce the removal capacity of ZVI towards zinc.

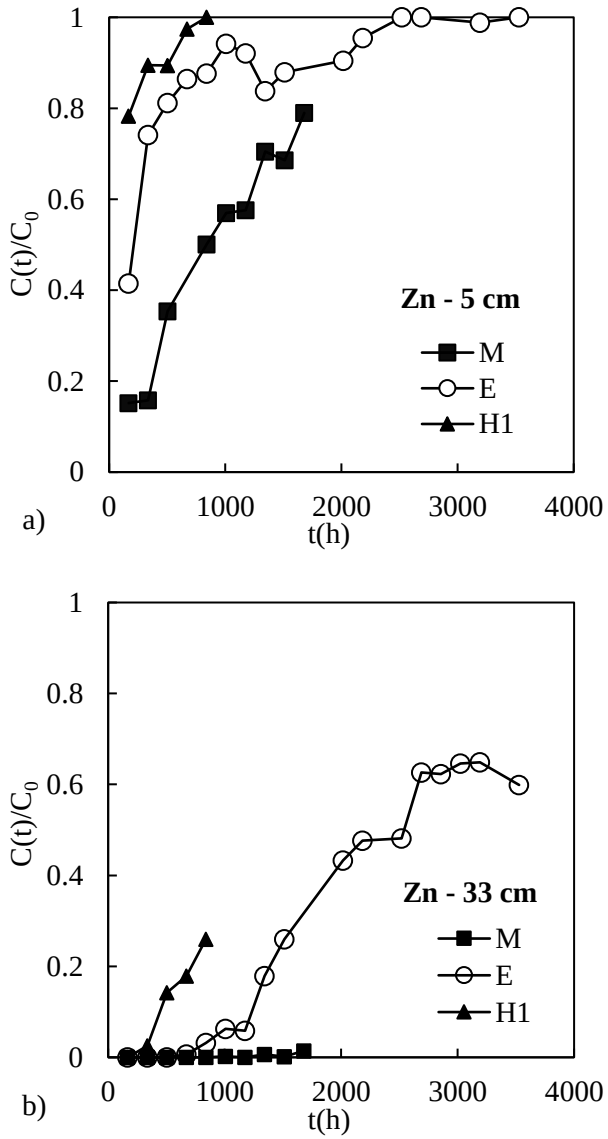

Figure 6.5 Relative Zn concentration for columns M, E and H_1 at a) 5 cm and b) 33 cm.

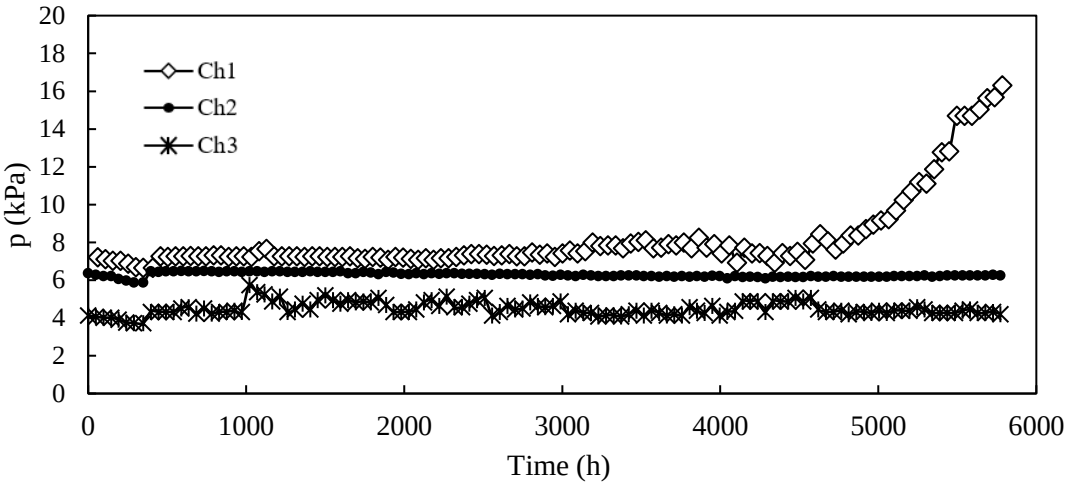

Figure 6.6 Pressure (kPa) detected at Channels 1, 2 and 3 vs. time (h) for column M.

Figure 6.7 compares the normalized permeability profiles for columns M, E and H, distinguishing for H the two phases H_0 and H_1. The permeability for the column H_0 (distilled water with $CaCO_3$) remains constant up to about 2000 hours; from 2000 to 4000 hours the values rapidly decrease by two orders of magnitude. From 4000 to 6000 hours (column H_1) the decrease in k slows down, but the values are still reduced by another order of magnitude.

The comparison between the trend of column H and that of columns M and E shows that the mixture aged through the passage of distilled water alone has a lower capacity to remove heavy metals if compared to that of a virgin mixture and that the reduction of permeability in the absence of contaminants is faster than in their presence. It is legitimate to hypothesize that the variation of the chemical composition of the inlet solution causes a variation of the corrosion kinetics of the iron. Figure 6.8 shows the H column test ongoing.

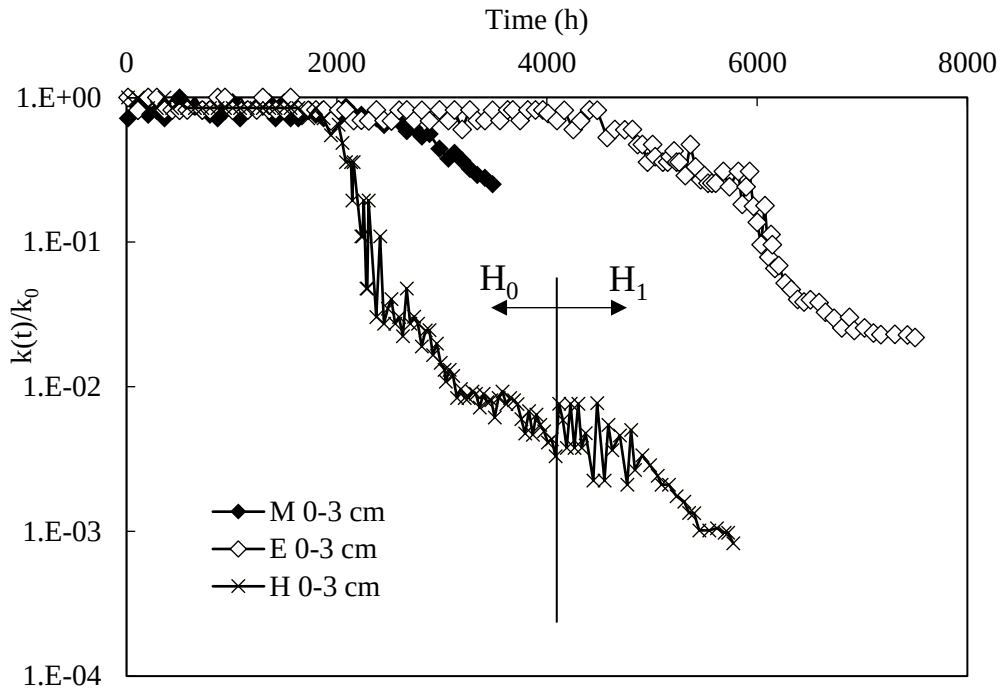

Figure 6.7 $k(t)/k_0$ profile over time for columns M, E and H.

Figure 6.8 Image of column H during the test.

7 CONCLUSIONS

In this thesis, several aspects not yet properly studied in the scientific literature and concerning the long-term behaviour of granular reactive mixtures of ZVI and lapillus, to be used in PRB for groundwater remediation, were investigated.
The first chapter provided an overview of the existing contamination and of the most used remediation technologies and a detailed description of the PRB technology, highlighting the design and construction aspects of the technology. Among the possible reactive materials of a PRB, particular attention was paid to ZVI. The aspects relating to the long-term hydraulic and reactive behaviour of a ZVI-PRB were studied through a description of the possible removal mechanisms activated by ZVI towards heavy metals and related to the corrosion phenomenon of iron in water.
The materials and methods used in the experimental activity carried out in this thesis, were described in the second chapter. Finally, results and discussion of the experimental activity were presented in chapters 3, 4, 5 and 6.
Chapter 3 dealt with the behaviour of a multilayer PRB configuration composed of two layers of a granular mixture of ZVI and lapillus each characterized by a different degree of iron dispersion. In the first layer, named "pre-treatment layer", ZVI particles were more dispersed in order to avoid the clogging phenomenon, which generally occurs at the barrier inlet.
The main results obtained from these tests can be summarized as follows:

- The presence of the pre-treatment zone is not beneficial in terms of nickel removal since it involves a rapid depletion of the barrier reactivity. Whereas in terms of zinc and copper removal, the pre-treatment zone can assure the simultaneous removal of the two contaminants with a moderate increase of the barrier thickness.

- When the PRB filling material revealed a short reactive lifetime, as in case of Nickel, it was possible to identify an optimal thickness of the barrier. In these cases, an increase in the thickness of the reactive medium does not correspond to a significant removal of the contaminant.

- As far as the hydraulic behaviour is concerned, the presence of the pre-treatment zone does not help to improve the hydraulic behaviour of a PRB if the ZVI particles are not properly dispersed. This dispersion is closely related to the iron corrosion processes, which are in turn linked to the flow velocity and chemical composition of the contaminated solution.

- Adopting the right dispersion of the iron particles, for example in this case a volumetric ratio of 5:95, the "pre-treatment" layer has not suffered a reduction in hydraulic conductivity and has allowed preserving the hydraulic conductivity of the subsequent layer assuring the correct hydraulic behaviour of the barrier. The long duration of this test (at least 8 months) suggested a strong slowdown in the corrosion process most likely linked to the reduction of its reactivity. Indeed, in the first centimetres the reactive medium reached the complete exhaustion of its reactivity. On the contrary, the formation of iron corrosion products that caused the permeability reduction observed in columns with a lower dispersion of ZVI particles, was likely responsible of the modest removal of contaminants. This behaviour confirmed the role of corrosion products in the removal of nickel and zinc.
- SEM images of the exhausted reactive medium extracted from the columns, revealed the presence of copper in the form of trapezoidal crystals or in the form of a bulbous formation, the presence of iron corrosion products having a spongeous nature and the presence of nickel and zinc most likely incorporated within iron corrosion products.

In Chapter 4, the behaviour of a ZVI/lapillus granular mixture (v.r. equal to 10:90) was investigated varying the geochemical conditions. In particular it was investigated i) the effect of $CaCO_3$ on the removal and hydraulic performance of the reactive medium permeated with a solution contaminated with Cu, Ni and Zn, and ii) the single effect of $NaHCO_3$ and the combined effect of $CaCO_3$ and $NaHCO_3$ using a solution contaminated with Ni and Zn. The main results obtained from these tests can be summarized as follows:

- In solutions contaminated by Cu, Ni and Zn the removal sequence observed was Cu>Zn>Ni.
- $CaCO_3$ affects the reactive and hydraulic behaviour of the reactive medium permeated with Cu, Ni and Zn. In terms of reactive behaviour, the removal efficiency of the Cu, Ni and Zn decreases in presence of $CaCO_3$. Whereas, in terms of hydraulic behaviour, the presence of $CaCO_3$ delays the hydraulic conductivity reduction.
- The removal efficiency of the ZVI/lapillus granular mixture towards Ni and Zn greatly increases in absence of copper.

- In a solution containing $NaHCO_3$, Ni and Zn, the presence of $CaCO_3$ does not affects the removal efficiency of the two heavy metals.

In Chapter 5, the efficacy of the lapillus towards Cu, Ni and Zn was investigated and the results compared with a ZVI/lapillus granular mixture. The main results obtained from this test are summarized as follows:

- Lapillus is selective in the removal of the three metals according to the following sequence Cu>Zn>Ni.
- With reference to Cu, the contamination front propagates linearly as the thickness of the lapillus increases, while for Nickel and Zinc the reactive medium shows a more rapid depletion. This behaviour has been attributed to the strong affinity of lapilli towards copper, which reduces the availability of adsorption sites for Ni and Zn.
- As expected, the hydraulic conductivity remained constant over time.
- From SEM-EDX analyses it was observed as there is no clear difference in the morphology of the grains between virgin and exhausted material. EDX analysis showed the presence of copper and zinc, whereas the absence of nickel was attributed to the lower removal efficiency of lapillus toward Ni compared to Cu and Zn.
- Comparing lapillus with the ZVI/lapillus 10:90 granular mixture it was observed as the addition of 10% by volume of ZVI allows to considerably increasing the longevity in terms of reactivity of a PRB.

In Chapter 6 the results of two column tests were presented. A ZVI/lapillus mixture at v.r. 10:90 was permeated in a first phase with a solution of distilled water and $CaCO_3$ (10 mg/l) for 23 weeks and, in a second phase, the reactive medium, aged with the above mentioned non-contaminated solution, was permeated with a tricontaminant solution with Cu, Ni and Zn in presence of $CaCO_3$. The main results obtained from this test are summarized as follows:

- The granular ZVI/lapillus mixture aged with water does not influence the removal capacity of ZVI towards Cu.
- The aging of the reactive medium with uncontaminated water strongly affects the removal capacity of ZVI towards Ni and Zn.

References

Benner, S., Blowes, D., Ptacek, C., Mayer, K., 2002. *Rates of sulfate reduction and metal sulfide precipitation in a permeable reactive barrier.* Appl. Geochemistry 17, 301–320. https://doi.org/10.1016/S0883-2927(01)00084-1

Bilardi, S., Calabrò, P.S., Moraci, N., Madaffari, M.G., Ranjbar, E., 2020. A comparison between Fe 0 /pumice and Fe 0 /lapillus mixtures in permeable reactive barriers. Environ. Geotech. 7, 524–539. https://doi.org/10.1680/jenge.17.00095

Bilardi S., 2012a. *Short and long term behaviour of Fe^0 and Fe^0/pumice granular mixtures to be used in PRB for groundwater remediation.* Ph. D. Thesis in Geotechnical Engineering at the Mediterranean University of Reggio Calabria.

Bilardi, S., Amos, R. T., Blowes, D. W., Calabrò P. S. and Moraci, N., 2012b. *Reactive Transport Modeling of ZVI Column Experiments for Nickel Remediation.* Ground Water Monitoring & Remediation 33(1): 97–104. https://doi.org/10.1111/j.1745-6592.2012.01417.x

Bilardi, S., Calabrò, P.S. and Moraci, N., 2012c. *Are accelerated column tests used in permeable reactive barriers design sufficiently reliable? Proceeding of the Third International Conference on Hazardous and Industrial Waste Management, Crete, Greece.* Technical University of Crete, Chania, Greece.

Bilardi, S., Calabrò, P.S., Caré, S., Moraci, N., Noubactep, C., 2013a. *Effect of Pumice and Sand on the Sustainability of Granular Iron Beds for the Aqueous Removal of Cu^{II}, Ni^{II}, and Zn^{II}.* Clean - Soil, Air, Water 41, 835–843. https://doi.org/10.1002/clen.201100472

Bilardi, S., Calabrò, P.S., Caré, S., Moraci, N., Noubactep, C., 2013b. *Improving the sustainability of granular iron/pumice systems for water treatment*. J. Environ. Manage. 121, 133–41. https://doi.org/10.1016/j.jenvman.2013.02.042

Bilardi S., Calabrò P.S., Moraci N., 2014. *Simultaneous removal of Cu^{II}, Ni^{II} and Zn^{II} by a granular mixture of zero-valent iron and pumice in column systems.* Desalination and Water Treatment 55(3): 767-776. https://doi.org/10.1080/19443994.2014.916234

Bilardi, S., Ielo, D., Moraci, N., & Calabrò, P. S., 2016. *Reactive and Hydraulic Behavior of Permeable Reactive Barriers Constituted by Fe^0 and Granular Mixtures of Fe^0/Pumice.* Procedia Engineering 158, 446–451. https://doi.org/10.1016/j.proeng.2016.08.470

Bilardi, S., Calabrò, P. S., Greco, R., & Moraci, N., 2018a. *Removal of heavy metals from landfill leachate using zero-valent iron and granular activated carbon.* Environmental Technology, 1-13. https://doi.org/10.1080/09593330.2018.1503725

Bilardi, S., Calabrò, P. S., Greco, R., & Moraci, N., 2018b. *Selective removal of heavy metals from landfill leachate by reactive granular filters.* Science of The Total Environment 644, 335–341. https://doi.org/10.1016/j.scitotenv.2018.06.353

Bilardi, S., Calabrò, P. S., Moraci, N., Madaffari, M. G., & Ranjbar, E., 2018c. *A Comparison between Fe^0/Pumice and Fe^0/Lapillus Mixtures in Permeable Reactive Barriers.* Environmental Geotechnics, 1–52. https://doi.org/10.1680/jenge.17.00095

Bilardi, S., Calabrò, P. S., & Moraci, N., 2019. *The removal efficiency and long-term hydraulic behaviour of zero valent iron/lapillus mixtures for the simultaneous removal of Cu^{2+}, Ni^{2+} and Zn^{2+}.* Science of The Total Environment 675, 490–500. https://doi.org/10.1016/j.scitotenv.2019.04.260

Bilardi, S., Calabrò, P.S., Moraci, N., Madaffari, M.G., Ranjbar, E., 2020. *A comparison between Fe_0/pumice and Fe_0/lapillus mixtures in permeable reactive barriers.* Environ. Geotech. 7, 524–539. https://doi.org/10.1680/jenge.17.00095

Birke, V., Burmeier, H., Jefferis, S., Gaboriau, H., Touze, S., Romain, C., Harald, B., Stephan, J., Herve, G., 2007. *Permeable reactive barriers (PRBs) in Europe: Potentials and expectations.* Ital. J. Eng. Geol. Environ. 1, 1–8. https://doi.org/10.4408/IJEGE.2007-01.S-04

Blowes, D.W., Ptacek, C.J., Benner, S.G., McRae, C.W., T., Bennett, T.A., Puls, R.W., 2000. *Treatment of inorganic contaminants using permeable reactive barriers.* J. Contam. Hydrol. 45, 123–137. https://doi.org/10.1016/S0169-7722(00)00122-4

Blowes, D.W., Ptacek, C.J., Cherry, J.A., Gillham, R.W., Robertson, W.D., 1995. *Passive remediation of groundwater using in situ treatment curtains*. Acar, Y.B., Daniel, D.E.

(Eds.), Geoenvironment 2000: Characterization, Containment, Remediation, and Performance in Environmental Geotechnics. pp. 1588–1607.

Calabrò, P.S., Moraci, N., Suraci, P., 2011. *Estimate of the optimum weight ratio in Zero-Valent Iron/Pumice granular mixtures used in permeable reactive barriers for the remediation of nickel contaminated groundwater.* Journal of Hazardous Materials, 207-208, 111–116. https://doi.org/10.1016/j.jhazmat.2011.06.094

Calabrò, P.S., Bilardi, S., Moraci, N., 2021. *Advancements in the use of filtration materials for the removal of heavy metals from multicontamined solutions*. Current Opinion in Environmental Science & Health, 20. https://doi.org/10.1016/j.coesh.2021.100241

Cantrell, K.J., Kaplan, D.I., Wietsma, T.W., 1995. *Zero-valent iron for the in situ remediation of selected metals in groundwater.* J. Hazard. Mater. 42, 201–212. https://doi.org/10.1016/0304-3894(95)00016-N

Carey, M.A., Fretwell, B.A., Mosley, N.G., Smith, J.W.N., 2002. *Guidance on the Use of Permeable Reactive Barriers for Remediating Contaminated Groundwater.* National Groundwater and Contaminated Land Centre Report NC/01/51, UK Environment Agency, Bristol. 140pp. 24.

Corniello, A., Ducci, D., Ruggieri, G., & Iorio, M., 2018. *Complex groundwater flow circulation in a carbonate aquifer: Mount Massico (Campania Region, Southern Italy). Synergistic hydrogeological understanding.* Journal of Geochemical Exploration, 190, 253–264. https://doi.org/10.1016/j.gexplo.2018.03.017

Corniello, A., Ducci, D., 2014. *Hydrogeochemical characterization of the main aquifer of the "Litorale Domizio-Agro Aversano NIPS" (Campania — southern Italy)*. Journal of Geochemical Exploration, 137, 1–10. https://doi.org/10.1016/j.gexplo.2013.10.016

Cundy, A.B., Hopkinson, L., Whitby, R.L.D., 2008. *Use of iron-based technologies in contaminated land and groundwater remediation: a review.* Sci. Total Environ. 400, 42–51. https://doi.org/10.1016/j.scitotenv.2008.07.002

De Vita, P., Allocca, V., Celico, F., Fabbrocino, S., Mattia, C., Monacelli, G., Musilli, I., Piscopo, V., Scalise, A. R., Summa, G., Tranfaglia, G., Celico, P., 2018. *Hydrogeology of*

continental southern Italy. Journal of Maps, 14(2), 230–241. https://doi.org/10.1080/17445647.2018.1454352

Dong, H., Li, L., Lu, Y., Cheng, Y., Wang, Y., Ning, Q., Wang, B., Zhang, L., Zeng, G., 2019. *Integration of nanoscale zero-valent iron and functional anaerobic bacteria for groundwater remediation: A review.* Environ Int 2019. https://doi.org/10.1016/j.envint.2019.01.030

Di Molfetta, A., Sethi, R., 2005. *"Barriere Reattive Permeabili". Bonifica di siti contaminati. Caratterizzazione e tecnologie di risanamento.* McGraw-Hill, ed. The McGraw-Hill Companies, S.r.l. Publishing Group Italia, cap. 26, pp.562-605.

Elder, C.R., Benson, C.H., 2018. *Performance and economic comparison of PRB types in heterogeneous aquifers.* Environ. Geotech. 6, 214–224. https://doi.org/10.1680/jenge.17.00063

Franklin, O.N., Jolanta, K.-M., Grzegorz, M., & Krzysztof, W., 2020. *Assessment of zeolite and compost-zeolite mixture as permeable reactive materials for the removal of lead from a model acidic groundwater.* Journal of Contaminant Hydrology, 103597. https://doi.org/10.1016/j.jconhyd.2019.103597

Galdames A., Ruiz-Rubio L., Orueta M., Sánchez-Arzalluz M., Vilas-Vilela J.L., 2020. *Zero-valent iron nanoparticles for soil and groundwater remediation.* Int. J. Environ. Res. Public Health. https://doi.org/10.3390/ijerph17165817.

Gavaskar, A., Gupta, N., Sass, B., Janosy, R., Hicks, J., 2000. Design Guidance for Application of Permeable Reactive Barriers for Groundwater Remediation.

Gazzetta Ufficiale della Repubblica Italiana, 2006. *Norme in materia ambientale. Poligrafico dello Stato, Roma.* Gazzetta Ufficiale n. 88 del 14 aprile 2006 (in Italian).

Gheju, M., Balcu, I., Vancea, C., 2016. *An investigation of Cr(VI) removal with metallic iron in the co-presence of sand and/or MnO_2.* J. Environ. Manage. 170, 145–151. https://doi.org/10.1016/j.jenvman.2016.01.013

Giroud, J. P. Raymond, G.P., 1996. *Granular filters and geotextile filters.* Geofilters. pp. 565–680.

Gong, L., Lv, N., Qi, J., Qiu, X., Gu, Y., He, F., 2020. *Effects of non-reducible dissolved solutes on reductive dechlorination of trichloroethylene by ball milled zero valent irons.* J. Hazard. Mater. https://doi.org/10.1016/j.jhazmat.2020.122620

Gupta, V.K., Jain, C.K., Ali, I., Sharma, M., Saini, V.K., 2003. *Removal of cadmium and nickel from wastewater using bagasse fly ash - A sugar industry waste.* Water Res. 37, 4038–4044. https://doi.org/10.1016/S0043-1354(03)00292-6

He Y., Lin H., Luo M., Liu J., Dong Y., Li B., 2020. *Highly efficient remediation of groundwater co-contaminated with Cr(VI) and nitrate by using nano-Fe/Pd bimetal-loaded zeolite: Process product and interaction mechanism.* Environ. Pollut. https://doi.org/10.1016/j.envpol.2020.114479

Henderson, A.D., Demond, A.H., 2011. *Impact of Solids Formation and Gas Production on the Permeability of ZVI PRBs.* J. Environ. Eng. 137, 689–696. https://doi.org/10.1061/(ASCE)EE.1943-7870.0000383

Henderson, A.D., Demond, A.H., 2007. *Long-Term Performance of Zero-Valent Iron Permeable Reactive Barriers: A Critical Review.* Environ. Eng. Sci. 24, 401–423. https://doi.org/10.1089/ees.2006.0071

Holmes, R.R., Hart, M.L., Kevern, J.T., 2017. *Heavy metal removal capacity of individual components of permeable reactive concrete.* J. Contam. Hydrol. 196, 52–61. https://doi.org/10.1016/j.jconhyd.2016.12.005

Hu, R., Yang, H., Tao, R., Cui, X., Xiao, M., Amoah, B.K., Cao, V., Lufingo, M., Soppa-Sangue, N.P., Ndé-Tchoupé, A.I., Gatcha-Bandjun, N., Sipowo-Tala, V.R., Gwenzi, W., Noubactep, C., 2020. *Metallic Iron for Environmental Remediation: Starting an Overdue Progress in Knowledge.* Water 12, 641. https://doi.org/10.3390/w12030641

ITRC, 2011. *Permeable Reactive Barrier: Technology Update PRB-5.* Interstate Technology & Regulatory Council.

Jeen, S.-W., Blowes, D.W., Gillham, R.W., 2008. *Performance evaluation of granular iron for removing hexavalent chromium under different geochemical conditions.* J. Contam. Hydrol. 95, 76–91. https://doi.org/10.1016/j.jconhyd.2007.07.012

Jeen, S.W., Jambor, J.L., Blowes, D.W., Gillham, R.W., 2007. *Precipitates on Granular Iron in Solutions Containing Calcium Carbonate with Trichloroethene and Hexavalent Chromium.* Environ. Sci. Technol. 41, 1989–1994. https://doi.org/10.1021/es0618393

Kenney, T.C., Lau, D., 1985. *Internal stability of granular filters.* Can. Geotech. J. https://doi.org/10.1139/t85-029

Kezdi, A., 1969. *Increase of protective capacity of flood control dikes.* Dep. Geotech. Tech. Univ. Budapest, Rep.

Khan, F.I., Husain, T., Hejazi, R., 2004. *An overview and analysis of site remediation technologies* 71, 95 122. https://doi.org/10.1016/j.jenvman.2004.02.003

Li, L., Benson, C.H., Lawson, E.M., 2006. *Modeling porosity reductions caused by mineral fouling in continuous-wall permeable reactive barriers.* J. Contam. Hydrol. 83, 89–121. https://doi.org/10.1016/j.jconhyd.2005.11.004

Li, L., Benson, C.H., Lawson, E.M., 2005. *Impact of mineral fouling on hydraulic behavior of permeable reactive barriers.* Ground Water. https://doi.org/10.1111/j.1745-6584.2005.0042.x

Li, S., Wang, W., Liang, F., Zhang, W.X., 2017. *Heavy metal removal using nanoscale zero-valent iron (nZVI): Theory and application.* J. Hazard Mater. https://doi.org/10.1016/j.jhazmat.2016.01.032

Li, S., Yang, F., Li, J., Cheng, K., 2020. *Porous biochar-nanoscale zero-valent iron composites: Synthesis, characterization and application for lead ion removal.* Sci Total Environ, 746:141037.

Lyu, H., Tang, J., Cui, M., Gao, B., Shen, B., 2020. *Biochar/iron (BC/Fe) composites for soil and groundwater remediation: Synthesis, applications, and mechanisms.* Chemosphere. https://doi.org/10.1016/j.chemosphere.2019.125609.

Liang, L., Korte, N., Gu, B., Puls, R., Reeter, C., 2000. *Geochemical and microbial reactions affecting the long-term performance of in situ "iron barriers"*. Adv. Environ. Res. 4, 273–286. https://doi.org/10.1016/S1093-0191(00)00026-5

Liu, T., Rao, P., Lo, I.M.C., 2009. *Influences of humic acid, bicarbonate and calcium on Cr(VI) reductive removal by zero-valent iron*. Sci. Total Environ. https://doi.org/10.1016/j.scitotenv.2009.01.043

Lo, I.M.C., Lam, C.S.C., Lai, K.C.K., 2006. *Hardness and carbonate effects on the reactivity of zero-valent iron for Cr(VI) removal*. Water Res. https://doi.org/10.1016/j.watres.2005.11.033

Madaffari, M.G., 2015. *New mixtures to be used in PBR for heavy-metals contaminated groundwater remediation: long-term removal efficiency and hydraulic behavior.* Ph. D. Thesis in Geotechnical Engineering at the Mediterranean University of Reggio Calabria.

Madaffari, M.G., Bilardi, S., Calabrò, P.S., Moraci, N., 2017. Nickel removal by zero valent iron/lapillus mixtures in column systems. Soils Found. 57, 745–759. https://doi.org/10.1016/j.sandf.2017.08.006

Mak, M.S.H., Rao, P., Lo, I.M.C., 2009. *Effects of hardness and alkalinity on the removal of arsenic(V) from humic acid-deficient and humic acid-rich groundwater by zero-valent iron*. Water Res. 43, 4296–4304. https://doi.org/10.1016/j.watres.2009.06.022

Moraci, N., 2010. Geotextile filter: Design, characterization and factors affecting clogging and blinding limit states, in: 9th International Conference on Geosynthetics - Geosynthetics: Advanced Solutions for a Challenging World, ICG 2010. Brazilian Chapter of the International Geosynthetics Society, pp. 413–438.

Moraci, N., Bilardi, S., Calabrò, P.S., 2017. *Fe^0/pumice mixtures: from laboratory tests to permeable reactive barrier design.* Environ. Geotech. 4, 245–256. https://doi.org/10.1680/jenge.15.00002

Moraci, N., Bilardi, S., Calabrò, P.S., 2016. *Critical aspects related to Fe^0 and Fe^0/pumice PRB design.* Environ. Geotech. 3, 114–124. https://doi.org/10.1680/envgeo.13.00120

Moraci, N., Bilardi, S., Calabrò, P.S., 2015. *Design of permeable reactive barriers for remediation of groundwater contaminated by heavy metals*. Riv. Ital. di Geotec. 49, 59–86.

Moraci, N., Calabrò, P.S., 2010. *Heavy metals removal and hydraulic performance in zero-valent iron/pumice permeable reactive barriers.* J. Environ. Manage. 91, 2336–2341. https://doi.org/10.1016/j.jenvman.2010.06.019

Moraci, N., Calabrò, P.S., Suraci, P., 2011. *Long-term efficiency of Zero-Valent iron - Pumice Granular mixtures for the removal of Copper or Nickel from groundwater.* Soils and Rocks 34, 129–138.

Moraci N., Calabrò P. S., Bilardi S., 2010b. *Efficiency of Zero valent iron/pumice granular mixtures in simultaneous removal of Copper and Nickel.* Proc. of the Second International Conference Hazardous and Industrial Waste Management, Chania (Creta).

Moraci N., Calabrò, P. S., Suraci, P., 2010c. *Estimate of the optimum weight ratio in zero valent iron/pumice granular mixtures used in permeable reactive barriers for the remediation of nickel contaminated groundwater.* Proc. of the Second International Conference Hazardous and Industrial Waste Management, Chania (Creta).

Moraci, N., Calabrò, P.S., Suraci, P., 2011. *Long-term efficiency of Zero-Valent iron/pumice granular mixtures for the removal of Copper or Nickel from groundwater.* Soils and Rocks 34 (2): 129-138.

Moraci, N., Ielo, D., Bilardi, S., Calabro, P.S., 2016. *Modelling long-term hydraulic conductivity behaviour of zero valent iron column tests for permeable reactive barrier design.* Can. Geotech. J. 53, 946–961. https://doi.org/10.1139/cgj-2015-0453

Moraci, N., Mandaglio, M.C., Ielo, D., 2012. A new theoretical method to evaluate the internal stability of granular soils. Can. Geotech. J. 49, 45–58. https://doi.org/10.1139/t11-083

Moraci N., Rigano G., Suraci, P., Calabrò P.S., Panzera G., Antonucci P.L., 2008. *Studio sperimentale sull'efficienza di barriere permeabili reattive per la bonifica di acque di*

falda contaminate da metalli pesanti. Atti del Simposio Internazionale di Ingegneria Sanitaria e Ambientale SIDISA 2008. Firenze, 24-27 Giugno 2008.

Noubactep, C., 2013. *Metallic iron for environmental remediation: The long walk to evidence.* Corros. Rev. 31, 51–59. https://doi.org/10.1515/corrrev-2013-0018

Noubactep, C., 2010. *The suitability of metallic iron for environmental remediation.* Environ. Prog. Sustain. Energy 29, 286–291. https://doi.org/10.1002/ep.10406

Noubactep, C., 2008. *A Critical Review on the Process of Contaminant Removal in Fe^0–H_2O Systems.* Environ. Technol. 29, 909–920. https://doi.org/10.1080/09593330802131602

Noubactep, C., Schöner, A., Meinrath, G., 2006. *Mechanism of uranium removal from the aqueous solution by elemental iron.* Journal of Hazardous Materials 132, 202–212. https://doi.org/10.1016/j.jhazmat.2005.08.047

Noubactep, C., Schöner, A., 2009. Fe^0-based alloys for environmental remediation: Thinking outside the box. Journal of Hazardous Materials, 165, 1210–1214. https://doi.org/10.1016/j.jhazmat.2008.09.084

Obiri-Nyarko, F., Grajales-Mesa, S.J., Malina, G., 2014. *An overview of permeable reactive barriers for in situ sustainable groundwater remediation.* Chemosphere 111, 243–259. https://doi.org/10.1016/j.chemosphere.2014.03.112

Obiri-Nyarko, F., Kwiatkowska-Malina, J., Malina, G., & Kasela, T., 2015. *Geochemical modelling for predicting the long-term performance of zeolite-PRB to treat lead contaminated groundwater.* Journal of Contaminant Hydrology, 177-178, 76–84. https://doi.org/10.1016/j.jconhyd.2015.03.007

Ou, J.H., Sheu, Y.T., Tsang, D.C.W., Sun, Y.J., Kao, C.M., 2020. *Application of iron/aluminum bimetallic nanoparticle system for chromium-contaminated groundwater remediation*. Chemosphere 256. https://doi.org/10.1016/j.chemosphere.2020.127158

Powell, R.M., Blowes, D.W., Gillham, R.W., Schultz, D., Sivavec, T., Puls, R.W., Vogan, J.L., Powell, P.D., Landis, R., 1998. *Permeable Reactive Barrier Technologies for*

Contaminant Remediation. Report EPA/600/R-98/125, U. S. Environmental Protection Agency, Washington, DC, 51pp.

Powell, R.M., Puls, R.W., Blowes, D.W., Vogan, J.L., Gillham, R.W., Powell, P.D., Schultz, D., Sivavee, T., Landis, R., 1998. *Permeable Reactive Barrier Technologies for Contaminant Remediation*. EPA/600/R-98/125. https://doi.org/EPA/600/R-98/125

Pratt, A.R., Blowes, D.W., Ptacek, C.J., 1997. *Products of Chromate Reduction on Proposed Subsurface Remediation Material*. Environ. Sci. Technol. 31, 2492–2498. https://doi.org/10.1021/es9607897

Puls, R.W., Blowes, D.W., Gillham, R.W., 1999. *Long-term performance monitoring for a permeable reactive barrier at the U. S. Coast Guard Support Center, Elyzabeth City, North Carolina.* Journal of Hazardous Materials, 68, 109–124. https://doi.org/10.1016/S0304-3894(99)00034-5

Qian, L., Shang, X., Zhang, B., Zhang, W., Su, A., Chen, Y., Ouyang, D., Han, L., Yan, J., Chen, M., 2019. *Enhanced removal of Cr(VI) by silicon rich biochar-supported nanoscale zero-valent iron.* Chemosphere 215, 739-745. https://doi.org/10.1016/j.chemosphere.2018.10.030

Rigano G., 2007. *Studio dell'efficienza di barriere permeabili reattive per la bonifica di acquiferi contaminati da metalli pesanti.* Ph. D. Thesis in Geotechnical Engineering in The Mediterranean University of Reggio Calabria.

Skinner, S.J., Schutte, C.F., 2006. *The feasibility of a permeable reactive barrier to treat acidic sulphate – and nitrate – contaminated groundwater.* Water SA 32 (2), 129–136.

Shan, C., Chen, J., Yang, Z., Jia, H., Guan, X., Zhang, W., Pan, B., 2018. *Enhanced removal of Se(VI) from water via pre-corrosion of zero-valent iron using H_2O_2/HCl: Effect of solution chemistry and mechanism investigation*. Water Res. https://doi.org/10.1016/j.watres.2018.01.038

Sherard, J.L., 1979. *Sinkholes in dams of coarse, broadly graded soils. Technology Review.* Int Comm on Large Dams, pp. 25–35.

Starr, R.C., Cherry, J.A., 1994. *In Situ Remediation of Contaminated Ground Water: The Funnel-and-Gate System.* Ground Water 32, 465–476. https://doi.org/10.1111/j.1745-6584.1994.tb00664.x

Suraci P., 2011. *Studio sperimentale dell'efficienza di barriere permeabili reattive per la bonifica di acque di falda contaminate da metalli pesanti.* Ph. D. Thesis in Geotechnical Engineering in The Mediterranean University of Reggio Calabria.

Tasharrofi, S., Rouzitalab, Z., Maklavany, D. M., Esmaeili, A., Rabieezadeh, M., Askarieh, M., Rashidi, A., Taghdisian, H., 2020. *Adsorption of cadmium using modified zeolite-supported nanoscale zero-valent iron composites as a reactive material for PRBs*. Science of The Total Environment, 736. https://doi.org/10.1016/j.scitotenv.2020.139570

Tosco, T., Petrangeli Papini, M., Cruz Viggi, C., Sethi, R., 2014. *Nanoscale zerovalent iron particles for groundwater remediation: A review.* J. Clean. Prod. https://doi.org/10.1016/j.jclepro.2013.12.026

Tratnyek, P.G., 2002. *Keeping up with all that literature: The IronRefs database turns 500.* Gr. Water Monit. Remediat. 22, 92–94. https://doi.org/10.1111/J.1745-6592.2002.TB00757.X

Ullah, S., Faiz, P., Leng, S., 2020. *Synthesis, Mechanism, and Performance Assessment of Zero-Valent Iron for Metal-Contaminated Water Remediation: A Review*. Clean - Soil, Air, Water 48(9). https://doi.org/10.1002/clen.202000080

USEPA, 2002. *Field Applications of In Situ Remediation Technologies: Permeable Reactive Barriers.* USEPA Publ. EPA 542-R-, 1–122.

USEPA, 1999. *Field Applications of In Situ Remediation Technologies: Permeable Reactive Barriers.* USEPA Publication.

Wang, M., Cheng, W., Wan, T., Hu, B., Zhu, Y., Song, X., Sun, Y., 2019. *Mechanistic investigation of U(VI) sequestration by zero-valent iron/activated carbon composites*. Chem. Eng. J. https://doi.org/10.1016/j.cej.2018.12.138

Wantanaphong, J., Mooney, S.J., Bailey, E.H., 2005. Natural and waste materials as metal sorbents in permeable reactive barriers (PRBs). Environ. Chem. Lett. https://doi.org/10.1007/s10311-005-0106-y

Xin, J., Tang, F., Yan, J., La, C., Zheng, X., Liu, W., 2018. *Investigating the efficiency of microscale zero valent iron-based in situ reactive zone (mZVI-IRZ) for TCE removal in fresh and saline groundwater*. Sci. Total Environ. 626, 638–649. https://doi.org/10.1016/j.scitotenv.2018.01.115

Zhao R., Zhou Z., Zhao X., Jing, G., 2019. *Enhanced Cr(VI) removal from simulated electroplating rinse wastewater by amino-functionalized vermiculite-supported nanoscale zero-valent iron*. Chemosphere 218, 458-467. https://doi.org/10.1016/j.chemosphere.2018.11.118

Zhang, Y., Gillham, R.W., 2005. *Effects of gas generation and precipitates on performance of Fe^0 PRBs.* Ground Water 43(1), 113–121.

Zhang, Z., Liu, J., Cao, X., Luo, X., Hua, R., Liu, Yan, Yu, X., He, L., Liu, Yunhai, 2015. *Comparison of U(VI) adsorption onto nanoscale zero-valent iron and red soil in the presence of U(VI)–CO_3/Ca–U(VI)–CO_3 complexes*. J. Hazard. Mater. 300, 633–642. https://doi.org/10.1016/j.jhazmat.2015.07.058

Web sites

http://www.eea.europa.eu/data-and-maps/indicators/progress-in-management-of-contaminated-sites-3/assessment